Neural networks linking crypt neurons to innate attractive behaviour in zebrafish

Inaugural-Dissertation

zur

Erlangung des Doktorgrades

der Mathematisch-Naturwissenschaftlichen Fakultät

der Universität zu Köln

vorgelegt von

Manish Tomar

aus

Moradabad, Indien

Köln, 2021

Berichterstatter:	Prof. Dr. Sigrun Korsching
	Prof. Dr. Peter Kloppenburg
Tag des mündlichen Prüfüng	12.08.2020

Abstract

Crypt neurons are one of the subtypes of sensory neurons in the olfactory epithelium of zebrafish. A single member of the ORA gene family, ORA 4, was found to be expressed in all crypt neurons. Crypt neurons project to a single glomerulus of the medio-dorsal cluster in the olfactory bulb. However, the function of crypt neurons still needs to be elucidated. Some studies have implicated the role of crypt neurons in kin recognition of larval zebrafish; however, the respective ligands have not been identified in those studies.

To understand the function of crypt neurons we generated an ORA4 knockout in our lab. First, I checked whether crypt neurons are viable without an ORA4 receptor. I found that crypt neurons do not require the ORA4 receptor to survive, and they also maintain their target glomerulus in the absence of functional ORA4 receptor. Interestingly the number of crypt neurons is significantly increased in the knockout, consistent with a compensatory mechanism. I then used neural activity markers such as p-Erk in wildtype and knockout fish, along with live calcium imaging in wildtype fish to investigate whether the activation of ORA4 receptor observed in heterologous expression system is also present in vivo. p-Erk results were variable, but calcium imaging reproducibly showed activated neurons in bo olfactory bulb. As a first step to analyze the function of ORA4 receptor signaling pathway I established that larval zebrafish prefer the activating stimulus irrespective of their metabolic state. However, the spatial distribution of activated neurons observed in calcium imaging does not support a mediation of this innate attraction by crypt neurons. For time reasons behavior could not be studied in the knockout fish.

Zusammenfassung

Kryptneuronen sind eine der Typen von Sinnesneuronen im Riechepithel des Zebrafisches. Es wurde festgestellt, dass ein einzelnes Mitglied der ORA-Genfamilie, ORA 4, in allen Kryptneuronen exprimiert wird. Alle Kryptneuronen projizieren auf einen einzigen Glomerulus des medio-dorsalen Clusters im Riechkolben, dem Bulbus olfactorius. Die Funktion der Kryptneuronen muss jedoch noch aufgeklärt werden. Einige Studien haben die Rolle von Kryptneuronen bei der Verwandtschaftserkennung von Zebrafischlarven impliziert, jedoch wurden die entsprechenden Liganden in diesen Studien nicht identifiziert.

Um die Funktion von Kryptneuronen zu verstehen, haben wir in unserem Labor einen ORA4-knockout erzeugt. Zuerst prüfte ich, ob Kryptneuronen ohne einen ORA4-Rezeptor lebensfähig sind. Ich fand heraus, dass Kryptneuronen den ORA4-Rezeptor nicht zum Überleben benötigen und dass sie ihren Ziel-Glomerulus auch in Abwesenheit eines funktionierenden ORA4 beibehalten. Interessanterweise ist die Anzahl der Kryptneuronen im knockout signifikant erhöht, was einen Kompensationsmechanismus implizieren könnte. Ich habe dann neurale Aktivitätsmarker, wie p-Erk bei Wildtyp- und knockout-Fischen zusammen mit der Kalzium-Live-Bildgebung bei Wildtyp-Fischen verwendet, um zu untersuchen, ob die im heterologen Expressionssystem beobachtete Aktivierung des ORA4-Rezeptors auch in vivo vorhanden ist. p-Erk-Ergebnisse waren variabel, aber die Kalzium-Live-Bildgebung zeigte reproduzierbar aktivierte Neuronen sowohl im Riechkolben. In einem ersten Schritt zur Analyse der Funktion des ORA4-Rezeptor-Signalweges stellte ich fest, dass Zebrafischlarven unabhängig von ihrem Stoffwechselzustand den aktivierenden Reiz bevorzugen. Die in der Calcium-Bildgebung beobachtete räumliche Verteilung der aktivierten Neuronen unterstützt jedoch nicht die Vermittlung dieser angeborenen Anziehung durch Kryptneuronen. Aus Zeitgründen konnte das Verhalten bei den knockout-Fischen nicht untersucht werden

Table of Contents

1. Introduction

To make sense of the environment, an animal possesses sensory systems which consist of sensory receptors, and subsequent neural circuits. In terrestrial and marine organisms, sensory systems are constantly processing information and making the organism aware of the stimuli such as smell, light, touch, taste and monitoring the internal state of organism. Sensory systems are expected to be present in all animals, and in vertebrates can be classified into three physical (vision, auditory, touch) and two chemical (olfaction and taste) senses.

Olfaction is an ancient sense and is one of the main tools that animals use to make sense of their environment. There are many chemical cues in the environment of the organism. Vertebrates, including fishes efficiently use their sense of smell for locating food, detecting danger, communicating with kin members and for reproduction. Fish including zebrafish detect and discriminate huge variety of odorants such as amino acids, nucleotides, bile acids, amines, steroids, and prostaglandins. Such odor signals evoke fundamental behaviors important for the survival of species (Yoshihara, 2014). In tetrapods, two majors anatomically and functionally separate sensory organs are present, the vomeronasal organ (VNO) and the main olfactory epithelium (MOE). VNO is specialized to sense pheromones (volatile and non-volatile), and MOE serves as a general odor detector for volatile molecules. The olfactory epithelium is connected to the olfactory bulb, whereas the projections from the VNO goes to the accessory olfactory bulb. In contrast to tetrapods fish have developed a single olfactory organ with a single sensory surface containing several distinct types of olfactory sensory neurons. All olfactory sensory neurons send their axons in the olfactory bulb, which is neuroanatomically and functionally segregated into different glomerular clusters (Baier and Korsching 1994; Braubach et al., 2012). Output neurons from the olfactory bulb called mitral and tufted neurons project axons to target areas in the higher brain regions such as ventral telencephalon and habenula, finally generating various behavioral phenotypes in response to different odors (Yoshihara., 2014).

Zebrafish as a model organism offers distinct advantage such as easy maintenance, ease of breeding, large progeny, and optical transparency during development. Olfactory system of zebrafish has been well studied and comprises 5 morphologically distinct types of

olfactory sensory neurons (ciliated, microvillous, crypt, kappe and pear shaped A2c neurons. Olfactory receptors such as OR, V1R, V2R, TAAR, and recently discovered A2c receptor appear to be expressed in different olfactory sensory neuron populations (Ahuja et al., 2014; Alioto and Ngai 2005, Hashiguchi and Nishida 2006, 2007; Saraiva and Korsching 2007, Wakisaka 2017). Each olfactory neuron type expresses lar sensory neurons Unexpectedly, one member of the ORA family ORA4 was found to be expressed in all crypt neurons (Oka et al., 2012), thus give rise to “one neuron - one receptor”, mode of expression, which is an unique mode of expression for a olfactory receptor as compared to “one neuron type-one receptor” mode of expression mentioned above. This makes crypt neurons interesting neurons to investigate. To understand the function of crypt neurons we generated an ORA4 knockout in our lab, to check whether crypt neurons survive without a receptor. Some studies have implicated crypt neurons in kin recognition of larval zebrafish (Biechl et al., 2016, Gerlach et al., 2019). This appears inconsistent with our results (Behrens and Korsching, unpublished observation) that the ORA4 receptor is activated by alkaline pH in heterologous expression system. The purpose of this study was to investigate the relationship of alkaline stimulus and ORA4 in zebrafish *in vivo* by comparing wildtype and ORA4 knockout fish, using a combination of methods.

1.1 Zebrafish olfactory system

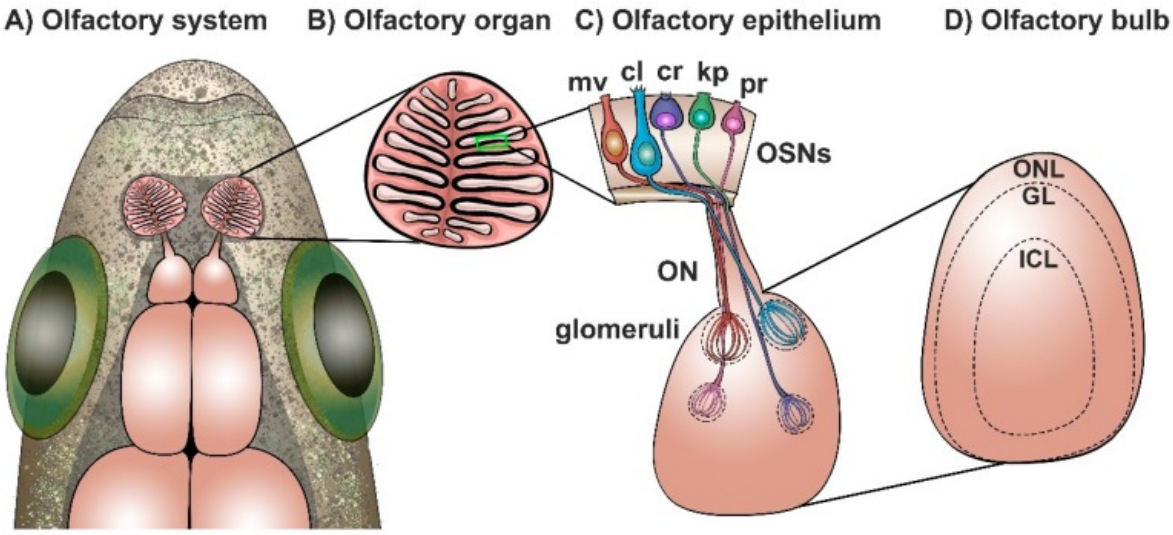

Figure 2: General organization of the zebrafish olfactory system (Figure taken from Ochoa and Jacobs, 2019)

General organization of zebrafish olfactory system

Interestingly, in teleost fish peripheral organization of the olfactory system is different from that of the mammals. Teleost including zebrafish have developed only a single type of olfactory organ called the olfactory rosette. In case of zebrafish the rosette contains five morphologically distinct olfactory sensory neurons: ciliated, microvillous, crypt (Hansen et al., 2004, Ahuja et al., 2013), kappe (Ahuja et al., 2014) and pear shaped adenosine receptor containing olfactory sensory neurons (Wakisaka et al., 2017). Individual neurons in the olfactory epithelium project their axons via olfactory nerve to olfactory bulb which comprises of glomerular clusters serving as the first relay station to receive the odor information (Baier and Korsching, 1994; Braubach et al., 2012). From the olfactory bulb mitral and tufted neurons target to different areas in the higher brain regions such as habenula and ventral nucleus of ventral telencephalon (Miyasaka et al., 2009).

1.2 Olfactory sensory neurons and receptor types

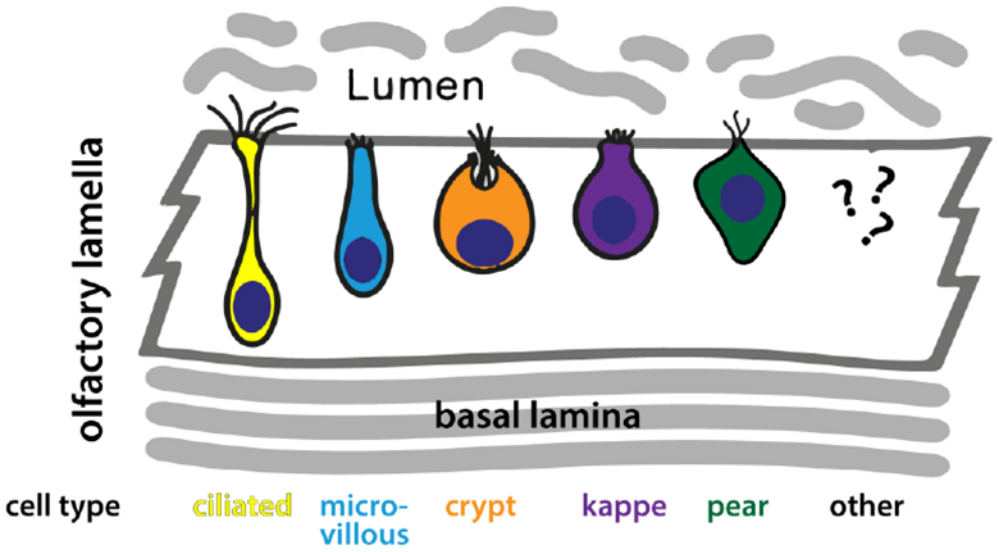

Figure 3: Types of olfactory sensory neurons (Image modified from Milan Dieris, Doctoral Thesis, 2018)

Olfactory sensory neuron expresses distinct receptors (Yoshihara, 2014) belonging to different olfactory receptor families. Zebrafish genome contains 150 OR-type, ~60 V2R-related Olfc genes, 7 V1R-related ORA genes, and ~100 TAAR type olfactory receptor genes. (Alioto and Ngai, 2005; Hashiguchi and Nishda, 2006, 2007; Sato et al., 2007; Saraiva and Korsching, 2007; Hussain et al., 2009; Zapilko and Korsching, 2016; Ahuja et al., 2018).

Ciliated neurons in the olfactory epithelium, possess long dendrites, and extend several long cilia into the lumen of the nasal cavity. The ciliated neurons express OR, TAARs (Cao et al., 1998; Speca et al., 1999; Hansen et al., 2004; Hussain et al., 2009).

Microvillous olfactory sensory neurons constitute a minor population in olfactory epithelium of zebrafish. Microvillous neurons exhibit a short dendrite and emanate short but numerous microvilli and express V2R-related OlfC genes (Sato et al., 2005).

Crypt neurons constitute third type of olfactory sensory neurons (Hansen and Zeiske,1998; Hansen et al., 2003, 2004) which are identified by large globular soma, along with the presence of both cilia and microvilli. Recently a small and highly conserved family of V1R-like genes have been identified: 7 highly conserved receptor genes were

reported in teleost fish and a new nomenclature was awarded to the gene family called “ORA gene family” (Saraiva and Korsching, 2007; Zapilko and Korsching, 2016). Unexpectedly, one member of the ORA family ORA4 was found to be expressed in all crypt neurons (Oka et al., 2012). This homogeneous expression of a single receptor in the entire cell type is different from the “one cell type - one receptor” mode of expression in the ciliated and the microvillous neurons leading to more restricted “one cell – one receptor” mode of expression. In recent studies functional role of crypt neurons has been suggested in kin odor recognition in zebrafish larvae (Beichl et al., 2016).

Kappe neurons have been reported as fourth type of olfactory sensory neurons with microvilli, but different from microvillous neurons (Ahuja et al., 2014), their functional importance has yet to be identified. So far, they have only been observed in zebrafish.

Pear-shaped neurons have been recently identified, which express adenosine receptor A2c (Wakisaka et al., 2017). They are located apically in the lamellae and project to a large lateral glomerulus (IG2), which reacts to AMP, ADP and ATP (Wakisaka et al., 2017). Since nucleotides are considered feeding stimulus for fish, pear shaped neurons are thought to involved in feeding behavior in zebrafish.

1.3 General mechanism of signal transduction in olfactory sensory neurons

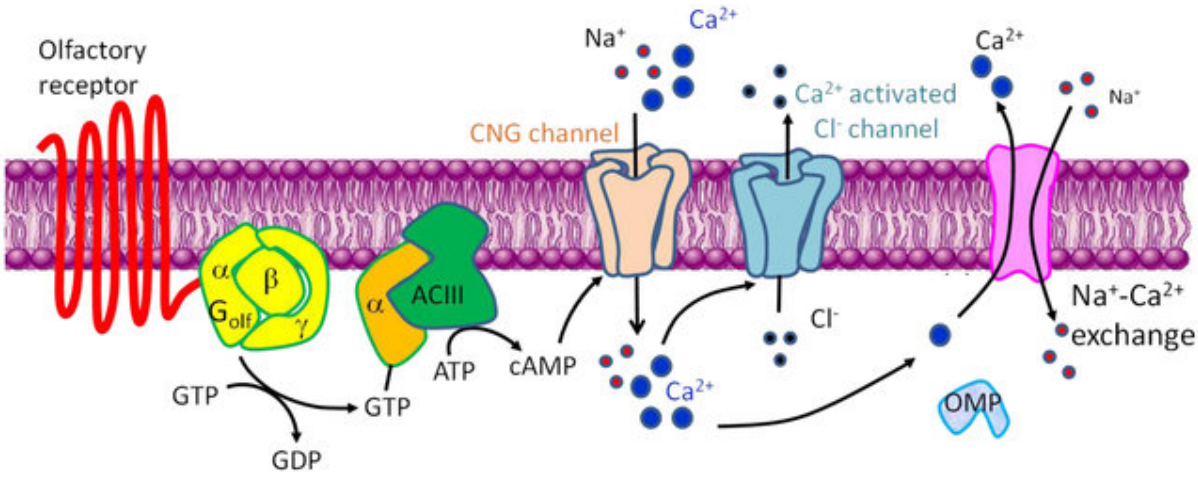

Figure 4: A schematic diagram of olfactory signal transduction. Olfactory signal transduction begins with the activation of an olfactory receptor (OR) in the ciliary membrane; this leads to an increase in cyclic AMP (cAMP) synthesis through the activation of adenylate cyclase type III (ACIII) via a G protein (Golf)-coupled cascade. The increase in cAMP concentration causes cyclic nucleotide-gated (CNG) channels to open, leading to an increase in intracellular Ca 2+ concentration and depolarization of the cell membrane by the Ca 2+-activated chloride channel. Among several molecules of the olfactory signal transduction, OR, olfactory marker protein (OMP), Golf protein α-subunit (Gαolf), and ACIII have known to be olfactory specific molecules. Figure taken from Kang and Koo, 2012.

The olfactory system senses the odorants in the environment via odorant receptors which are in the cilia of olfactory sensory neurons (OSNs) in the olfactory epithelium of terrestrial and aquatic organisms. When an odorant binds the olfactory receptor, it triggers a signaling cascade leading to generation of action potential. Once activated leads to an increase of intracellular cAMP caused by the membrane form of adenylate cyclase III (ACIII) (Wong et al 2000). Increased intracellular cAMP causes an external cation influx by activating a cation-selective cyclic nucleotide gated (CNG) channel (Nakamura and Gold 1987). Plasma membrane depolarization is further triggered by calcium-activated chloride channels (Berg et al., 2012). Elevated intracellular calcium concentration is brought back to resting levels by expelling calcium ions through the plasma membrane by sodium/potassium exchanger (NCX), a potassium-dependent sodium potassium exchanger (NCX4), and a plasma membrane Ca^{2+} ATpase (PMCA) (Brini and Carafoli, 2011). OMP olfactory

marker protein facilitates NCX activity and allows for the rapid Ca2+ extrusion (Kwon et al., 2009).

The inhibitory G protein (Gi1b) has been found to be expressed with ORA 4 receptor (Oka et al., 2012), which supports the notion that signal transduction of ORA4 is mediated by an inhibitory G protein

1.4 Phosphorylated Erk (p-Erk) as a marker for neuronal activity

The extracellular signal-regulated kinase (Erk, including Erk1 and Erk 2), is a member of mitogen activated protein kinase (MAPk) family. Activation of ERK occurs by its upstream kinase MEK (MAP kinase or ERK kinase) (Widmann et al., 1999). Studies have reported that ERK is involved in neuronal and synaptic plasticity underlying learning, memory, and pain sensitivity (Ji et al., 2002). GPCRs have been shown to stimulate MAP kinase phosphorylation cascade which is used as an indicator of neural activity in wide variety of cell types and species., because of its better temporal resolution as compared to other markers of neuronal activity for example the immediate early gene c-fos (Gao and Ji., 2009) (Wetzker and Bohmer, 2003). Phosphorylation of the extracellular signal-regulated kinase (Erk), has been used as an activity marker for neuronal activation in larval and adult zebrafish (Randlett et al., 2015; Dieris et al., 2017; Hussain et al., 2013).

1.5 Functional organization of olfactory bulb in zebrafish

Different set of odorants excite different type of olfactory sensory neurons in zebrafish (Friedrich and Korsching, 1998; Hussain et al., 2013; Dieris et al., 2016). Olfactory neurons project their axons to the olfactory bulb, which is further segregated into individual glomeruli acting as a first relay station for the segregation of olfactory information (Baier and Korsching, 1994; Braubach et al., 2012). Numerous neuroanatomical tracing studies were conducted to reveal the pattern of projection of olfactory sensory neurons to the olfactory bulb (Morita and Finger, 1998; Doving et al., 2011; Hamdani and Doving 2002, 2006; Hansen et al 2003). Further, introduction of genetic labelling and gene trap provided detailed insight of the axonal wiring from olfactory epithelium to olfactory bulb (Miyasaka et al., 2009; Sato et al., 2005, 2007; Koide et al., 2009).

The ciliated olfactory sensory neurons project their axons to the maG, vaG, dG, and dlG clusters, mpG glomerulus, IG2 glomerulus and the most of vmG glomeruli, whereas microvillous OSNs project their axons to all glomeruli in the IG cluster except for IG2, one of the two vpG glomeruli and several mdg glomeruli (Sato et al., 2005) (Braubach et al., 2012). Crypt neurons which contain ORA4 receptor have been shown to project to the large medio-dorsal glomerulus mdg2 (Ahuja et al., 2013), while kappe neurons project to the mdG5 glomerulus (Ahuja et al., 2014). The segregation of neural pathways forms the basis for the distinction of olfactory information at the level of olfactory bulb and represented on the olfactory bulb as “odor map”. (see Figure on next page)

A series of studies measured the activity from the glomerulus using either voltage sensitive dyes or calcium indicators gave the evidence of an odor map in olfactory bulb of zebrafish (Friedrich and Korsching 1997, 1998; Fuss and Korsching 2001) Adult Zebrafish displays strong attraction to amino acids. (Steele et al., 1990, Koide et al., 2009). Microvillous olfactory sensory neurons detects amino acids (Hansen et al., 2003) and as a result activation of multiple glomeruli was seen in the IG cluster (Friedrich and Korsching 1997, 1998; Fuss and Korsching, 2001). Fish produce bile acid derivative specific to their own species (Hagey et al., 2010), suggesting their role in olfactory-mediated social interaction. Bile acids elicit strong responses in the dG and parts of vmG cluster (Friedrich and Korsching, 1998). Amines, for example cadaverine has been shown to selectively activate dlG (Dieris et al., 2017). Prostaglandin PGF2α elicits response in a specific

ventral glomerulus (Yabuki et al., 2016), and nucleotides are processed by lateral glomerulus (Wakisaka et al., 2017)

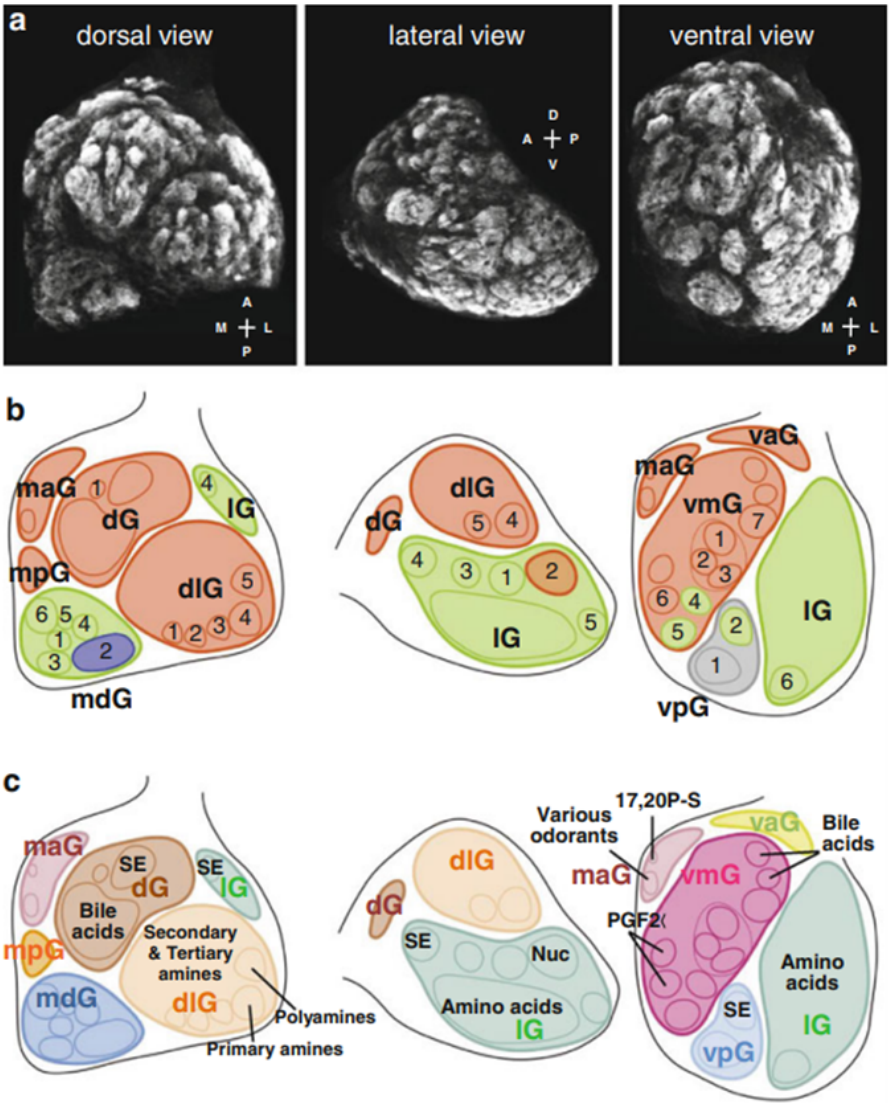

Figure 5: Glomerular clusters and odor map in the adult zebrafish olfactory bulb (OB). (a) Whole-mount OB immunostained with anti-SV2 antibody, viewed from dorsal, lateral, and ventral sides. (b) Eight glomerular clusters and 29 identifiable glomeruli. (c) Odor map, nucleotides, SE skin extract, dG dorsal glomerular, dlG dorsolateral, lG lateral, maG medio-anterior, mpG medioposterior, mdG medio-dorsal, vaG ventro-anterior, vmG ventro-medial, vpG ventro-posterior (Figure taken from Yoshihara, 2014)

1.6 Organization of olfactory bulb in larval zebrafish

As mentioned in the previous section, glomeruli are anatomically and functionally arranged in olfactory bulb of mature zebrafish OB (Braubach et al., 2012). The anatomical and neurochemical organization in zebrafish larva resemble the mature olfactory bulb as early as 72 hpf (Braubach et al., 2013)

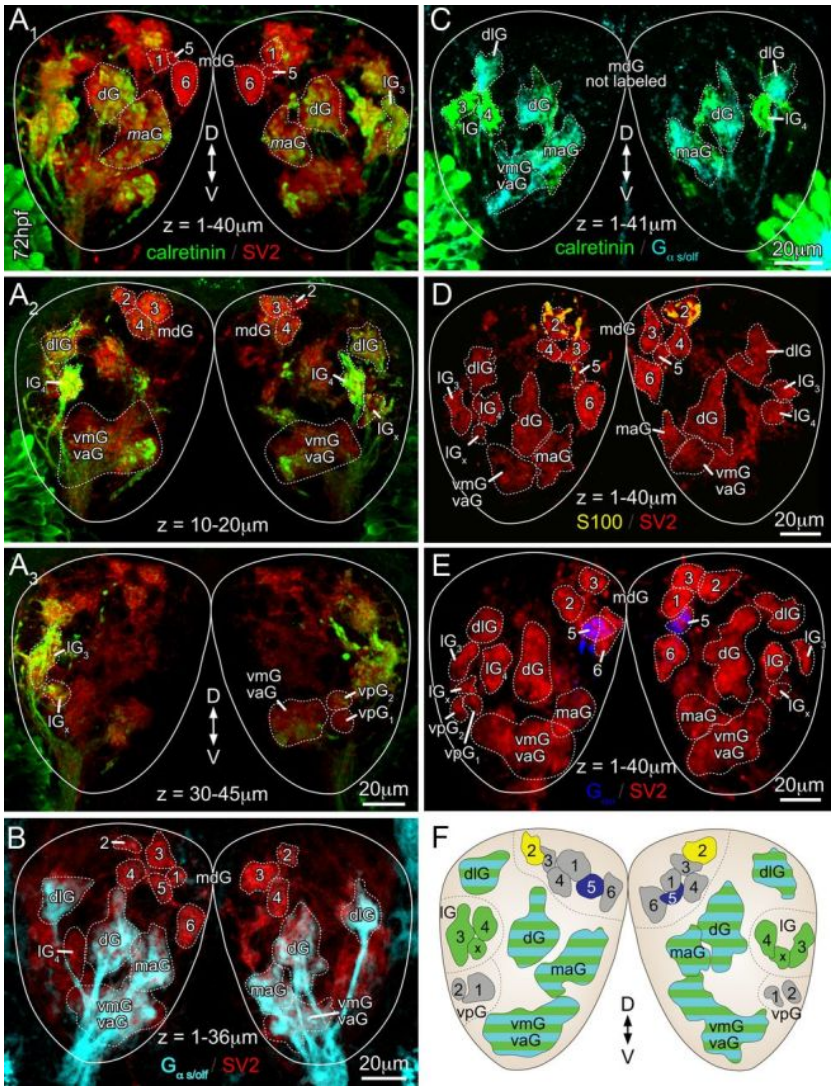

Figure 6: Frontal views of OBs from five 72 hpf embryos, as seen through the skull. Glomeruli labeled selectively with anti-calretinin (A1–A3, substacks of optical sections from same specimen), anti-Gαs/olf (B), anti-S100 (D), and anti-Gαo (E) antibodies. Four large and irregularly shaped regions (dG, dlG, maG, and vmG/vaG) were always labeled by anti-calretinin and anti-Gαs/olf antibodies (C,F). A1–A3, C, IG labeled only with the anti-calretinin antibody. The mdG2 and mdG5 were selectively immunoreactive (IR) to anti-

S100 (D) and anti-Gαo (E), respectively, and displayed inconsistent staining with the anti-calretinin antibody (compare A1–C). The remaining mdG were labeled only with general structural markers, such as anti-SV2. F, The schematic summarizes the distributions of glomeruli at 72 hpf. The scale bar in A3 also applies to A1, A2. (Figure taken from Braubach et al 2013)

From 36 hpf onwards, olfactory sensory axons send their projections to the olfactory bulb where they target individual glomeruli (Dynes and Ngai, 1998). Glomeruli in zebrafish larvae undergoes a process of activity dependent maturation (Li et al., 2005; Braubach et al., 2013) leading to the appearance of discreet glomerular clusters such as (mdg) and other glomerular regions (Braubach et al., 2013)

1.7 Olfactory processing in the higher brain areas of zebrafish

The fish olfactory system detects variety of compounds, which are responsible for crucial behaviors important for survival of the animal such as feeding, reproduction, social interaction and avoiding predation. Odorants are detected by the olfactory sensory neurons in the olfactory epithelium, and then the information is sent to olfactory bulb, which acts as the first relay station for processing of olfactory information. Mitral and tufted neurons (Glutamatergic) are the major neurons in the olfactory bulb of zebrafish (Edwards and Michael, 2002). Dendrites of mitral neurons and tufted neurons receive synaptic input from the olfactory sensory neurons and project their axons to higher brain regions such as telencephalon and diencephalon (Fuller et al., 2006; Miyasaka et al., 2009).

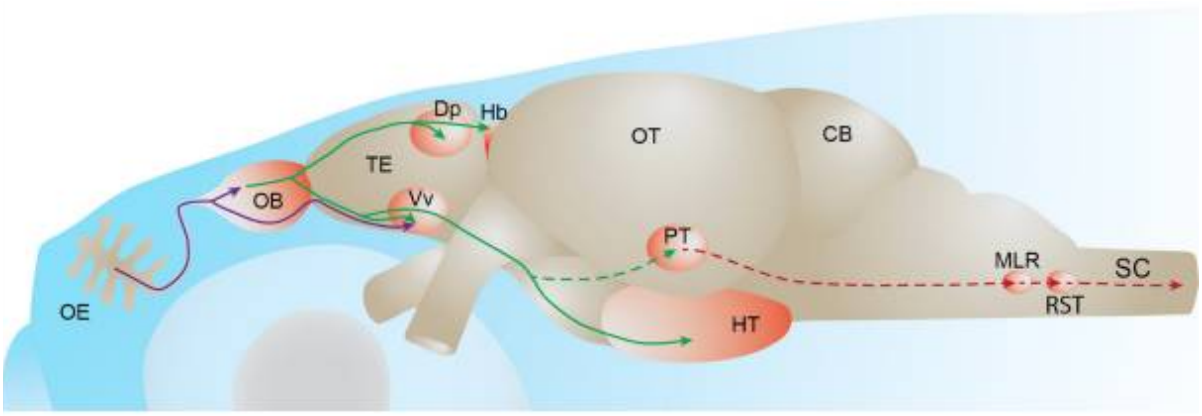

Figure 7: Targets of Mitral neurons from olfactory bulb

OE: olfactory epithelium, OB: olfactory bulb, TE: telencephalon, Dp: dorsal-posterior part of the telencephalon, Hb:habenula, Vv: ventral nucleus of the ventral telencephalon, OT: optic tectum, PT: posterior

tubercle, HT: hypothalamus, CB: cerebellum, MLR: mesencephalic locomotor region; RST: reticulo-spinal tract, SC: spinal cord. Figure adapted from Kermen et al., 2013)

In telencephalon, the mitral neurons project axons to Vv (Ventral nucleus of Ventral Telencephalon, Dp (dorsal posterior part of telencephalon) which (in teleost) is homologous to the mammalian primary olfactory (piriform) cortex, and to Vv (Ventral nucleus of ventral Telencephalon) which is a homolog to septal area, part of limbic system in mammals (Rink and Wullimann, 2004; Miyaska et al., 2009; Gayoso et al., 2011). The lateral olfactory tract contains fibers which originates in the lateral olfactory bulb, whereas medial olfactory tract contains the fibers which originate in the medial olfactory bulb (Sheldon.,1912). Medial and lateral olfactory tracts are separate, anatomically defined axon bundles, which allowed the researchers to experimentally manipulate these tracts across different fish species (Doving et al., 1980). Dye tracing studies and genetic labelling approaches gave an insight on different brain regions which are targeted by mitral neurons and are involved in olfactory processing (Rink and Wullimann 2004; Miyaska et al., 2009, 2014)

Different higher brain areas are activated by different set of odorants. Bile acids activate the medial pallium, whereas amino acids and nucleotides activate lateral pallium which is a part of Dp (Nikonov et al., 2005). Habenula has gained popularity in recent years due its role in processing value-related information, which receives diverse sensory inputs due to its unique asymmetrical pattern (Miyasaka et al., 2009). Right dorsal habenula which is innervated by mitral neurons in olfactory bulb (Miyasaka et al., 2014) has been shown to mediate social interaction in larval zebrafish (Krishnan et al., 2014).

Hypothalamus is in the ventral diencephalon and plays a key role in mediating several vital physiological functions (Machluf et al., 2011). In zebrafish hypothalamus receives input from olfactory sensory neurons via mitral neurons (Reinig et al., 2017) and is responsible for mediating behavioural phenotypes such as stress response along the HPA axis (Joels and Baram., 2009), feeding (Wee et al., 2019) and reproductive behaviour (Zohar et al., 2010).

1.8 Larval zebrafish behavior

Zebrafish larvae are sensitive to various sensory stimuli such as chemo sensation, touch, olfaction, audition, heat sensation and vision (Kalueff et al., 2013). Reflexive responses to touch appear around 21 hours post fertilization (Amant and Drapeau, 1998). Zebrafish larvae displays occasional tail flicks from 3 dpf onwards (Lindsay and Vogt, 2004). Various studies have described commonly observed behaviours of zebrafish larvae, which include thigmotaxis (tendency to remain close to the walls of the petri-dish), and startle response (Colwill and Creton, 2011). Other well studied behaviour characteristics includes optokinetic response-eye movement in response to moving object (Orger and Baier, 2005), and prey capture (Muto and Kawakami, 2013).

In the last decade zebrafish larvae became an attractive model to study pharmacological manipulations. With the introduction of high throughput screening techniques, ease of replication, commercially available software for data analysis it was made possible to screen the behavior of larvae at different stages of development on presentation with different stimuli. In neuroscience research zebrafish became an attractive model because their advantage of optical transparency, and small size which makes it possible to screen the effect of stimulants over a large sample size (Kokel et al., 2010).

The behaviour repertoire of zebrafish larvae has been utilized for studying effects of drugs for psychiatric illness such as anxiety and mood disorders, and also for the identification of novel compounds for the treatment of psychiatric illness (Kokel et al., 2010; Luna et al., 2017). Behaviour of larval zebrafish has also been utilized to trace the neural circuits associated with innate behaviour such as attraction, aversion (Krishnan et al., 2014) and prey capture (Muto and Kawakami, 2013). Zebrafish larvae undergo a process of rapid embryogenesis in the first few days after successful hatching, and as they continue to grow their reliance on the yolk sac as their food source diminishes. From 5dpf onwards zebrafish larvae need to be supported with external food sources for their survival, as they begin to display swimming bouts which could be seen as exploratory, for avoidance from predators or for food foraging (Chen et al., 2019). Thus, the first week of development acts as a crucial transitional period in the feeding behaviour of zebrafish larvae. Zebrafish larvae in their first week of development are attracted to intermediate

concentration of bile salts but tend to avoid higher concentration. Larvae displayed aversion to 10μM of GCDA, while 1μM of GCDA was an attractive odor (Krishnan et al., 2014), which suggests that larvae can discriminate between different concentrations of the same olfactory cue, processing it as either rewarding or aversive stimuli. Food extract acts as a positive rewarding stimulus for zebrafish larvae and they display significant increase in the swimming speed after the addition of food odor (Chen et al., 2019). On analyzing the calcium levels in higher olfactory brain regions in *elavl3*::GcaMP5 5 dpf larvae in response to food odor, it was observed that neurons of right dorsal habenula responded on the addition of food odor. In zebrafish, habenula is divided into dorsal and ventral habenula. Dysfunction or lesion of right dorsal habenula resulted in significant impairment of food seeking behavior (Chen et al., 2019). In lower vertebrates habenula acts as modulator in processing emotion related information by modulating the release of neurotransmitters. The role of habenula has been well studied in fear and anxiety-related behavior in rodents and zebrafish (Hikosaka, 2010), while in zebrafish besides receiving fear and anxiety related inputs, role of habenula has also been studied modulating inputs from visual and olfactory pathways (Zhang et al., 2017).

In the last decade development of genetically encoded calcium indicators and with the development of functional imaging (confocal/two photon microscopy) has given an added advantage to study the neural networks that are activated on the activation of olfactory sensory neurons.

1.9 Imaging Calcium in neurons

Calcium ions mediate a variety of intracellular signals that regulate the fate of multitude of functions in a living biological organism (Berridge et al., 2000). The function of calcium ions ranges from the control of heart muscle to the regulation of cell cycle, cell proliferation and cell death (Orrenius et al., 2003). In nervous system, the functional role of calcium ions is vitally important as it triggers the exocytosis of neurotransmitters containing synaptic vesicles (Neher and Sakaba, 2008). In the post-synapse a transient rise of calcium ions in the dendritic spines is essential for the activity induced synaptic plasticity of the neurons (Lyons and West, 2011). Thus, making calcium ions as the hallmark for the vitally essential processes in the nervous system. Intra cellular calcium signals can function over a wide variety of time scales, with different amplitudes and at varied location in the cellular environment of the organism, for example neurotransmitters release take milliseconds while the regulation of gene transcription in the nucleus could take over hours to execute (Berridge et al., 2003). This unique characteristic of calcium ions has given rise to the possibilities for investigation of multiple cellular processes in the living organism.

Investigation of calcium signals in the last decade has benefitted enormously from the development of visualization techniques which greatly improved the qualitative and quantitative estimation of intracellular calcium signals. Historically, aequorins a bioluminescent calcium binding photoprotein was first used for monitoring the dynamics of cellular calcium signaling, (Ashley and Ridgway, 1968). Calcium indicators then evolved to synthetic dye for example arsenzaro (III) (Brown et al. 1975) which provided invaluable insight into the functioning of neuronal processes. However, their application was tedious and time consuming (Smith and Zucker, 1980). Furthermore, more sensitive dyes were developed by the hybridization of highly selective chelators like EGTA or BAPTA which were responsible for the chelation of free calcium ions with fluorescent chromophore (Tsien et al., 1980). These developed fluorescent indicators were called as quin-2, fura-2, indo-1, and fluro-3 (Tsien et al., 1980). Quin-2 is excited by ultraviolet light and was one of the first dye among fluorescent indicators to be used for biological experiments (Pozzan et al., 1982; Tsien et al., 1980). Over the years many synthetic calcium indicators have been introduced, for example Oregon Green BAPTA and fluo-4 dye families (Paredes et al.,

2008), which have been widely used for neuroscience research because of their ease of implementation and provided a better signal to noise ratio as compared to Fura family dyes (Paredes et al., 2008).

The next crucial development in calcium imaging research came in the form of development of protein based genetically encoded calcium indicators (GECI) (Miyawaki et al., 1997). The early versions of GECIs had limited application as their response kinetics were slow and had low signal to noise ratios, in the last decade there has been tremendous improvements in improving the response kinetics of genetically encoded calcium indicators such as GCaMP (Chen et al., 2013)

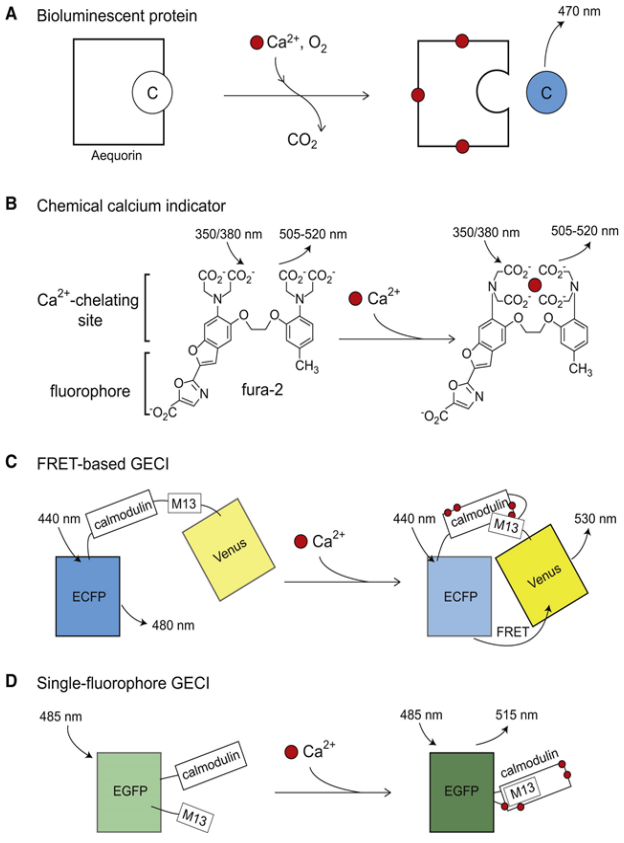

Figure 8: Calcium Indicators

(Figure legend on next page)

(A) **Bioluminescent protein**. Binding of calcium ions to aequorin leads to the oxidation of the prosthetic group coelenterazine (C, left side) to colenteramide (C, right side). Colenteramide relaxes to the ground state while emitting a photon of 470 nm.

(B) **Chemical calcium indicator**. Fura-2 is excitable by ultraviolet light (e.g., 350/380 nm) and its emission peak is between 505 and 520 nm. The binding of calcium ions by fura-2 leads to changes in the emitted fluorescence.

(C) **FRET-based genetically encoded calcium indicator (GECI).** After binding of calcium ions to yellow cameleon 3.60 the two fluorescent proteins, ECFP (donor) and Venus (acceptor), approach. This enables Fo¨ rster resonance energy transfer (FRET) and thus, the blue fluorescence of 480 nm decreases, whereas the fluorescence of 530 nm increases.

(D) **Single-fluorophore genetically encoded calcium indicator (GECI)**. After binding of calcium to GCaMP conformational intra-molecular changes lead to an increase in the emitted fluorescence of 515 nm, modified from (Greinberger and Konnerth., 2012)

GECI provides an added advantage over traditional calcium indicators with the cell and tissue specific expression, making the process non-invasive. The development of genetically encoded calcium indicators has paralleled the advanced imaging methods (Eilers and Konnerth, 2009) which made possible to record and analyze real time fluorescence signals of the biological processes at a single cell resolution. Two-photon microscopy further developed the area of calcium imaging research in many laboratories around the world (Helmchen and Denk, 2005; Svoboda and Yasuda, 2006).

1.9.1 Neuronal Calcium signaling

As described above intracellular calcium acts as an important messenger to facilitate a variety of functions in a living organism. Inside the cell calcium dynamics constantly change and the balance between the calcium influx and efflux in the cell is determined by the exchange of calcium from the cellular environment as well as the release of calcium from internal stores (Schwaller et al., 2010).

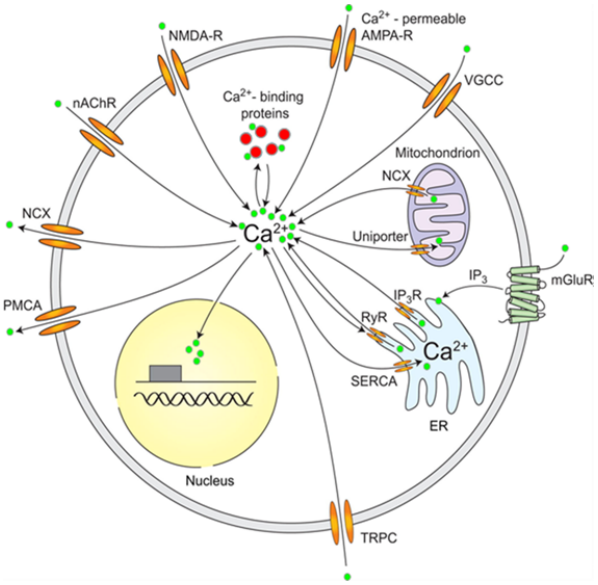

Figure legend on next page

Figure 9: Neuronal Calcium Signaling: Sources of calcium influx are calcium-permeable-a-amino-3-hydroxy-5-methyl-4-isoxazolepropionic acid(AMPA) and N-methyl-D-aspartate (NMDA) glutamate type receptors, voltage-gated calcium channels (VGCC),nicotinic acetylcholine receptors (nAChR), and transient receptor potential type C (TRPC) channels. Calcium release from internal stores is mediated by inositol trisphosphate receptors (IP3R) and ryanodine receptors (RyR). Inositol trisphosphate can be generated by metabotropic glutamate receptors (mGluR). Calcium efflux is mediated by the plasma membrane calcium ATPase (PMCA), the sodium-calcium exchanger (NCX), and the sarco-/endoplasmic reticulum calcium ATPase (SERCA). Also, the mitochondria are important for neuronal calcium homeostasis. (Modified from Greinberger and Konnerth, 2012)

The calcium ions which are responsible for giving rise to calcium spikes are the free calcium ions.

Endoplasmic reticulum acts as a store house for intracellular calcium, and the release of calcium ions from ER is mediated by inositol triphosphate and ryanodine receptors (Berridge, 1998). The high level of calcium within the endoplasmic reticulum is maintained by sarco-endoplasmic reticulum calcium ATPase (SERCA) which is responsible for the transport of calcium ions from the cytosol to the lumen of ER (Berridge, 1998). Mitochondria are another source of intracellular calcium ions, and they acts as a calcium buffer by taking up calcium during calcium elevations in the cytosol and then releasing them back to the cytosol (Duchen, 1999). The exchange of calcium between the cell and the extracellular space is mediated by multiple receptors and ion channels, for example voltage gated calcium channels, ionotropic glutamate receptors, nicotinic acetylcholine receptors (nChR), and transient receptor potential type C (TRPC) channels (Fucile, 2004).

The cellular calcium levels are determined by multiple processes, which co-ordinate with each other to regulate processes such as neurotransmitter release (Grienberger and Konnerth, 2012). Thus, developing a mechanistic understanding of a pathway for specific source of calcium inside the cell is still unclear and under investigation.

1.9.2 GCaMP6 as a Calcium indicator

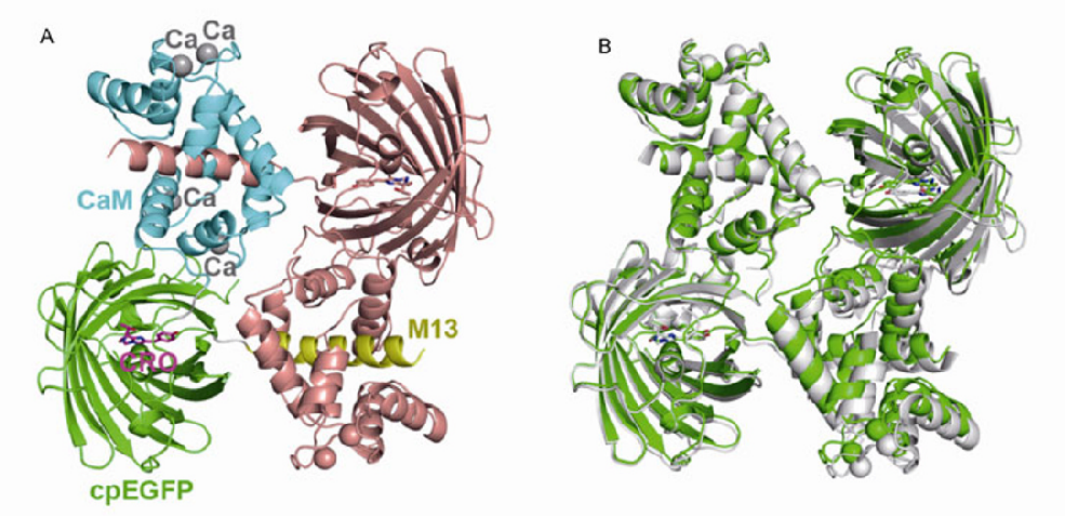

Figure 10: Crystal structure of GCaMP (Figure taken from Akerboom et al., 2012)

In the last 10 years of Calcium Imaging research Genetically Encoded Calcium Indicators (GECI), have been extensively used for imaging intracellular calcium levels in zebra fish, flies and mouse in vivo (Zariwala et al., 2012, Tian et al., 2009, Muto et al., 2017). In the layer 2/3 of pyramidal neurons in the mouse visual cortex, GCaMP6 was able to detect single action potentials in the neurons, and also responses evoked by light in the ganglion neurons in adult rodent tissue (Zariwala et al., 2012). GCaMP6, as calcium sensors provides useful insights into the organization and dynamics of calcium influxes in the cellular environment.

As shown in Figure11, GCaMP comprises of circularly permuted green fluorescent protein (cpGFP) (Baird et al., 1999), calmodulin (CaM)- calcium binding protein, and CaM-interacting M13 peptide (Crivici and Ikura, 1995). The CaM / M13 complex sits close to the chromophore inside cpGFP β barrael (Akerboom et al., 2012). Calcium ions on binding to the calcium binding domain in calmodulin results in making conformational changes in the CaM/M13 domain modulating the solvent access resulting in increased brightness. Multiple studies were conducted involving protein mutagenesis and screening for calcium activity giving rise to different version of GCaMP (Tian et al., 2009), (Akerboom et al., 2012), (Nakai et al., 2001).

Based on sensitivity and response kinetics Chen et al. (2013) have screened GCaMPs as a sensor for calcium sensitivity in cultured assay of rat hippocampal neurons containing GCaMP variants. The study made a quantitative comparison among different variants of GCaMPs.

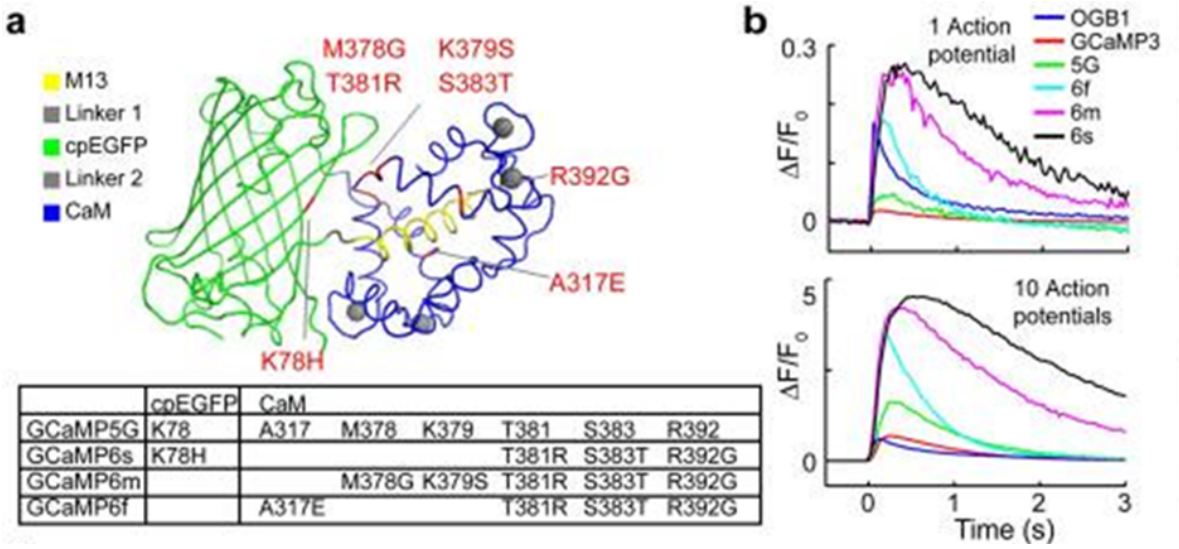

	cpEGFP	CaM					
GCaMP5G	K78	A317	M378	K379	T381	S383	R392
GCaMP6s	K78H				T381R	S383T	R392G
GCaMP6m			M378G	K379S	T381R	S383T	R392G
GCaMP6f		A317E			T381R	S383T	R392G

Figure 11: GCaMP structure27,64 and mutations in different GCaMP variants relative to GCaMP5G. b, Responses averaged across multiple neurons and wells for GCaMP3, 5G, 6f, 6m, 6s, and OGB1-AM. Top, fluorescence changes in response to 1 action potential. Bottom, 10 action potentials (Figure taken from Chen et al., 2013)

When compared to GCaMP5G, the GCaMP6 sensors displayed similar baseline brightness and a dynamic range (described as ΔF/F0 at 160 action potentials) was increased by 1.1-1.6. When stimulated with small numbers of action potentials GCaMP6s produced >10-fold larger signals than GCaMP3. When compared to GCaMP5G, GCaMP6s exhibited 3-fold higher affinity for calcium, while maintaining the same baseline fluorescence. Further mutagenesis of the calcium binding domain in the GCaMP6 variants resulted in the development the jGCaMP7 series, which are characterized by improved sensitivity to one action potential and higher signal-to-noise ratio due to enhanced brightness (Dana et al., 2018).

1.9.3 Imaging neuronal activity in vivo using GCaMP6s

GCaMPs have been tested as neural indicators in vivo by various research groups leading to a better understanding of neuronal activity in vivo different organisms ranging from C.elegans (Luo et al., 2014) , *Drosophilla* (Simpson and Looger, 2018), zebrafish (Aherns et al., 2013 ; Barker and Baier, 2015), and rodents (Niell and Stryker, 2008 ; Chen et al., 2013).

Zebrafish larvae encoding GCaMP6 have proved to be helpful in providing insights in visualization of neural circuits activated by certain goal directed behaviors such as prey capture, and attraction/aversion in zebrafish, thus making GCaMP6 a forefront tool in understanding of neural circuits (Bahl and Engert, 2019; Haesemeyer et al., 2018).

2. Aim of the thesis

Crypt neurons are a type of olfactory sensory neurons which project their axons to the medio-dorsal cluster 2 (mdg2) in the olfactory bulb (Ahuja et al., 2013). One receptor from the ORA gene family, ORA 4 was found to be expressed in crypt neurons and was activated by alkaline pH in heterologous expression system. The purpose of this study was to investigate the relationship of alkaline stimulus and ORA4 in zebrafish in vivo by comparing wildtype and ORA4 knockout fish, using a combination of methods. I used neural activity markers and calcium imaging with *elavl3*::GCaMP6s larvae to study the neural circuits activated in response to an alkaline stimulus.

3. Material and Methods

3.1 Organisms

3.1.2 Zebrafish strains and Animal care

Fish was housed in groups of up to 30animals in tanks with day/night cycle 14-hour light and 10-hour darkness. Fish water consisted of equal parts mixture of desalted water and tap water. pH of the circulating water was maintained between pH 7,0 – 7,4. Fish were fed twice a day, with brine shrimp artemia (Sanders, USA) and flake food (Terta, Germany). The following zebrafish strains were used in the study:

Strain	**Feature**	**Origin**
WT/KS	wildtype	Cologne
WT/Ab	wildtype	Tübingen
Casper(*elavl3*:: GCaMP6s)	Calcium sensor in neurons	HHMI, Janelia Farms
Tg(*elavl3*::nls-GCaMP6s)mpn400Tg	Calcium sensor in neurons	AG Arrenberg, Institute for System Neuroscience, Tübingen

Male and female zebrafish were kept in the plastic mating tanks overnight separated by a plastic separator, which was removed the next morning within the first 15 minutes at the start of light cycle for zebrafish. The eggs that fall on the bottom of the mating tank through the grid are collected and washed with first tap water, and then were kept in the E3 medium until further use. From 5 dpf onwards larvae were fed with fresh paramecium (cultured in the lab) 20ml/day, and supplemented with red breeze (reefdepot.de), until 20 dpf with 15-20 embryos in a mouse cage. At 20 dpf, the fish were transferred to fresh mouse cages (a maximum of 4 fish/ mouse cage) and were connected to the facility water

for the next 3-4 weeks. In the mouse cages fishes were supplemented with artemia along with finely grinded fish food flakes.

ORA4 -/- fish

ORA 4 -/- fish was generated in our lab using CRISPR/Cas 9 (Liu and Korsching, unpublished). The knockout fish had a frameshift mutation in ORA 4 gene. Mutated sequence is shown below:

```
>AM778166.1 Danio rerio partial mRNA for olfactory receptor class A (V1r-like
homolog) (ora4 gene)
ATGTCTGAGGTCCTGACGGTGGACGCGGTTCTCTTCGGCCTGCTGGTGTTCTCTGGTATCATTGGAAACARiqui
Liu
TCATGGTCATCTATGTGGTGTTTGACTGTGCTAAATTGTGCGCCTCTCGCCACCTGCCGCCGTCTGACAC
CATCCTGGTGCACCTGTGTCTGGCTAACCTGCTGACGTCAGTGTTCCGCACGGTGCCGATCTTCGTGTCG
GACCTGGGCCTGCAGGTGTGGCTGACGGCGGGCTGGTGCCGCGTCTTCATGCTGCTGTGGGTGTGGTGGC
GGGCGGTGGGCTGCTGGGTCACCTTGGCTCTCAGCGCCTTCCACTGCGCCACCCTGCGTCGCCAGCATGT
CTCCATGGGGCCGCTGGGTCACTCGCGGGAGCGTCGCCGCGTCTGGGTCGTCCTGGCGGTGGTGTGGGCT
GCAAACCTGCTGTTCTCGCTGCCGGCGCTGGTCTACACCACACAGGTGCGTGGGAACGCTACCGTGGAGC
TGATGGTGATTAGCTGCACCAC
```

ORA4 (WT): GGGCCTGCAGGTGTGG-CTGACGGCGGGCTGGTGGTGCCGCGTCTT

ORA4 -/-: GGGCCTGCAGGTGTGGGCT----GGCGGGCTGGTGCCGCGTCTT

3.1.3 Bacterial Strains

For transformations and cloning of plasmids the electroporation-competent strain E. *coli* XL1 blue (Agilent Genomics, USA) was used.

The animal handling was approved by the governmental animal care and use office (Landesamt für Natur, umwelt und Verbraucherschutz Nordrhein-Westfalen, Protocol No. 8.87-51.05.20.10.217), and was in accordance with the German Animal Welfare Act as well as with the General Administrative Directive for the execution of the Protection of Animal

3.2 Technical equipment, chemicals, and disposables

3.2.1 Technical equipment

Type	Model	Manufacturer
Cryostat	CM 1900	Leica
Electrophoresis Chamber		Bio-Rad
Electrophoresis Power supply	Power Pac 300 Bio-Rad	Bio-Rad
Fluorescence Microscope	BZ-9000	Keyence
Gel Documentation System	GelDoc XR	Bio-Rad
Halogen Lamp	iLux 150NL	Visitool
Heating Plate	MEDAX	StörkTronic
Incubator (dry)		Memmert
Incubator (wet)	GFL	KMF
Laser Scanning Microscope	LSM 510	Zeiss
Laser Scanning Microscope	SP8	Leica
Microcentrifuge	Micro Star 17	VWR
Microcentrifuge (cooling)	Z233 MK-2	Hermle
Micropipette Puller	P-97	Sutter Instruments
Microwave	900 & Grill	Severin
Peristaltic Pump		Cole-Parmer
pH-Meter	Calimatic 766	Knick
Pipets (10/20/200/1000 µl)	Research Plus	Eppendorf
Precision scale	LA 120 S	Sartorius
Rasberry Pi-Camera Module	Model V2.1	Rasberry

Rotary Mixer	**R1**	**Pelco**

Scale	**Universal**	**Sartorius**
Shaker	**Bio Shaker 3D**	**BIOSAN**
SLR Camera	**D5100**	**Nikon**
Spectrophotometer	**Nanodrop one**	**Thermo Fisher**
Stereomicroscope	**Stemi 2000**	**Zeiss**
Thermal Mixer	**Thermomixer Comfort**	**Eppendorf**
Thermal Cycler	**LifeEco**	**BIOER**
Vortex	**Vortex Genie 2**	**Benden and Hobein AG**

3.3 Chemicals, reagents, and pre-mixed solutions

If not stated otherwise all chemicals were obtained from VWR at molecular biology grade. All chemicals from other sources are listed below:

Description	**Manufacturer /Supplier**
A-Lysine	Sigma
Acetic anhydride	Sigma
BCIP (5-bromo-4-chloro-3-indolyl-phosphate)	Roche
Blocking Reagent	Roche
BSA (Bovine Serum Albumin) ≥ 96%	Sigma
Cadaverine	Sigma-Aldrich
D-Fructose	Applichem
Dimethyl sulfoxide	Sigma
di-Sodium hydrogene phosphate	Merck
EDTA	Sigma
Instant Ocean Sea Salt	Instant Ocean
Low-melting point agarose	Sigma
Methylene Blue	Sigma
MS-222	Sigma-Aldrich
Phenol Red	Fluka

Phenol-Chloroform-Isoamyl alcohol mixture (25:24:1)	Sigma
Phenylthiocarbamide	Sigma
Sheep Serum	Sigma
TAE buffer 50x (Rotiphorese)	Roth
TissueTek cryo-embedding medium	Sakura
Triton X-100	Merck
Tween20	Sigma
Vecta mount permanent mounting medium	Vector Labs
Vecta mount permanent mounting medium (w/ DAPI)	Vector Labs
yeast tRNA	Thermo Fischer Scientific

3.4 Disposables

Plastic and glass beakers, flasks and bottles were autoclaved prior to use

Disposables	Specifications	Manufacturer/Supplier
Borosilicate Capillary	GB100F -10	Science Products
Conical Tubes	15ml, 50ml	Falcon
Coverslips	24×60 mm	VWR
Hypodermic Needles	Sterican	Braun
Laboratory Film		PARAFILM
Latex Gloves	powderfree	VWR
Microcentrifuge Tubes	1.5 ml, 2 ml	Axygen
Microloader Tips	20 µl	Eppendorf
Microscope Slides	Superfrost	VWR
Microscope Slides	Standard	VWR
Pasteur Pipet		VWR
PCR-Tubes		VWR

Petri Dish	Ø 34.5mm, Ø 60mm, 100 mm	VWR
Pipet Tips	10/200/1000 µl	VWR
Pipet Tips with Filter	SurPhob	Biozym
Syringes	2/5/10/20 ml	Braun

3.5 Enzymes and premixed enzymes

Proteinase K	**Roche, CH**
GoTaq Green Mastermix	**Promega, GER**
BsaI	**New England Biolabs**
EcoR1	**New England Biolabs**

3.6 Antibodies

Antibody	**Source**	**Catalogue number**
anti-TrkA (763) antibody	**rabbit IgG; 1:100,** **(Ahuja et al., 2013),** **Santa Cruz Biotechnology**	**#sc-118**
α-p-Erk rabbit IgG, polyclonal	**Cell Signaling Technology, USA**	**#9101**
α-S100 rabbit IgG	**Agilent, former Dako, USA**	**#Z0311**
Alexa Fluor 488 goat α-rabbit IgG	**Invitrogen, GER**	**#A21206**
Alexa Fluor 594 goat α-mouse IgG	**Invitrogen, GER**	**#A11005**

3.7 Media

LB-medium 1 litre	**10g** **10 g** **5 g** **pH to 7.5**	**NaCl** **Tryptone** **yeast extract** **NaOH**
Ampicillin	**stock solution** **100mg/ml**	**Working concentration** **100 µg/ml**
Kanamycin	**50mg/ml**	**50 µg/ml**

3.8 Buffers and solution

60x E3 solution (Stock Concentration)	**34.8 g** **1.6 g** **5.8 g** **9.78 g**	**NaCl** **KCl** **CaCl2·2H2O** **MgCl2·6H2O**
1x PBS (Tween /Triton)	**137 mm** **2.7 mm** **10 mm** **1.8 mm** **(0,1% v/v** **(0,1% v/v** **pH 7.3**	**NaCl** **KCl** **Na2HPO4** **KH2PO4** **Triton X100)** **Tween20)** **with NaOH**
Paraformaldehyde	**1x** **4% w/v**	**PBS** **Paraformaldehyde**
Primary antibody solution	**1x** **1,5% w/v** **5% v/v**	**PBS-Triton** **BSA** **Sheep Serum**

DNA extraction buffer	**100 mm** **100 mm** **250 mm** **1% w/v** **200 µg/ml**	**Tris-HCl** **EDTA** **NaCl** **SDS** **Proteinase K**
“Quick” DNA extraction buffer	**10 mm** **2 mm** **0,2% w/v** **200 µg/ml**	**Tris-HCl** **EDTA** **Triton X100** **Proteinase K**

3.9 Kits

The following Kits were used according to instruction manual

Name	Manufacturer
NucleoSpin® Plasmid	**Macherey-Nagel, GER**
NucleoSpin® Gel and PCR Clean-up	**Macherey-Nagel, GER**

3.10 Molecular Biology Techniques

3.10.1 DNA extraction from embryos or tissue by phenol/chloroform method

To get DNA from tissue in larger amounts this method is used

The embryo/tissue is lysed in 30 µl of DNA extraction buffer freshly added with 200 ng/µl Proteinase K. Tissue lyses was done either by mechanically with a pestle or mortar or by shaking the tissue in a thermomixer at 700 rpm and 56 °C for a maximum of 1 hour. 70 µl of extraction buffer was added and it was mixed by inverting the tissue several times. 50µl of phenol/chloroform/iso-amylalcohol (25:24:1) was added to the mixture and the tube was inverted several times. Spinning of tube was done on a bench top spinner for 5 minutes at 13,000 g the aqueous phase carefully collected and transferred into a new tube. The DNA was pelleted by spinning for 5-8 minutes at high speed at the tabletop spinner. The supernatant was discarded, and the tubes were left to dry at room temperature for few minutes. The pellet was dried was washed with 200 µl 80% ethanol and centrifuged again. After drying the pellet, it was re-suspended in 20-50 µl 10 mm Tris-HCl pH 8. The DNA concentration was measured and determined with a NanoDrop™ Photometer.

3.10.2 “Quick” genomic DNA preparation for PCR

This protocol was used as a relatively quicker method than phenol/chloroform to screen larger amounts of embryos/tissue for genotyping by PCR. After obtaining the tissues from tissue biopsy it was incubated in the DNA extraction buffer at 56°C for 2-3 hours (if required overnight) on a thermomixer. The tubes were then centrifuged for 30s at 11,000 g to pellet the tissue after being digested. 10µlof supernatant was used for PCR reactions. DNA samples were stored at -20 °C until further use.

3.10.3 DNA amplification by using polymerase chain reaction

Polymerase chain reaction (PCR) is used for the amplification of DNA templates using appropriate forward and reverse primers. Primers were designed using primer 3 tool (http://primer3.ut.ee/). 10-100 ng of DNA was used as a template for PCR reactions.

The standard protocol was followed for amplifying the DNA templates: -

Initial denaturation	**95 °C, for 3 minutes**
denaturation	95 °C, 45 s
primer annealing	51-58 °C, 45 s 35 x
extension	72°C, 30-90 s
final extension	72°C, 5 minutes
end	4°C, ∞

The annealing temperature was calculated by using an online tool Tm-calculator, provided by Thermo Fischer website. The typical temperature that is used for annealing is 55°C, which can have a different range depending upon the GC contents of oligonucleotides .The length of the elongation was for 5 minutes at 72°C which can also vary depending on the length of the fragment which is being amplified. Taq-based polymerases generally process around 1 kb/min.

3.10.4 DNA sequencing

DNA sequencing was used to check for the sequence of amplified PCR product. DNA sequencing was conducted using Eurofins Genomics (Germany) sequencing services. PCR samples were purified using PCR purification kit from Machery Nagel. Samples were prepared as instructed by sequencing service and usually contained 10-50 ng/µl template DNA which was either a purified PCR product, plasmid, or genomic DNA. Either forward or reverse primer (2,5 µM), 10-20µl was added with DNA sample. Results were analysed using the GATC viewer and/or NCBI blast, where sequence alignments were analysed

3.11 Histological Methods

3.11.1 Anti-TrkA labelling for crypt neuron in zebrafish larvae whole mounts

Anti-TrkA antibody has been reported as a sensitive marker for crypt neurons (Ahuja et al., 2013). To check for the presence of crypt neurons in ORA4-/- embryos, healthy fertilized eggs were collected and kept at 28°C in E3 medium until day 5 post fertilization. On day 5 embryos were collected and transferred to 4%PFA for one hour (short fixation). Following fixation, embryos were washed thoroughly with 1X PBST, (3 times for 20 minutes each), and treated with 150 mM Tris pH 9.0, for 5 minutes at room temperature. Embryos in Eppendorf tubes were then heated at 70°C for 15 minutes and allowed to cool for the next 20 minutes. Embryos were washed with 1X PBST, (3 times for 20 minutes each). Blocking solution (5% sheep serum/normal goat serum in 1X PBST), was added and embryos were kept in incubation for 1 hour at room temperature. Anti-TrkA antibody rabbit polyclonal IgG (Santa Cruz Biotechnology) 1:400 was added to the embryos and left for overnight incubation at 4°C.

The next day embryos were again given washes with 1X PBST, (3 times for 20 minutes each). Secondary antibody Alexa-conjugated-498 donkey anti-rabbit IgG (1:400) in blocking solution was added and left for overnight incubation at 4°C.

Microscopy

On the following day embryos were given several washes with PBST and embedded in 0.8% low gelling agarose for microcopy with Zeiss LSM confocal microscope.

3.11.2 Anti-TrkA labelling for crypt neurons in adult zebrafish OE (WT/ ORA 4-/-)

The protocol followed has been described by Ahuja et al. (2013)

Adult wild type and ORA 4-/- fish were to cold anesthetized on ice, and after de-capitation the heads were transferred to 4% PFA and for 15-20 minutes (short fixation). Dorsal cranium was further removed, and olfactory epithelium was carefully dissected out and transferred to Tissue Tek (Sakura). Tissue Tek was frozen at -80 degrees for few minutes. 20µm sections were cut using a cryostat and picked on a slide and left for drying for 15 minutes. After drying, slides were transferred to 100% acetone maintained at -20°C for 15 minutes. Slides were then washed in a glass jar filled with PBST (3 times 10 minutes each) at room temperature. Blocking solution (0.5% in PBS) was added to the slides and left for incubation for one hour at room temperature in a moist chamber. Anti-TrkA rabbit polyclonal (Santa Cruz Biotechnology) (1:1000 dilution), around 100µl was added to the slides and incubated overnight in a moist chamber at 4°C. The next day slides were washed with PBST again (3 times for 10 minutes each) and secondary antibody in PBST (goat anti-rabbit IgG, Alexa conjugated-498, 1:200 dilution), was added to the slides. Slides were kept in incubation for 2 hours in a moist chamber. The slides were then washed with PBST (3 minutes each 3 times) and mounted with Vecta sheild with DAPI for microscopy.

3.11.3 Labelling of the crypt neuron glomerulus by Anti-TrkA antibody

It has been reported that the single mediodorsal glomerulus mdg2, is also labelled by Anti-TrkA antibody (Ahuja et al., 2013). So, I decided to use the same antibody to locate the glomeruli in the olfactory bulb of ORA 4 -/- adult zebrafish.

3.11.4 Cryosectioning of the olfactory bulb

WT and ORA 4 -/- fish were cold anesthetized and decapitated and transferred to 4% PFA at 4°C for an overnight fixation. The next morning heads were given a gentle wash in PBST to remove the excess PFA. Dorsal cranium was removed, and exposed olfactory bulbs along with telencephalon was dissected out and transferred to Tissue Tek (Sakura) and frozen. 10 um coronal section were thawed mounted on Super-frost plus glass slides (Thermo). Slides were left to dry for 15 minutes and then incubated in acetone at -20°C

for next15 minutes, washed several times with PBST and blocked with 5% Normal Goat Serum in PBST for one hour at room temperature. After blocking, slides were incubated with two separate antibodies (Zns2, mouse monoclonal IgG Oregon), 1:1000 dilution in blocking solution for labeling all the glomeruli, and Anti-TrkA rabbit polyclonal IgG (1:1000) dilution in the blocking solution for labelling the mdg2 cluster, and kept for overnight incubation in a moist chamber. The next day slides were given several washes with PBST and incubated with secondary antibodies for two hours at room temperature. Slides were then washed with PBST and mounted with Vecta sheild with DAPI and observed under fluorescence microscope

3.11.5 Whole mount p-Erk staining for olfactory bulb

Protocol followed has been described in Dieris et al., 2017

Both WT and the ORA 4 -/- fish were given a 3-minute exposure to the stimulant. After 3 minutes fish were transferred to ice for cold anesthetization. Once anesthetized, fish head were removed, and transferred to 4% PFA and further kept at 4°C for overnight incubation.

Following overnight incubation, next day dorsal cranium was dissected, and brain tissue was taken out and washed several times in PBST to remove excess PFA and transferred to −20 °C methanol for overnight incubation.

Following incubation, the next day brains were re-hydrated in a dilution series of 75%, 50%, 25% methanol in PBST (5 min each). After rehydration they were washed again in PBST. Blocking solution was then added containing 10% calf serum/1% DMSO in PBST for 1 h. Samples were then incubated with primary antibody α-p-Erk (1:50 in blocking solution) at 4 °C for 5–7 days on a vertical rotator (~12 rpm).

Following several PBST washes, incubation with secondary antibody (1:200 in blocking solution) was performed and samples were left to incubate at 4 °C for 3 days. After three days brain tissues were again washed several times in PBST and then a fructose gradient series was used to clear the tissue (20%, 40%, 60%, 80%, and 100%) fructose in PBS (w/v) on a vertical rotator at room temperature for 4 h or at 4 °C overnight.

3.11.6 Anti-TrkA Labelling of medio dorsal glomeruli in the olfactory bulb in zebrafish embryo

The protocol for staining was first described by Braubach et al., 2013

5-6 larvae at 9 dpf AB/TU Zebrafish larvae were anesthetized by dipping them in ice cold water maintained at 4 degree centigrade. Larvae were then transferred to 2% PFA in PBS maintained at 4 degrees centigrade and left overnight at 4 degrees centigrade for fixation in 1.5 ml Eppendorf tubes.

Next day PFA was carefully removed from the Eppendorf tubes. The larvae were washed with PBST 3 times for 20 minutes each at room temperature. Larvae were then left for incubation in PBS-based blocking solution containing 0.25% v/v Triton X-100, 2% v/v dimethyl sulfoxide, 1% v/v normal goat serum and 1% w/v bovine serum albumin, in PBS for 48 hours.

After 2 days embryos were incubated with primary antibody Anti-TrkA (1:100, Rabbit IgG,Sigma) in blocking solution for 4 days. After 4 days, blocking solution containing primary antibody was removed and embryos were washed thoroughly with PBST 5 times for 20 minutes at room temperature. Further, larvae were incubated with secondary antibody (Alexa Fluor 488 goat α-rabbit IgG (1:50), Invitrogen) in PBST for 3 days. After 3 days, secondary antibody was washed thoroughly by giving PBST washes 5 washes for 20 minutes.

Glycerol clearing

After PBST washing larvae were incubated for 24 hours in a 3:1 solution of glycerol with 0.1 M Tris buffer pH 8.0, containing 2% (w/v) n-propyl gallate (Sigma).

Sample preparation

Larvae were carefully transferred to another eppendorf tube and immersed for one hour in 99% percent glycerol in A drop of 99 % glycerol was placed on the microscopic glass slide and embryo was added to it, aligned under the light microscope in dorso-lateral position.

Microscopy

Leica Sp8 confocal microscope was used for taking the confocal stacks. 20x water immersion objective was used for taking confocal stacks. Once the position of embryo was aligned under objective, He-Ne laser was switched on and a zoom factor of 1.50 was selected from the control panel located at the graphic user interface.

Anti-TrkA staining was identified as the bright green fluorescence against light green background. Optical section of 0.88µm were taken covering a maximum depth of 108 um dorso-ventrally. Confocal stacks were processed using the Image J software, and maximum projections of the confocal stacks was obtained for the final visualization of the olfactory bulb.

3.12 Calcium Imaging using Zebrafish larvae

Sample Preparation

9 dpf larvae were used for the imaging experiments. *elavl3*: GCaMP6s larva were anesthetized using 0.01% MS-222. The larva was carefully observed for 2 minutes, and when movement completely seized, the animal was picked up and embedded in 1.2% low gelling agarose on a sylgard plate. Agarose was carefully removed from the mouth of the animal so that stimulus could reach to the mouth of the animal. The animal was dipped in E3 medium and transferred to the microscope.

Microscopy

Leica Sp8 Confocal microscope at the imaging facility at the University of Koln was used for the microscopy. Sylgard plate containing the larva was placed on the stage of the microscope. 20x water immersion lens was used for the microscopy. A flow of 7.5 ml/minute of E3 medium was maintained throughout the experiment. 30µlof stimulus was added with a difference of at least 40 s between two intermittent stimuli.

Imaging movies were further analyzed by using Fiji and custom written scripts using MATLAB.

Stimulus application If not stated otherwise 10mM Tris pH 7.00 was used as neutral pH and 10mM Tris pH 8.60 was used as alkaline pH for calcium Imaging experiments. Cadaverine was used at a concentration of 100µM for all experiments.

4. Results

4.1 Crypt neurons survive in ORA4-/- background and maintain their target glomerulus

Crypt neurons containing ORA 4 receptor project their axons to medio-dorsal glomerulus 2 (mdg 2), (Ahuja et al., 2013). We wanted to check whether crypt neurons survive in the absence of ORA 4 receptor. ORA4 -/- was generated our lab using CRISPR/Cas9 methodology (Lui and Korsching, unpublished). Anti-TrkA antibody has been reported as specific marker for crypt neurons (Ahuja et al., 2013). On performing immuno-histochemistry on the olfactory epithelium of ORA 4 -/- adult fish (see material and methods /histological methods) it was observed that crypt neurons survive in ORA4 -/- background.

Olfactory bulb was removed and sectioned, Anti-TrkA staining was performed on the 10µm sections of olfactory bulb and it was observed that crypt neurons also maintain their target glomerulus (mdg2) in ORA4-/- (Figure12, 2nd last panel from below).

5 dpf larval zebrafish (WT and ORA4-/-) were stained using Anti-TrkA antibody, and at 5 dpf crypt neurons were observed in WT as well as in ORA4-/- fish. This data indicates that that loss of ORA4 receptor has no effect on the survival of crypt neurons, in adult as well as larval zebrafish. `

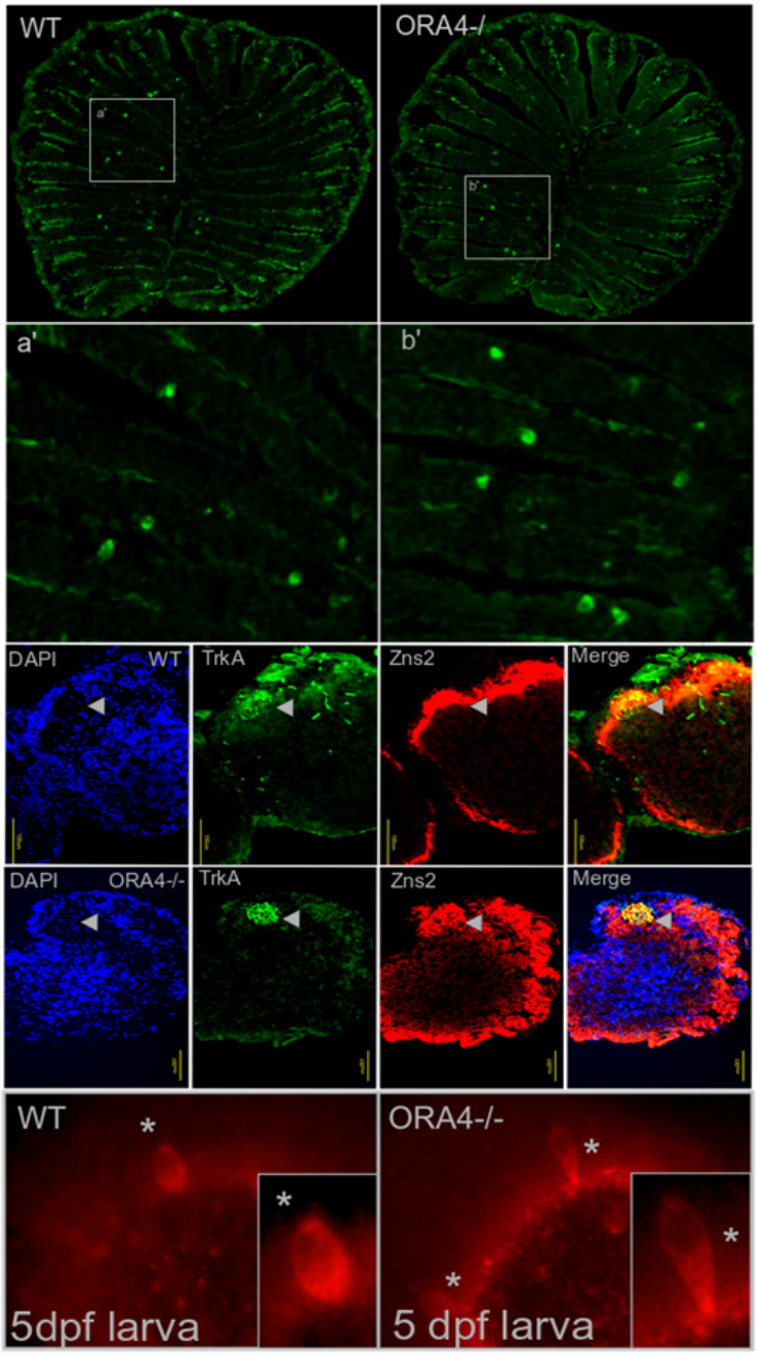

Figure 12: Crypt neurons survive in ORA4-/- background and maintain their target glomerulus Anti TrkA staining in wild type and ORA4-/- adult zebrafish (topmost panel). Magnified view of the selected are below. Crypt neurons maintain their target glomerulus (middle panel). Anti-TrkA staining in zebrafish larvae (WT vs ORA4-/-) bottom panel.

4.2 Changes in crypt neuron abundance and morphology in the ORA4 knockout

After staining with Anti-TrkA antibody diameter ratios of crypt neurons (width/height) were measured for 6 dpf larval zebrafish (WT and ORA4-/-). On plotting the ECDF (Empirical Cumulative Distribution Function) for diameter ratios, no significant difference was observed (Figure 13, Panel A), indicating in larvae crypt neurons tend to maintain their globular morphology

Blind evaluation was done for the diameter ratios of crypt neurons stained with Anti-TrkA antibody in adult zebrafish (WT vs ORA4-/-). A significant difference in ECDF of diameter ratio was observed (**p=0.0019, KS test), between WT and ORA4 -/- indicating that the absence of ORA 4 receptor affects the morphology of the crypt neurons in adult zebrafish. Crypt neurons were significantly slender in ORA4-/-, Figure 13, Panel B.

In larval zebrafish crypt neurons were stained with Anti-TrKA antibody for 3 ,4 5, and 6 dpf, in WT and ORA4-/-. Significantly more number of crypt neurons were seen at 6 dpf in ORA4-/- larval zebrafish (**p=0.0048), Figure 13 Panel C. In adult zebrafish olfactory epithelium, again more number of crypt neurons were observed/section in ORA4-/- zebrafish as compared to WT (**p<0.001), Figure 13 Panel D

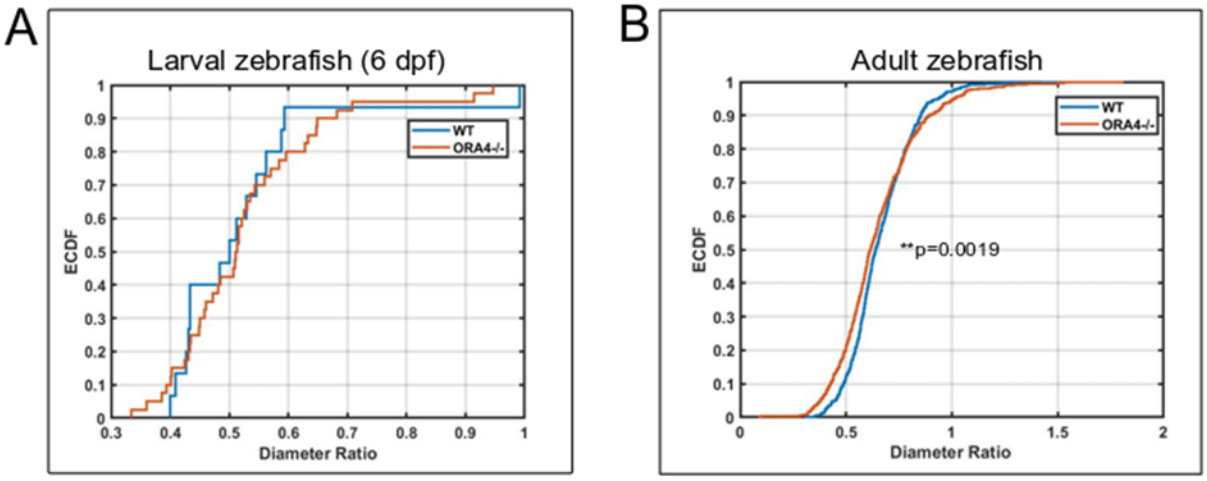

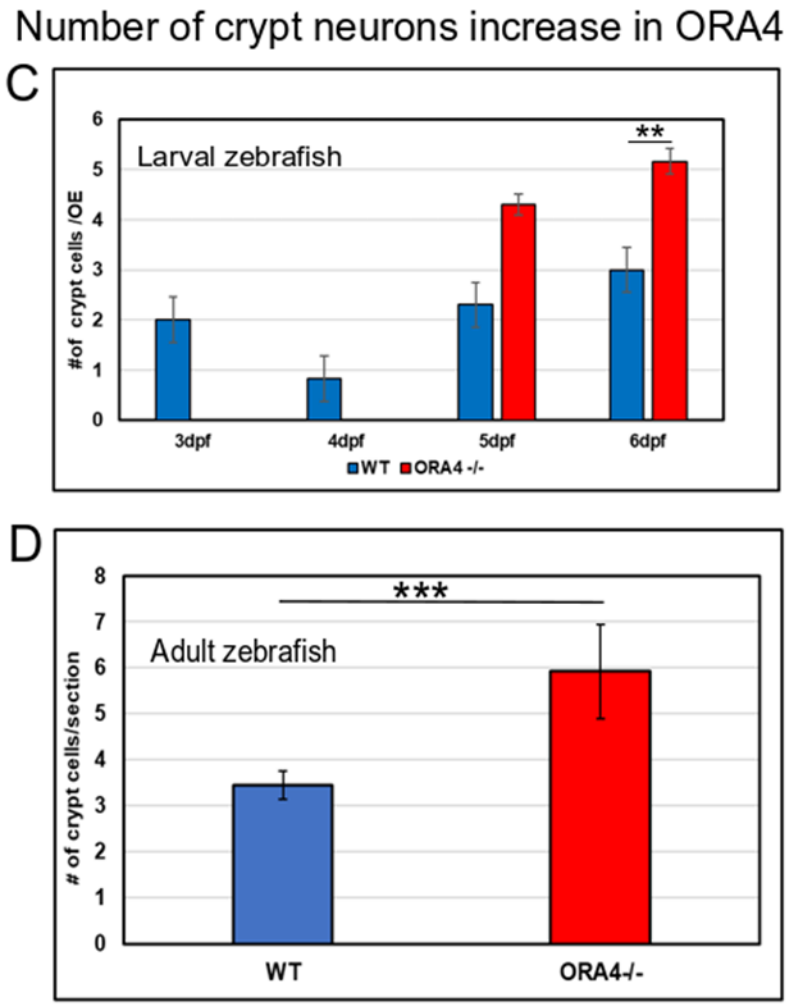

Figure Legend on next page

Figure 13: Changes in crypt neuron abundance and morphology in the ORA4 knockout. Panels A and B show the distribution of diameter ratios (cell width/height) for larval (panel A) and adult (panel B) zebrafish in WT and ORA4-/-, given as ECDF (empirical cumulative distribution function). No significant difference was observed for larval zebrafish, but in adult zebrafish crypt neurons of the knockout fish were significantly more slender (**p=0.0019). Panels C and D show number of crypt neurons in zebrafish larvae (Panel C, 3, 4, 5 and 6dpf) and adult zebrafish (panel D). Significantly more crypt neurons were seen in the knockout compared to wildtype (** p=0.0048 for 6dpf larvae), and (***p<0.001 for sections of adult olfactory epithelium, blind evaluation).

4.3 Anti-TrkA labelling for medio-dorsal cluster 2 (mdg2) in larval zebrafish

9 dpf and 12 dpf embryo (WT and *elavl3*::GCaMP6s) were stained with Anti-TrkA antibody. Crypt neurons and mediodorsal cluster (mdg2) was labelled as shown in the Figure14 (top, middle, and bottom panel).

After staining, optical sections of olfactory bulb 0.88µm in depth were obtained dorso-ventrally for both WT and *elavl3*::GCaMP6s larva covering a total of approximately 108 µm. In the olfactory bulb, Anti-TrKA staining was observed in the first 10 optical sections dorso-ventrally, covering a total depth of 8-10µM in both WT and elavl*3*::GCaMP6s strain see Figure 14.

Hence, while performing calcium imaging experiments, the dorsal surface of the olfactory bulb was kept in focus keeping medio-dorsal cluster 2 in the field of view.

Additionally, 0.88µm deep optical sections of olfactory bulb for 9 dpf live head strained elavl*3*::GCaMP6s larvae were also obtained.

On carefully examining these stacks of WT 9 dpf Anti-Trka stained larvae with the stacks of *elavl3*:: GCaMP6s 9 dpf live head strained larva, it was found that location of medio-dorsal cluster co-indices with the location of fibers of pallial commissure which can be seen in live *elavl3*:: GCaMP6s larvae but disappear on staining, see Figure 14 and 26 B.

Fibers of pallial commissure are among the major fiber tracks appearing at 48hpf in zebrafish larvae (Abraham et al., 2008), and connecting the two olfactory bulbs. The fiber bundle is visible in a live 9 dpf *elavl3*::GCaMP6s larva, which additionally served as an anatomical marker for locating medio-dorsal cluster in live *elavl3*::GCaMP6s larvae while performing calcium imaging experiments.

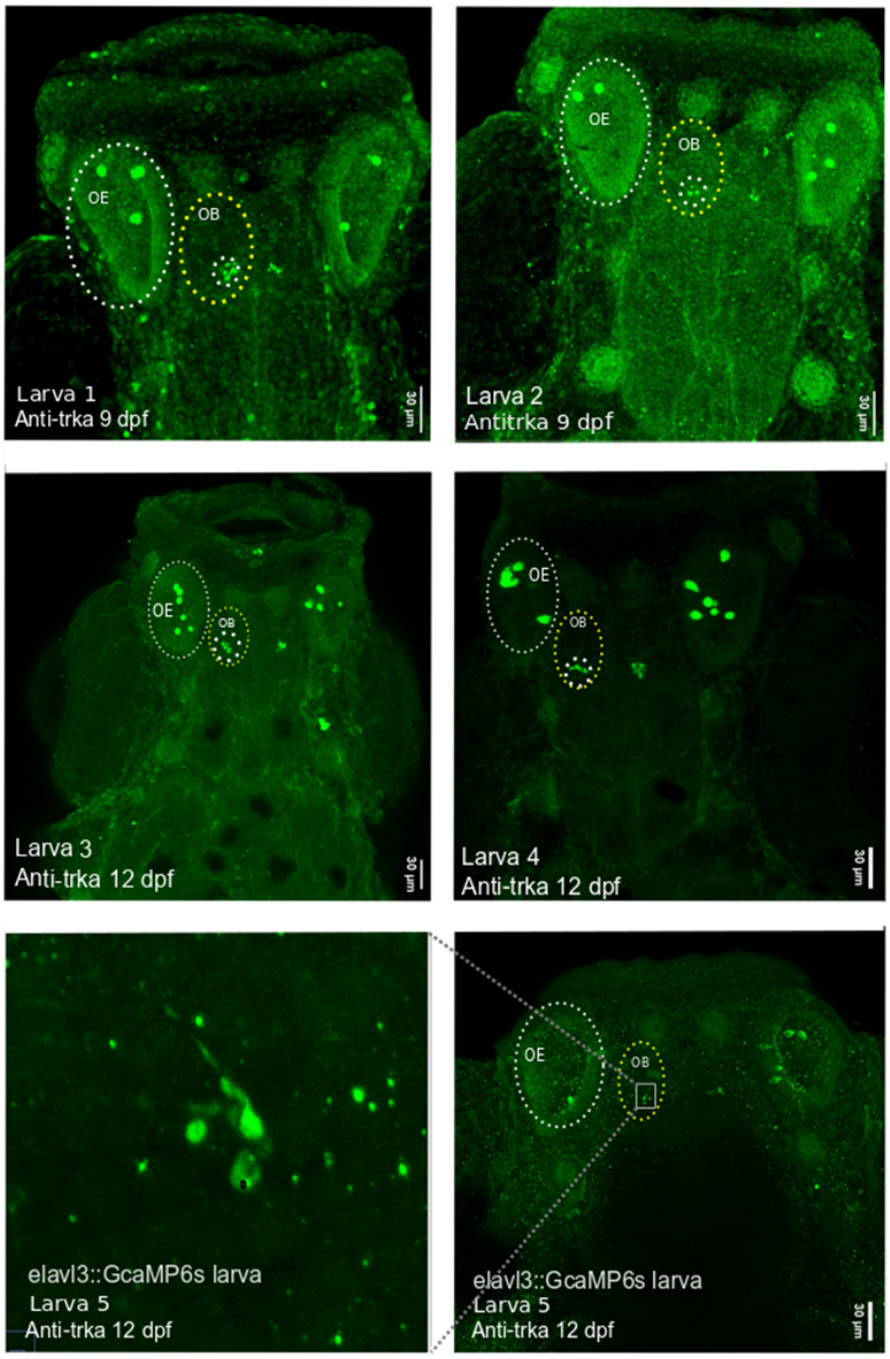

Figure 14: **Anti-TrkA labelling for medio-dorsal cluster 2 (mdg2) in larval zebrafish.** Crypt neurons are labelled in green against a faint background. Projections from crypt neurons are also labelled in green and could be seen on the dorsal surface of olfactory bulb both in 9 and 12 dpf WT larvae. In the bottom panel a magnified image of medio-dorsal cluster (mdg) can be seen

4.4 Multilane setup for larval behavior

9 dpf larvae were kept in the behavior room overnight, so that they are acclimatized to the environment of the room. All behavioral experiment was performed in between 9 am until 4 pm., as it was observed that larvae were active during this span of time (data not shown)

The testing setup consisted of a 20 cm long and 21 cm wide apparatus divided into 16 lanes of 1.5 cm each. Each lane was filled with 10 ml of E3 medium, and 100µl of stimulus was added at one end and E3 at other end of the lane. Each lane was further divided into 10 segments of 2 cm each, to mark the position of larvae while swimming. Each segment was given a score depending on their position from the point of stimulus introduction. The segment at the point of stimulation was assigned a position index of 100 and the segment farthest away was assigned position index of 0.

Before testing, embryos were starved for 3 hours exactly 2 hours in the petri dish and for one hour in the elongated tanks) so that they are motivated to move in the behavior setup. After an hour, the embryos were relaxed until they displayed normal swimming behavior.

100 µl of E3 medium was used as a negative control. Food odor was prepared by mixing 40 mg of food odor in 100 ml of E3 medium, incubated on a rotor for one hour and filtered.

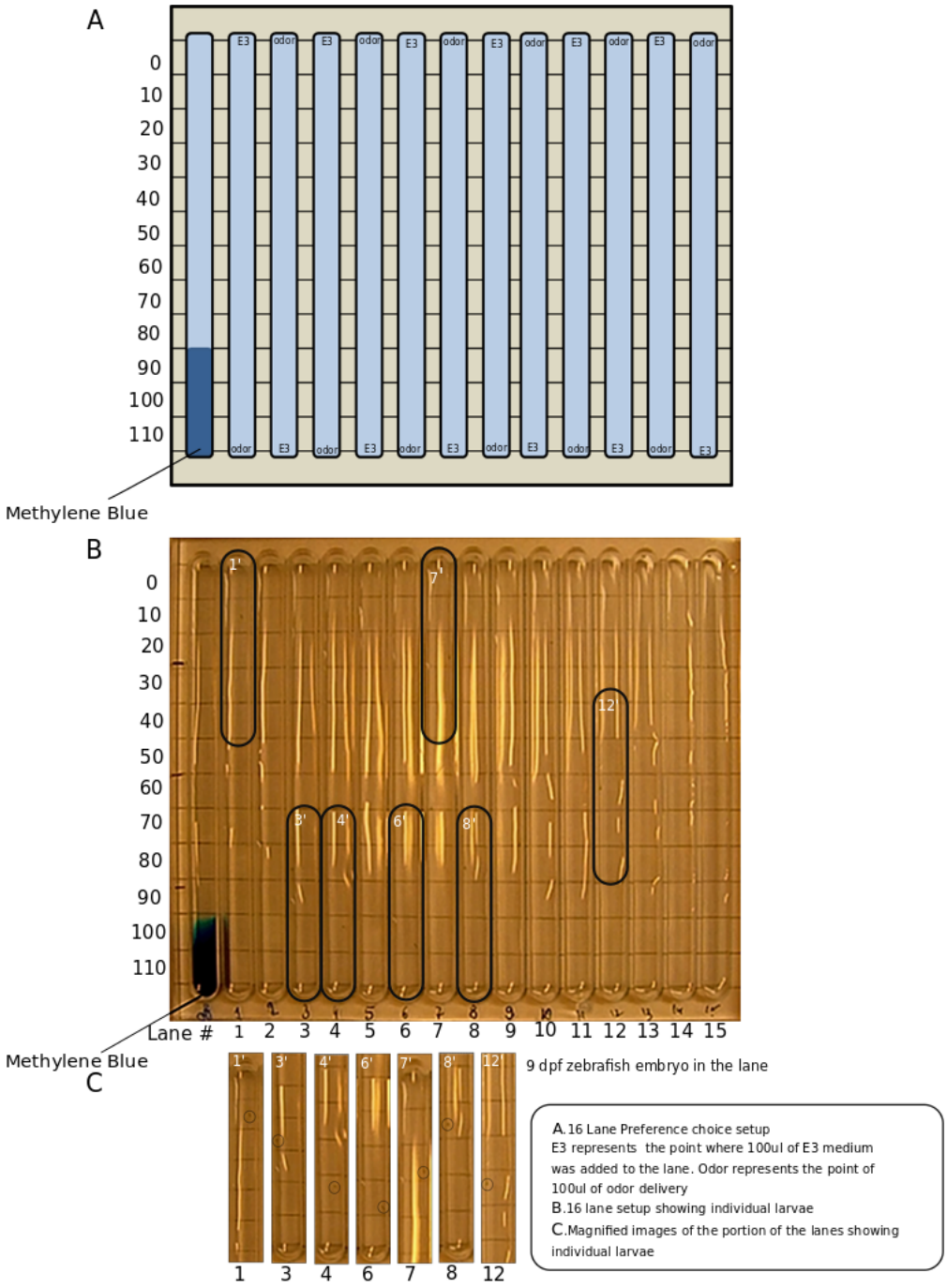

Figure15: Multilane setup for behavioral analysis of zebrafish larvae.

4.5 Larval Zebrafish response to food odor

9 dpf zebrafish were used for this experiment. The night before larvae were transferred from the fish room and kept at the behavior room maintained at 37 degrees for overnight acclimatization. In the morning at fresh food odor was prepared by dissolving the 0.4g/L of baby food in E3 medium and incubating it on a magnetic stirrer of an hour. After an hour, the solution was filtered using a standard filter paper to remove the undissolved particles and filtered solution was collected in a glass beaker.

Simultaneously, overnight acclimatized embryos were given the food odor in a petri dish for 15 minutes, after that larvae were removed from petri dish and transferred into the fresh petri dish containing E3 medium. 4-5 larvae were kept in a single petri dish. The larvae were left for starving for a total of 3 hours (2 hours in the petri dish and 1 hour in the lanes of multi-lane setup).

After 3 hours of incubation larvae were given 100 µl of the stimulus on one end of the multi-lane setup. The setup was divided into compartments 12 compartments 2 cm each to identify the position of larvae in any given frame of time. Each compartment was given a position index between 0 to 110. For evaluation, the position of E3 was designated as 0 and position of the stimulus being tested against E3 was designated as 110. If the larvae displayed attraction/preference for a given stimulus they would spend most of their time towards higher position index. If the animals are aversive for a stimulus, they would run away from it and spend much of their time towards the values of lower position index. Animals were recorded for a total of 20 minutes, 10 minutes pre-stimulus and 10 minutes of post-stimulus phase. At the start of post-stimulus phase 100 µl of E3 medium was given at the position index 0, and 100 µl of food odor was given at the position index of 110 and recorded for 10 minutes.

For evaluation, the video was stopped every 30s and the position index of the larvae in each lane was noted down. Hence each larva consisted of 40 data points consisting of 20 points pre-stimulus and 20 points post-stimulus. The data was further evaluated using

custom written scripts and position index of the larvae was calculated using scripts provided by Malvina Kuschmann, a masters student in the lab.

In the Figure 16 each larva is indicated by a single graph. The first graph shows position index of the larvae. Blue line indicates the position index of the larvae before and after the stimulus. The food stimulus was always given at the value 110, and hence it can be seen that the larva 2, 6, 7, 8, and 12 the position index values get shifted towards the food odor source. In the larvae 3, 4, 5 and 11 no major shift towards the food odor source was observed.

The next graph is the Empirical cumulative distribution function (ECDF). The blue curve in the graph indicates the position index in the pre-stimulus phase while the orange curve indicates the position index in the posts-stimulus phase.

When the orange and the blue ECDF curves are further away from each other indicates a difference in the position index before and after the stimulus. If the position index pre and post stimulus are remarkably similar, then there would no major difference in the pattern of curves i.e. they would overlap each other indicative of no effect of the stimulus on the larvae. When 100 µl of E3 and food odor was administered at opposite ends of each lane it can be observed from the ECDF graphs that larvae 1, 2, 6, 7, 8 and 9 showed strong preference for food odor. It needs to be noted that statistical tests for individual larvae were not performed. Larva 4 was aversive as it spent much of its time away from the food odor in post stimulus phase and larva 10 did not move much from the position index of 110 during experiment. Larva 5 and Larva 12 only showed slight preference for the food odor as indicated by the ECDF post stimulus curves. Overall, 6 out of 12 larvae showed strong preference for the food odor, which 2 of them displayed a slight preference for food odor (see also Figure19)

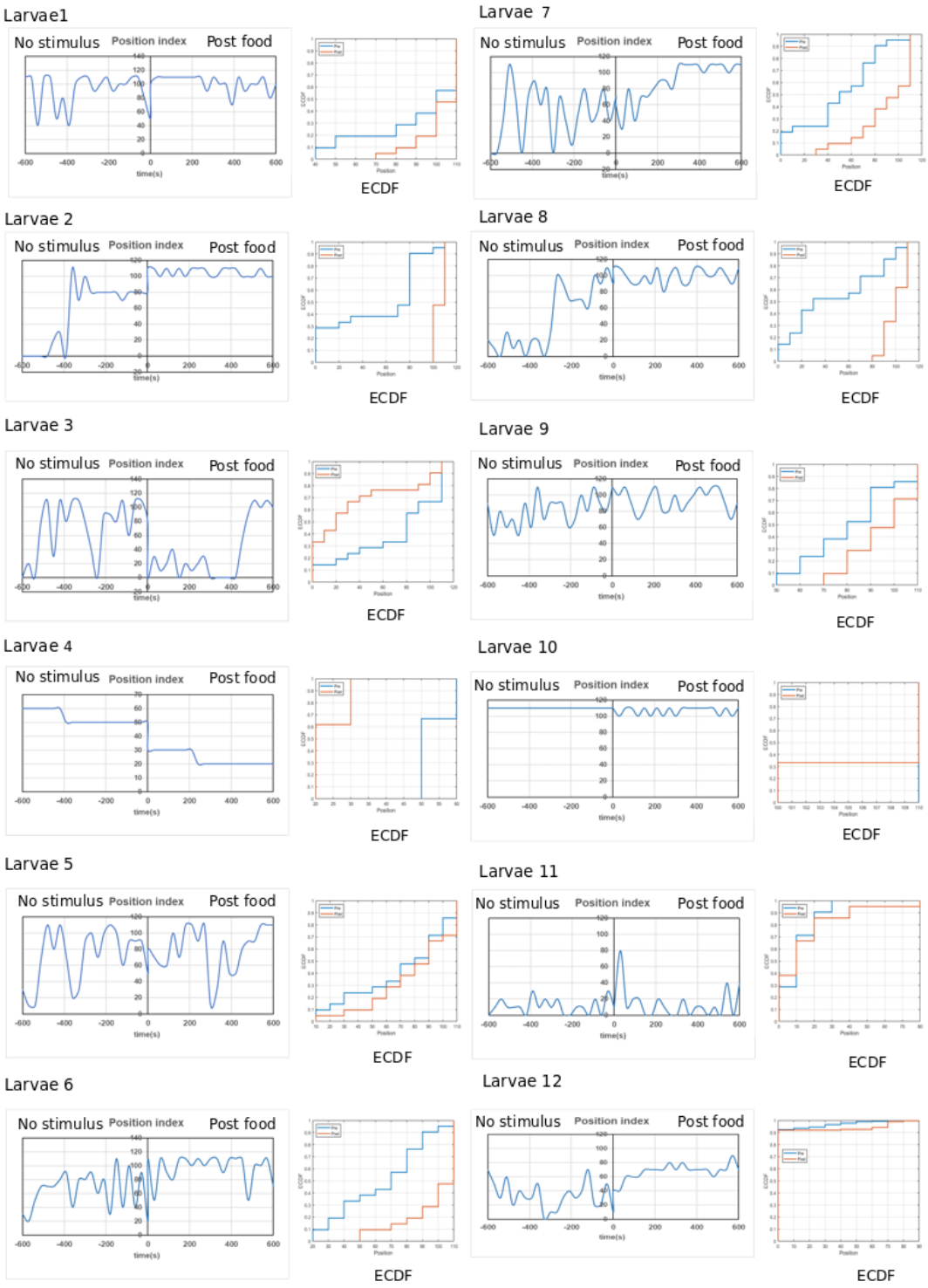

Figure 16: Position index of individual larvae pre and post stimulus of food odor. Food odor is introduced at timepoint 0 on y axis. Graph on the right-hand side indicate position index of the larvae 10 minutes (600s) pre stimulus and 10 minutes (600s) post stimulus. ECDF graphs to the right indicates the change in the position index pre and post stimulus

4.6 Larval zebrafish response to alkaline pH

The experimental conditions were similar as for testing alkaline pH as they were for the food odor. Larvae were brought into the behavior room on the evening before the experiment was to be performed. Larvae were fed in the evening with baby food and left overnight. The next morning, they were fed again for 15 minutes with freshly prepared baby food extract as described earlier. Then taken out from the food source and starved for 3 hours as described earlier.

100 µl of E3 medium was always given at the position 0 while 100 µl of Tris was given always given at the position 110. Larvae behavior was recoded for 20 minutes, 10 minutes pre stimulus and 10 minutes post stimulus. The first graph in Figure17 describes the position index of the larvae before and after stimulus

Larvae 6 and Larvae 9 displayed a strong preference to alkaline pH. As indicated by the graph of their position index they tend to spend time closer to the alkaline pH in the post stimulus phase. The effect can be easily seen in the pre and post stimulus ECDF of the same animals. The post stimulus ECDF graph of both animals displays strong preference for alkaline pH, as they get shifted towards the values of higher position index.

Larvae 2, larvae 5 and larvae 11 displayed only a slight preference for the alkaline pH. These three animals seemed to be oscillating between the segments of E3 and alkaline pH. Larva 1, 3, 8 and 10 showed no preference for alkaline pH, as it can be easily seen in position index graph of larvae 8 it did not display a preference for any of the stimuli presented, hence the ECDF post and pre stimulus graphs are overlapping with each other.

However, some of the larvae displayed aversion to alkaline. This can be easily seen from the position index graphs (Figure17) of larvae 4, larvae 7 and larvae 12. Larvae 12 displays a clear aversion from alkaline pH, as it moves away from the odor stimulus source in the post stimulus phase of the experiment. ECDF graph of the same animal shows a clear aversion as it can be seen position index is shifted away from the alkaline stimulus source. Larva7, also moves away from the alkaline stimulus source, and it can also be interpreted from the data that it shows some preference for E3 medium.

Whereas, larvae 4 displays only a slight aversion for the alkaline stimulus source. Overall, at an individual level 16% of the larvae (2/12) displayed a strong preference for alkaline pH, 40% (4/12), displayed a slight preference for alkaline pH where as 25% (3/12), displayed an aversion to alkaline pH. When the data was pooled a preference for alkaline pH was observed (see also Figure19)

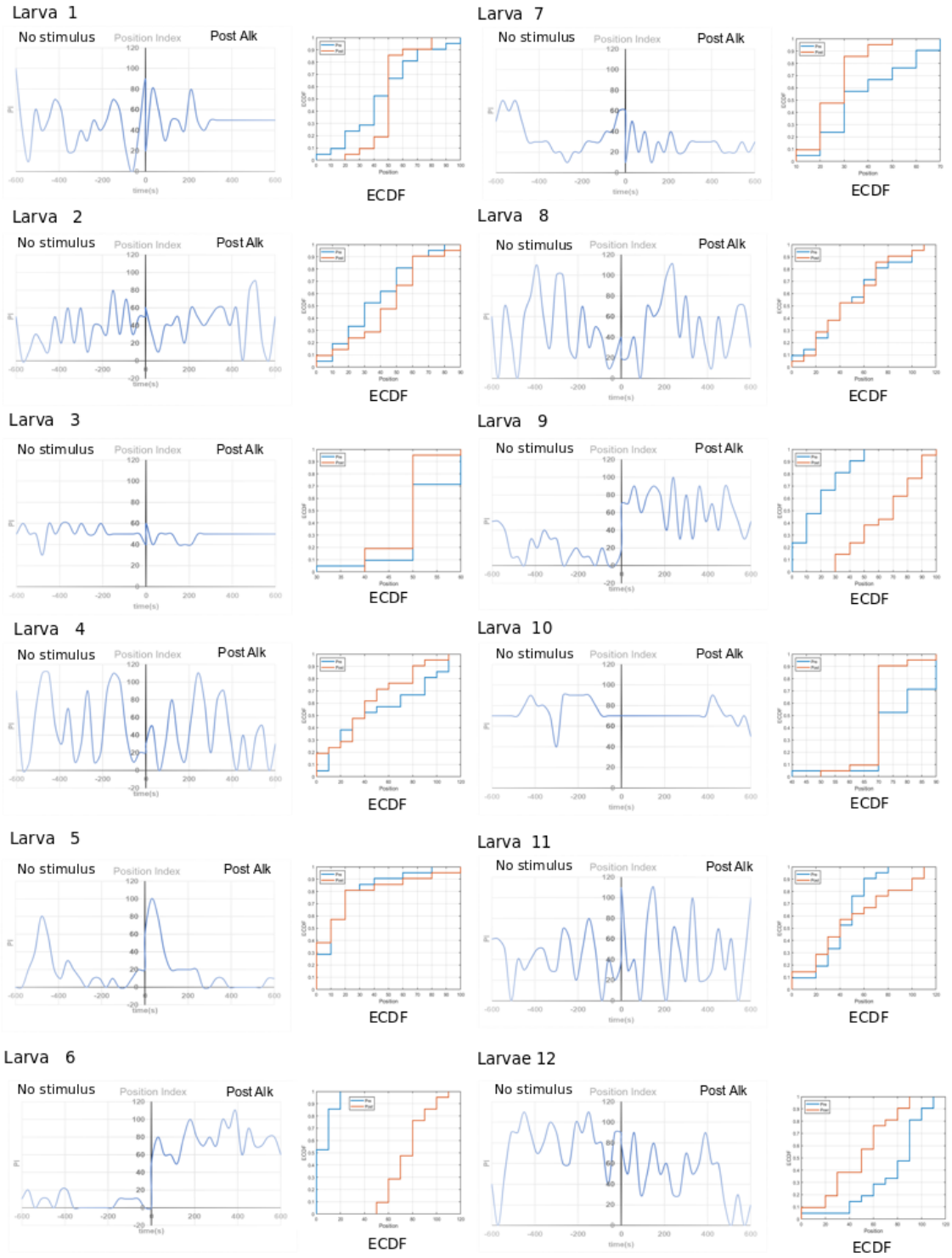

Figure 17: Larval zebrafish response to alkaline pH. Position index of individual larvae pre and post stimulus of alkaline pH introduced at time point 0. Graph on the right-hand side indicate position index of the larvae 10 minutes (600s) pre stimulus and 10 minutes (600s) post stimulus. ECDF graphs to the right indicates the change in the position index pre and post stimulus

4.7 Larval zebrafish response to neutral pH

Neutral pH of 7.00 buffered with Tris was used as a negative control to check the effect of neutral pH on 9 dpf zebrafish larvae behavior. Larva were carried from the fish facility and kept in the behavior room for overnight acclimatization maintained at 37 degrees. The next morning larvae were fed with food odor extract prepared as described earlier for 15 minutes and transferred into different petri dishes, 3-4 larvae per dish. Larvae were starved for 2 hours in the petri dish and 1 hour in the multi-lane setup. Recordings were done for 20 minutes, 10 minutes of pre-stimulus and for 10 minutes in the post-stimulus phase.

The experimental conditions with respect to lighting in the behavior and timing of the experiment were kept the same as they were for food odor and alkaline pH. All the behavior experiments were performed between 9.00 am in the morning until 4.00 pm in the evening. Throughout the experiment the temperature of the multi-lane setup was kept at 37 degrees.

A total number of 11 larvae were tested to check where whether they have any preference for neutral pH. Concluding from the observation as seen in the Figure on the next page, larvae 1, 4, 8 and 11 displayed aversion to Neutral pH, as seen by their ECDF graphs larvae moved away from the source of stimulus in the post stimulus phase of experiment. Larvae 3, larvae 6 and larvae 7 displayed no preference for neutral pH, as their pre and post stimulus graphs are overlapping with each other. (see Figure18)

Strong attraction was displayed by larvae 2, 9 and 10. It can also be seen from their position index as well ECDF graphs (see Figure18)

Overall, it can be concluded that neutral pH evokes mixed behavior from 9 dpf zebrafish larvae, ranging from strong attraction to strong aversion. However, a clearer picture was obtained when ECDF for all the larvae was pooled together (see also Figure19)

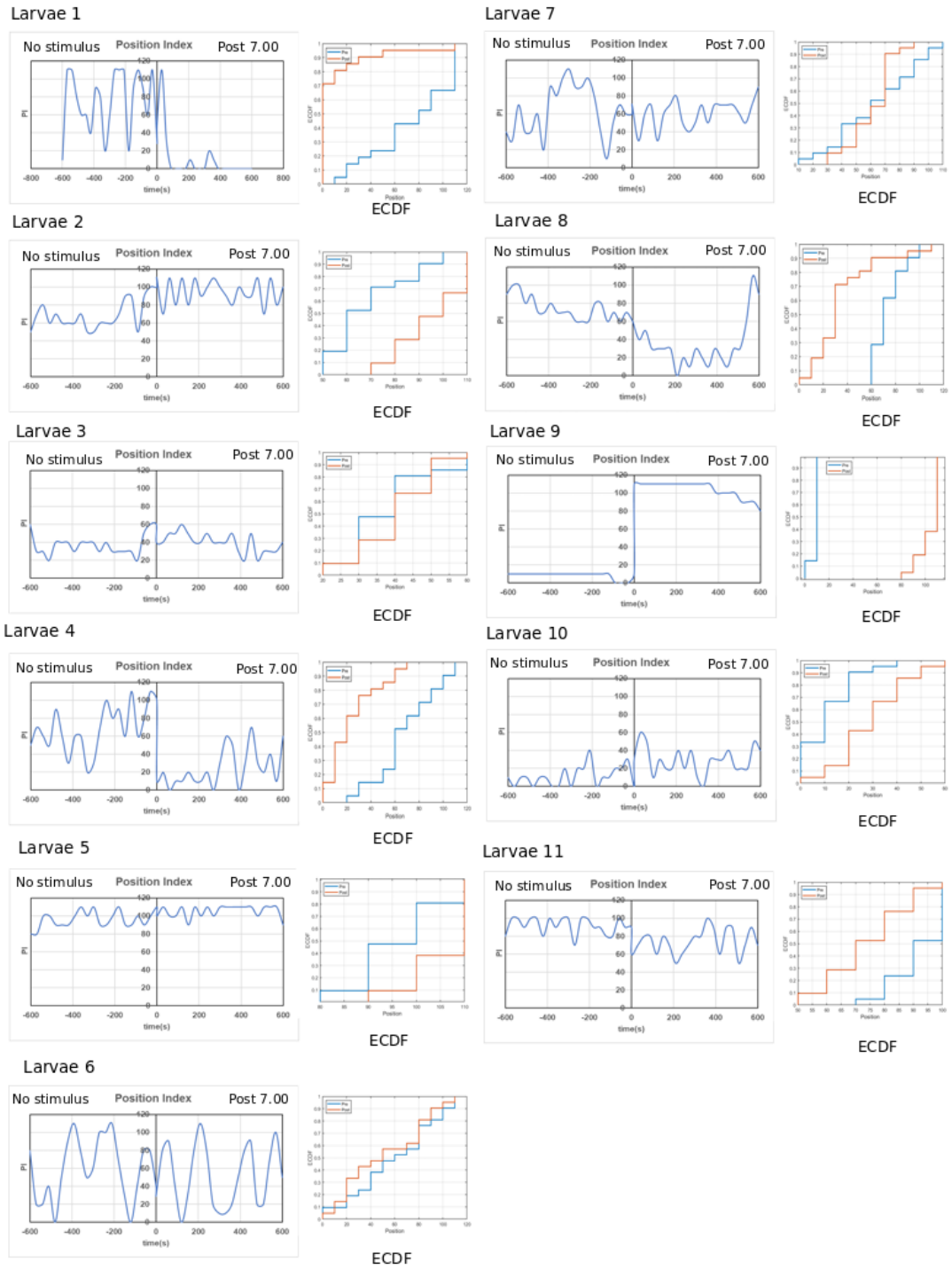

Figure 18: Position index of individual larvae pre and post stimulus of neutral pH introduced at time point 0 on y axis. Graph on the right-hand side indicate position index of the larvae 10 minutes (600s) pre stimulus and 10 minutes (600s) post stimulus. ECDF graphs to the right indicates the change in the position index pre and post stimulus

4.8 Pooled ECDF for larval behavior

Data collected from individual larvae was pooled together and evaluated. It was observed as shown in the Figure19 first panel that 9 dpf zebrafish larvae displayed strong attraction to 0.4g/L food odor with ***p <0.001(KS test). It can also be seen from the ECDF graphs that post food odor ECDF curve is strongly shifted towards the odor source i.e towards the preference index value 120. Thus, food odor served as a positive control for multilane behavioral setup.

Neutral pH has overall no effect on the behavior of 9 dpf larvae. As could be seen in the Figure 19 middle panel, pre and post ECDF curves are overlapping with each other with p=0.170 (KS test) which is non-significant. Indicating no net effect of Tris itself on zebrafish behavior. Thus, serving as a negative control for larval behavior (see Figure 19)

However, when the pH of Tris is slightly alkaline, 9 dpf larvae displays preference for the odor source (bottom panel Figure19), with *p=0.031 (KS) test. This indicates that animals were able to sense a slight change in the pH of the solution and that influences the overall behavior of the animal. This gives us a possibility that the attractive/preference behavior in 9dpf larvae might be mediated through ORA4 receptor sitting in crypt neurons (Oka et al., 2012). Alkaline pH reacted with ORA 4 receptor in vivo in cell culture (Behrens and Korsching unpublished). The evaluation was done manually which proved to be a cumbersome and tedious process, raising the possibility of manual errors, thus I setup an automated tracking setup for tracking larval zebrafish.

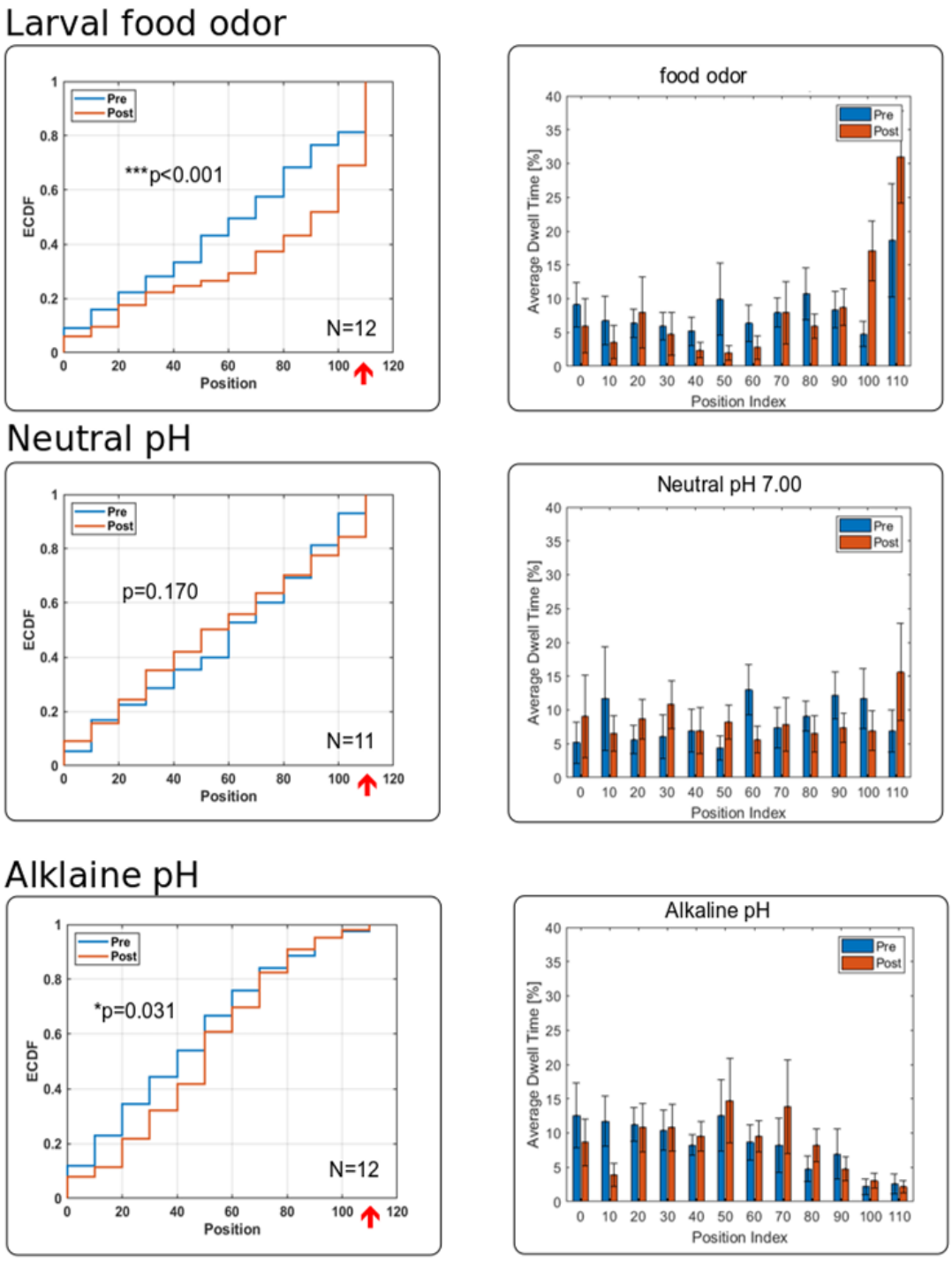

Figure 19: Pooled ECDF for larval Behavior (N=12, significant attraction to food odor, ***p<0.001(top left panel) Average dwelling time for individual larvae in response to food odor (0.4g/L) (top right panel). Pooled ECDF showing no significant attraction to neutral pH. (middle left panel). Average dwelling time of larvae in response to neutral pH (middle right panel). Pooled ECDF showing significant attraction to alkaline pH, *p= 0.031 (Bottom left panel). Average dwelling time of the larvae in response pH (Bottom right panel). Red arrow indicates the point of stimulus application

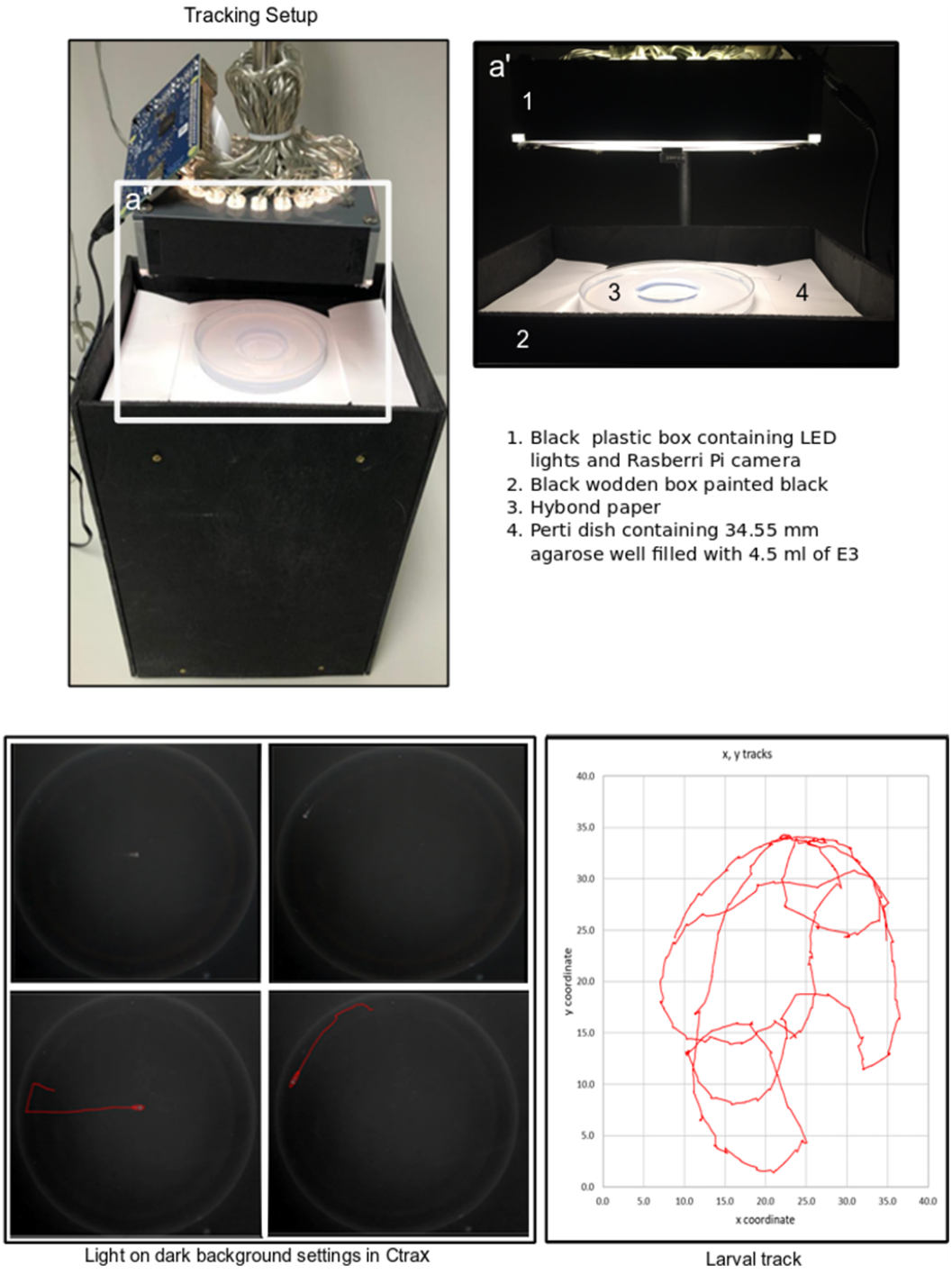

Figure 20: Automated behavior setup for zebrafish larvae

4.9 Automated tracking setup in petri plate

1. 9 dpf larvae were used for monitoring the behavior of the fish under IR background.
2. A black wooden box was constructed and painted black, 26 cm in height, with a platform for recording made of transparent plastic sheet 15 cm wide and 16 cm long, covered with sheets of hy-bond paper to evenly spread IR light
3. Petri dish was filled with 2% agarose gel and allowed to solidify at room temperature.
4. 34.5 mm of agarose well was cut out in the center of petri dish and filled with 4.5ml of E3 medium. Having walls of the well with agarose gel completely removes reflection.
5. 9dpf larvae was gently placed in middle of petri dish and allowed to acclimatize in the setup for 15 minutes
6. Rasberry pi camera could be connected directly to a working laptop via bluetooth, and activity of the animal could be seen live on the computer screen.
7. Before recording, for an experiment the image acquisition was selected to “negative”, from Rasberry’s graphic user interface, which greatly improves the contrast between animal and the background

4.10 Tracking larval zebrafish using Ctrax

1. Rasberry Pi cam and the video recording software gives the image movie recorded at 25 frames per second in the format of .mpeg file, which can be converted into .avi format recommended by Ctrax.
2. Once the video is uploaded to Ctrax, a graphic user interface opens giving three options as below, light on dark background option was selected as the recorded videos had a uniform black background the larvae can be seen as a white spot with sharp contrast to the background. Click next (as shown in the Figure below)

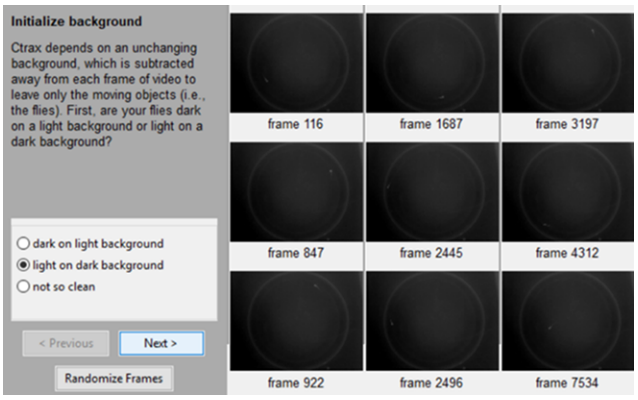

3. Ctrax then asks to define the region of interest, since the background evenly dark and edges are not recognized by Ctrax as animals select “don’t use region of interest Click next (as shown below in the figure)

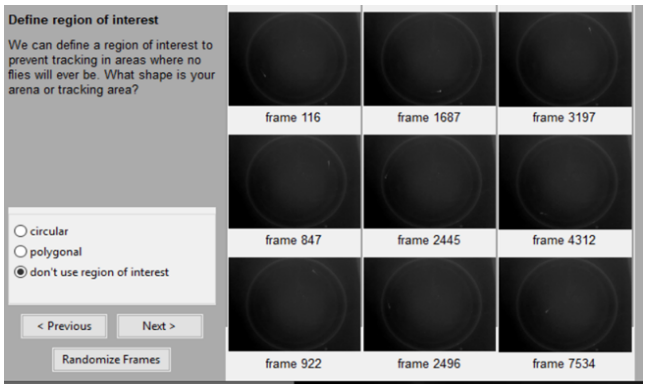

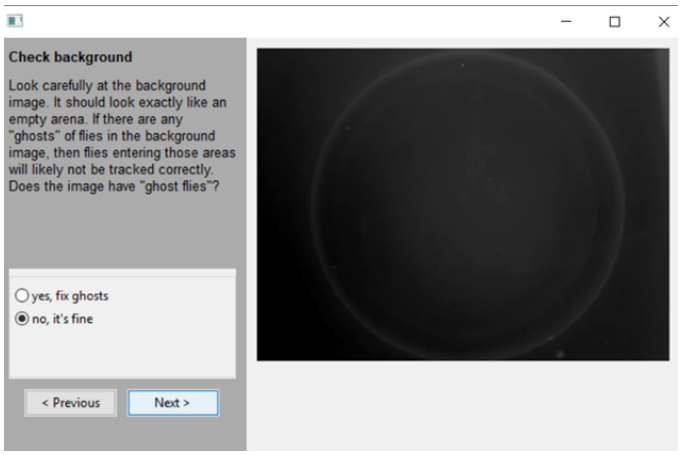

4. Check the image for “Ghost flies”, if the larvae had been moving constantly and was not stuck to one part of the petri dish for longer than 10 seconds, the image will look like an empty arena. If that is the situation as below, choose the option, no its fine from the graphic user interface. If Ctrax recognizes the ghost flies or ghost larvae, draw the rectangle around the ghost larvae. Click next (as shown in the UI above)

5. Ctrax then asks to decide a low threshold value to define the edges of the larvae making each larva distinct. Since in the setup we had one larva per condition a low threshold of 5 was enough. Larvae should be covered with a red outline in every frame, indicating that Ctrax is detecting exactly one larva per frame. Click next

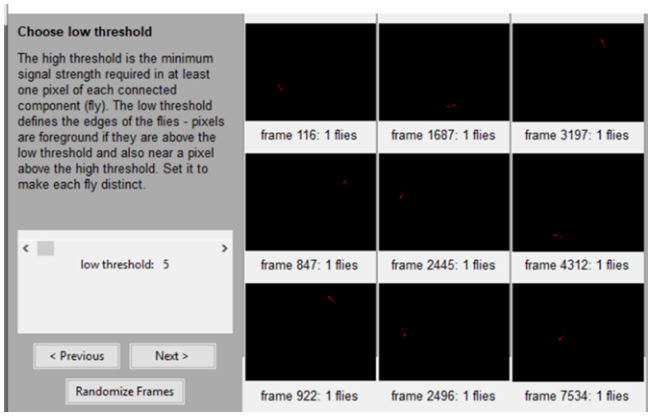

6. Ctrax then asks to choose a high threshold for the for the animals. This allows the background to be subtracted and identify the pixels that truly belongs to the animal. A high threshold of 15 was selected which allowed Ctrax to identify exactly one animal per frame. Click next

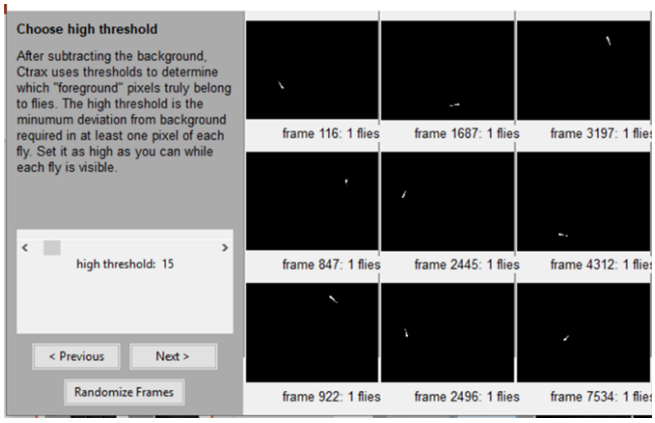

7. Next select “do not use shape bounds “, since in the setup we are using a single larva/arena. Click next.

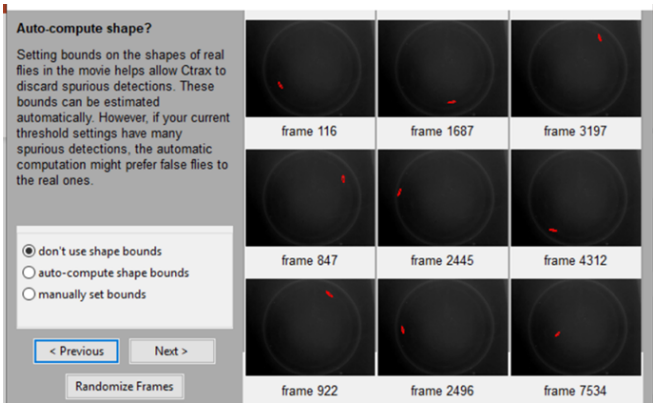

8. By clicking on randomize frames multiple times cross check to ensure that the larva is covered by a red circle in every single frame. If you find a red circle missing in any of the frames from the larva go back to the settings and adjust the thresholds. Then click on start tracking. Ctrax will open a window and start tracking the larva in real time. After tracking is done data can be exported as a MATLAB file. The

software generates 2 files that can be used for the post processing of the data, a MATLAB file(.mat) and a backup file(.ann). If everything went smoothly, we get 3 files in the folder the original .avi file, mat file and. ann file.

Post -processing of the tracked movie and fixing errors in the data

9. Fix error tool is needed to be installed from the online repository provided by Ctrax, which is a script written in MATLAB, and requires a MATLAB graphic user interface, hence MATLAB needs to be prior installed on the computer. While downloading the fix error tool, make sure to save it in the same folder as MATLAB was originally downloaded, otherwise MATLAB might not be able to read it. Once the script is downloaded, run the script in MATLAB.

10. To run the fix error GUI three files would be required, the original .avi file,.mat file, which is exported from MATLAB, and. ann back up file that Ctrax creates.

11. Once the GUI is started it will first ask to open the original movie file and the exported file from MATLAB. Then it will ask to enter the frame rate of the movie, in our case it was 25 frames/ second.

12. On clicking next, it will ask to enter the size of the arena in mm, the size of the arenas shown in Figure20 (bottom panel, left) was 34.55 mm in diameter

13. Fix error tools starts a GUI in which one can see the quality of the tracking video. First click on **Flip image** option. The recording quality of the tracks was fine and as a result there was no sudden birth/death of the tracks. Suddenly the embryo would flip itself or jump quickly from one frame to another and hence fix error tools only asked to confirm the identity on the basis of suspicion of the identity of the animal in both of the frames, if that option comes us click “correct” , and the tool will preserve the identity of the fish throughout the track.

14. When all the errors have been sorted out the tool will close itself and save the results as a new MATLAB file.

15. Open the new MATLAB file saved from fix error tool in MATLAB. In the workspace

the MATLAB file will be displayed as trx (1) file with a column, since there was only a single zebrafish larva in the arena

16. Use the command xpos=(trx(1).x_mm) and xpos=(trx(1).y_mm). This command will separate the x and Y co-ordinates in to two separate columns and will give the output two separate MATLAB sheets.

17. The x and y co-ordinates can be used as copied to another program for example excel to create a track. Alternatively, use the command (plot(trx(1).x_mm), plot (trx (1). y_mm)), to get a MATLAB figure of the tracks

4.11. 9 dpf larvae (not starved) displayed significant attraction to alkaline pH in petri plate setup

Larvae were kept in the behaviour room maintained at 37 degrees, for overnight habituation. The next morning larvae were fed with 100 µl food odor mixture in a petri dish (0.4g/L), and through the experiment food mixture was supplied to animals, and care was taken not to starve larvae during experiment. The protocol is modified from (Chen et al., 2019) and (Kaniganti et al., 2019)

Before the start of experiment, every animal was acclimatized in the recording chamber for 10 minutes (not recorded), at the end of 10 minutes behaviour of larvae was recorded for 3 minutes and this phase is designated as NS (no stimulus phase). At the end of NS phase another break of 3 minutes was given (not recorded), so that the larvae could relax.

After 3 minutes, 10 µl E3 medium with a pipette was gently placed in the centre of petri dish, and the behaviour of larvae was recorded for the next 3 minutes followed by rest for another 3 minutes (not recorded). After that 10 µl of neutral pH was placed in the middle of petri dish and behaviour of larvae was recorded, followed by another rest for 3 minutes (not recorded) followed by introducing 10µlTris alkaline pH and larvae was further recorded for 3 minutes.

The same pattern was applied to 10 different animals, giving 6 videos per larvae, and 60 videos from a single experiment were obtained. All 60 videos were tracked using Caltech Fly tracking software Ctrax (Branson et al.,2009). After post processing of the videos and fixing errors, as described in the previous section mean velocity of the larvae and the distance from the centre was calculated and plotted for, all 10 animals as shown in Figure 21.

The mean velocities obtained for individual larvae for each condition was compared and the ratio of Post-Pre/Pre was calculated. From Figure 21 (top left panel) addition of any stimulus into recording well has no significant effect on the mean velocities of the larvae.

This indicates that animals were not excited just by the addition of a new stimuli. Hence the system was stable, and embryos were not stressed during experiment.

On comparing the ratios Post-pre/Pre for mean velocities (E3 vs neutral pH) and (E3 vs Alk) there was a significant difference in the ratios for the mean velocities (**p=0.0071 paired t test). This data indicates that 9dpf larval zebrafish were excited on the addition alkaline pH.

Zebrafish larvae also displayed a significant decrease in the mean ratios of Post-Pre/Pre (E3 vs neutral pH) and (E3 vs Alk pH) for the distance from the centre on the addition alkaline pH. (Figure 21 bottom right graph, *p=0.0407), indicating an attraction for alkaline pH

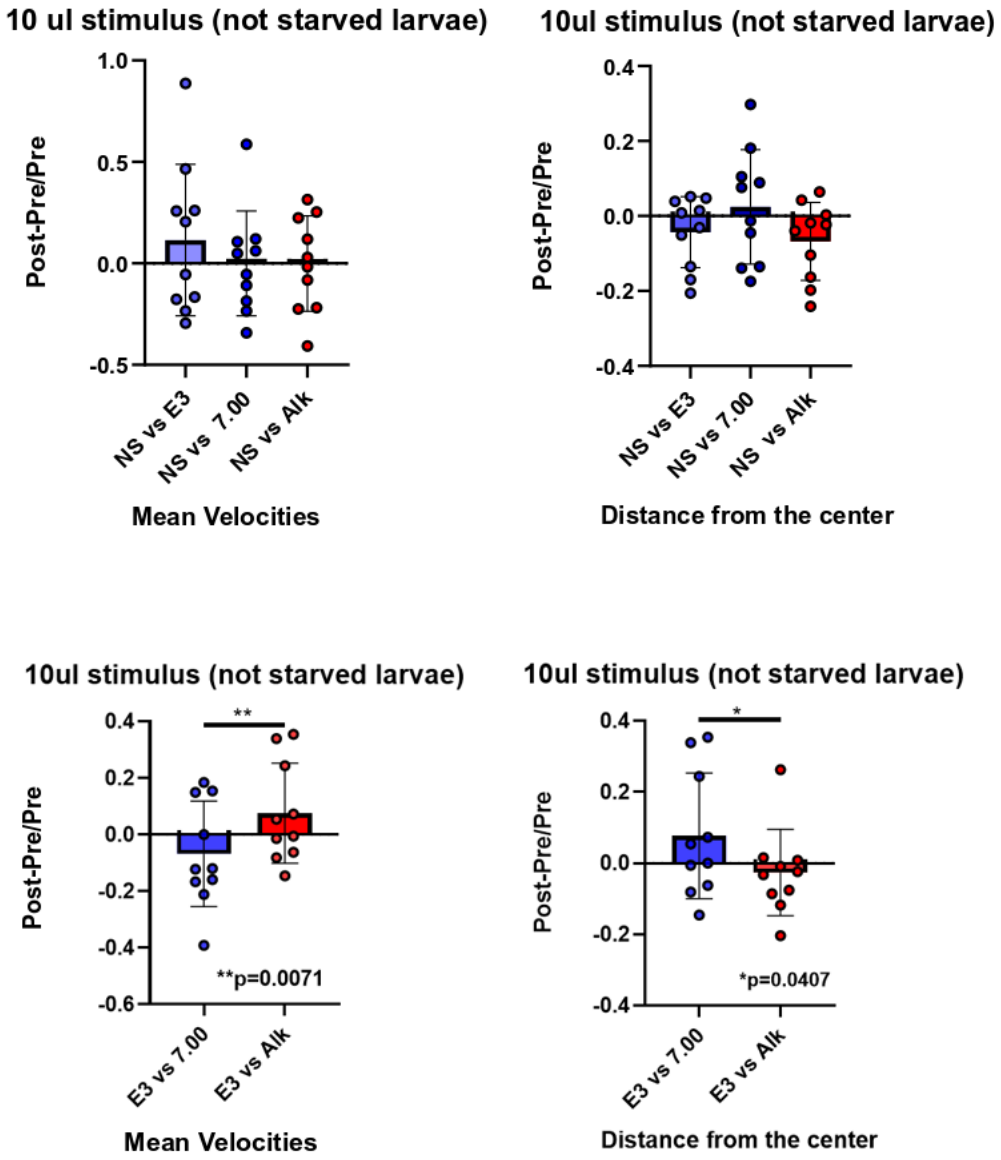

Figure 21: Significant attraction to alkaline pH Significant difference in the mean velocities (pH 7.00 vs Alkaline pH (**p=0.0071, paired t-test and distance from the centre (*p=0.0407 paired t test) was observed No significant difference in the mean velocities or distance from the centre was seen on the addition of pH 7.00 or Alkaline pH (Alk) when compared to no stimulus (NS) condition (top panel)

4.12. 9 dpf larvae (starved) displays no significant attraction to food odor in petri plate setup

The temperature of behaviour room was kept at 37 degrees and the conditions for experiments were kept similar as described in the previous section.

For testing food odor as an attractive stimulant for 9 dpf zebrafish larvae I used the same concentration of (0.4g/L) like the multilane lane setup to test the effect of food odor (see Figure19)

Larvae were transported to the behaviour room a day before the experiment and kept overnight to acclimatize to the conditions of behaviour room. The next morning larvae were pooled in a petri dish and given 100 µl of food odor, for 15 minutes. After 15 minutes, larvae were separated from the petri dish containing food odor, and individually starved in separate petri dishes for exactly 3 hours.

After 3 hours, individual larvae were kept in the recording chamber and acclimatised for 10 minutes so the animal get used to the recording chamber, thus reducing stress on the animal.

After 10 minutes, recording was switched on and embryos were recorded for 3 minutes for a no-stimulus (NS) phase. After that 3 minutes resting period was given (not recoded), and at the end of resting phase a 10 µl stimulus of E3 medium was given and behaviour of larvae was recoded for 3 minutes, again followed by a resting phase of 3 minutes. After that 10 µl of food odor was given to the larvae and response of animal was recorded for 3 minutes.

Once videos for experiments were obtained, Ctrax was used to obtain the trajectory, and the data for mean velocity and the distance from the centre of stimulus application was evaluated.

On calculating the ratios of Post-Pre/Pre (Preference Index), for different conditions it was observed as seen in the (Figure 22 top right graph), there was an increase in the mean velocities of larvae after the addition of E3 medium and food odor, when compared to no

stimulus condition. Indicating that embryos were excited on the addition of E3 medium and food odor however, the difference in mean velocities was not significant.

Mean distance from the centre also increased for larvae on the addition of E3 medium and food odor, (Figure 22 top right graph). Larvae tend to move away from the stimulus source, both with E3 and food odor. Since the animals were fed well before the experiment, as it can be observed that they were not motivated to explore the stimulus source.

Different set of animals were starved for exactly 3 hours before experiment. On evaluating the mean velocities, it was observed that the Post-Pre/Pre ratios for mean velocities of the animals decreased on the addition of E3 medium and food odor (Figure 22 left bottom graph). However, the difference was not significant.

Although, when comparing the ratios of distance from the centre for no stimulus (NS) vs E3 and NS vs Food, (Figure 22 bottom right panel), it can be observed that larvae tend to come closer to the food source, however this difference was not significant. Indicating that larvae in a well plate setup was not significantly attracted to food odor, as an attractive stimulant. Another set of 9 dpf larvae were starved as described previously, and 100 µl of food odor was given at the centre of petri dish. The protocol was described first by (Chen et al., 2019). Inconsistent with their data, in our setup zebrafish larvae did not display a significant increase in mean velocity on presentation of 100 µl of food odor, (Figure 22 right graph), also there was no significant difference in the distance from the centre indicating no attraction to food odor.

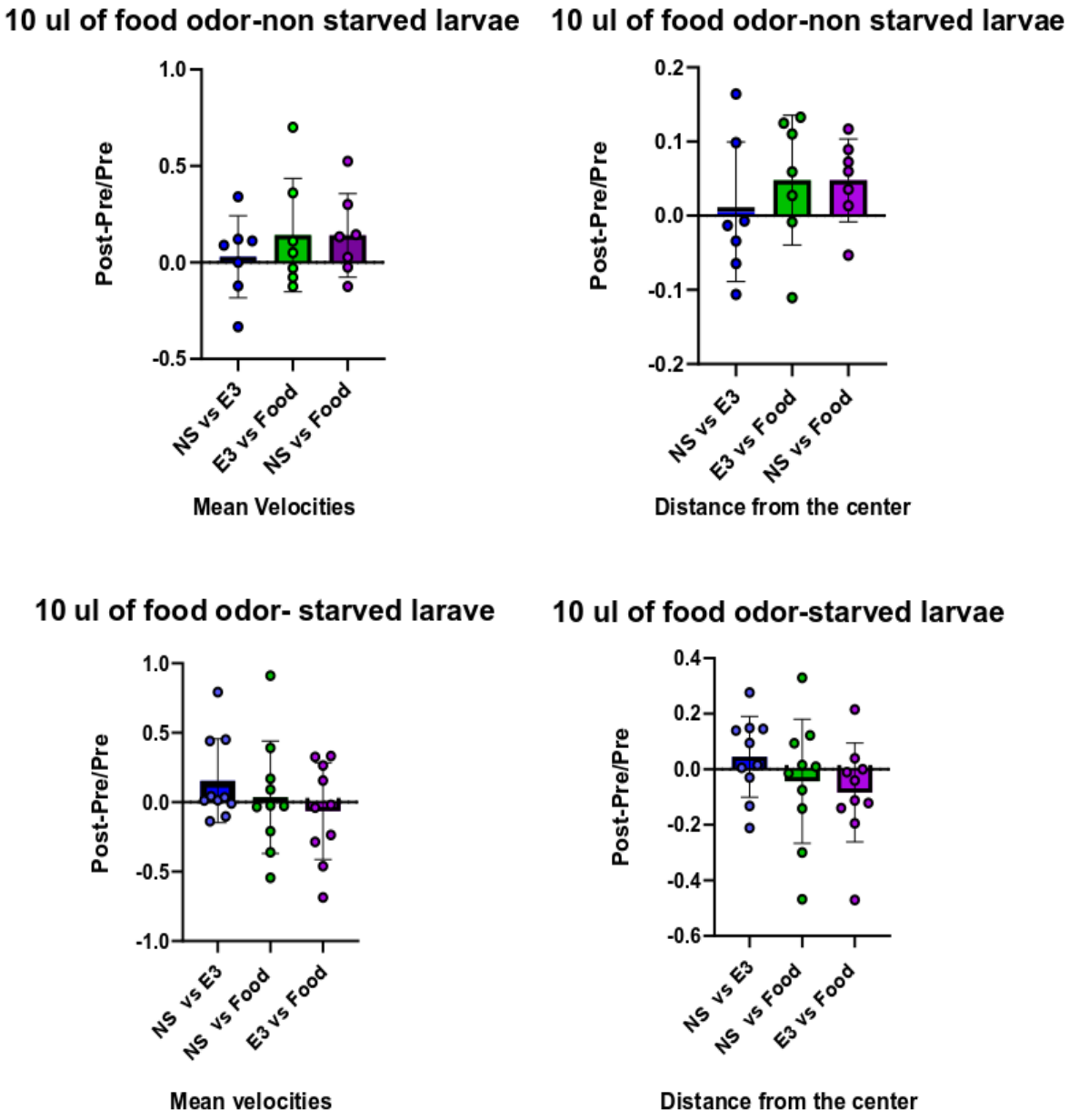

Figure 22 A: Larvae were not attracted to food odor (0.4g/L) in automated tracking setup. No significant difference was observed in the mean velocities or distance from the center on the addition of either 10 of E3 or food odor to non-starved larvae when compared to No stimulus (NS) recording (top panel). 3-hour starved larvae also did not show any significant attraction to food odor, in terms of increase in mean velocity or decrease in the distance from the center (Bottom panel).

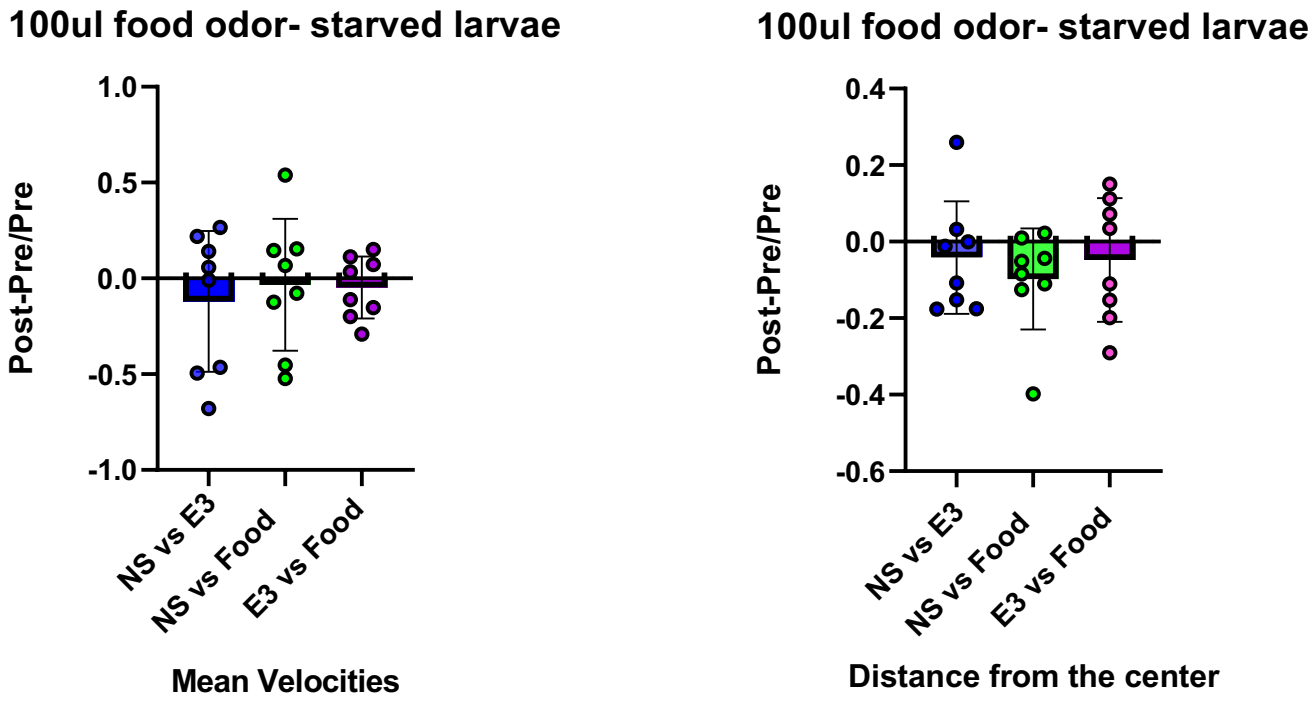

Figure 22 B*:* Larvae were not attracted to 100 µl of food odor 100 µl of food odor also did not significantly increases the velocity of the larvae or decreases the distance from the centre of perti-dish (odor source of the stimulus).

4.13 p-Erk labelling with Alkaline pH

Phosphorylated Erk has been used as an activity marker to trace the activity of neurons on stimulation of a specific ligand for example cadaverine (Dieris et al., 2017). I used the same approach to look for the neural activity in olfactory bulb in response to alkaline pH

A stimulating chamber was constructed, that allows for the minimum interference between the animal and the experimenter. The stimulating chamber consisted of black box (8.5x18.5cm) that is completely opaque, and the fish cannot see the experimenter. It is further divided in to two compartments that can hold about 500 ml of water each. The compartment is divided by a transparent divider that separates the two compartments and prevents the leakage between them. The frictional resistance initially offered by the rubber holding the barrier together was reduced by the application of graphite which reduced the friction to quarter of the originally experienced. Before starting the experiment, I decided to check the stability of the pH in the prototype as a function of time. It was observed that change in the pH on both the sides of the compartment was stable until 4 minutes and prototype could be used for stimulation with alkaline pH. Before stimulating, fishes were kept for overnight acclimatization with system water supplemented with 0.03% sea salt and buffered with 10 millimolar Tris pH 7.0.

Next morning, fishes were bought to the behavior room and acclimatized for one hour so that they are familiar with the new environment which helps them to remain as relaxed as possible during the experiment. One of the compartments was filled with 500ml of system water supplemented with 0.03% sea salt and buffered with 10 mM Tris with pH 7.0. Other compartment was also filled with 500ml of system water (Buffered with 10 millimolar Tris alkaline pH with 0.03%sea salt)

Fishes were acclimatized in pH 7.0 compartment for 30 minutes. After 30 minutes the divider was lifted, and a time frame for two minutes was given to the fish to enter towards the alkaline compartment. Once fish entered the alkaline compartment, divider was pushed down, and a stimulus time of 3 minutes was given to the fish. After 3 minutes fish was swiftly taken out of the apparatus and put on ice for cold anesthetization.

Cadaverine was used as a positive control, as it has been shown to evoke p-Erk signals in the dorsolateral cluster of olfactory bulbs (Dieris et al., 2017). Neutral pH was used as a negative control and alkaline pH was used as a test control. Next, fish was decapitated and transferred to 4% PFA for overnight. The olfactory bulb was stained using the protocol described by Dieris et al. (2017). After immuno-histochemistry, stained olfactory bulbs were subjected to tissue clearing, using gradient of 20%, 60%, 80% w/v sucrose solution in PBS overnight in each condition. After immersing the tissue overnight in 80% sucrose solution, tissue was separated and mounted between two coverslips, with a drop of 80% sucrose as a mounting medium. Whole mount stacks of olfactory bulb were taken with SP8 confocal microscope at imaging facility Biozentrum.

After obtaining confocal stacks maximum projections were obtained using FIJI software.

As it has been mentioned earlier that crypt cells project their axons to medio-dorsal glomerulus (Ahuja et al., 2013). A lot of variability in the signal intensity was observed as shown in Figure 23. Medio-dorsal cluster was faintly labelled in both WT and ORA4-/- fish, which is inconsistent to the findings in the heterologous expression system (Behrens and Korsching, unpublished observation). A lot of variability in p-Erk signal intensity was observed in the dorsal cluster (DG) and dorsolateral cluster (DLG) both in WT and ORA4-/- fish.

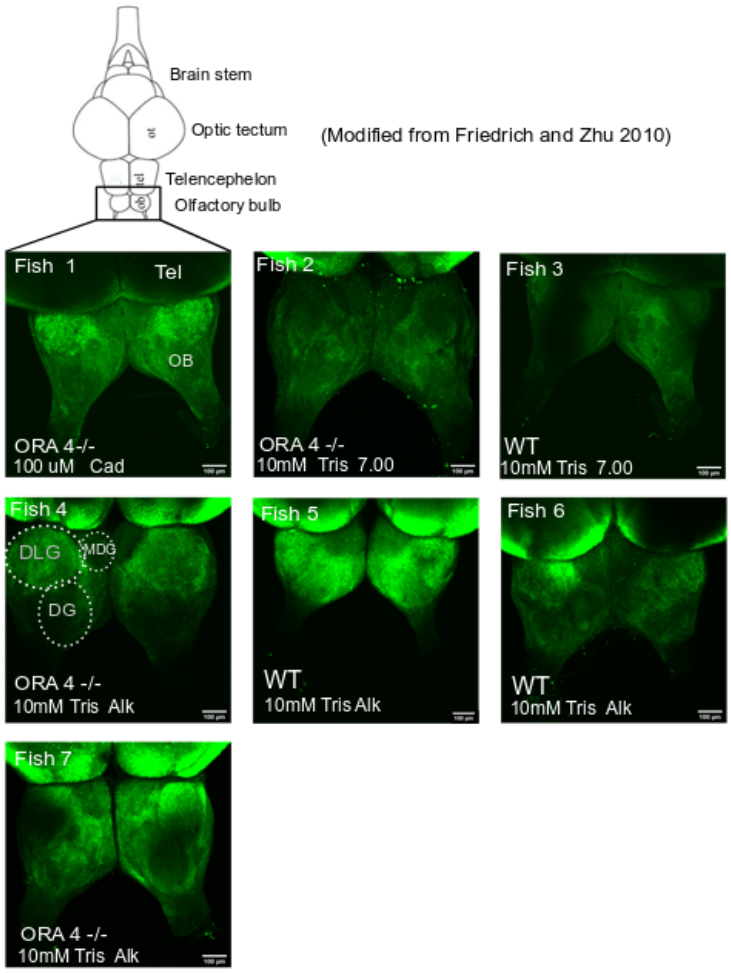

Figure 23: p-Erk labelling with alkaline pH. Cadaverine was taken as a positive control which distinctly labels dorsolateral cluster, in ORA4-/- (Fish 1), as seen in WT fish (Dieris et al., 2017) top panel left. Neutral pH was taken as negative control (top panel). On stimulating with Tris (alkaline pH) a lot of variability in labelling was observed (middle panel), in both WT and as well as OR A 4 -/- fish.

.

4.14 Calcium imaging for odor stimulation

Calcium ions generate a wide variety of signals that mediate a large variety of function in the cellular environment (Berridge et al., 2000). To trace the activity of calcium ion in the cellular environment a wide variety of calcium indicators have been developed and have been successfully used to visualize the activity of neurons using confocal microscopy (Grienberger and Konnerth, 2012). Fluorescent calcium indicators such as GCaMP6, have been widely used in a wide variety of organisms ranging from C.elegans to rodents (Nguyen et al., 2016) , (Chen et al., 2017). Stably expressing GCaMP6s under the control of elavl3 promoter (previously called HuC) were obtained from Janelia Farms Research, courtesy Misha Ahrens lab. Another line of *elavl3*::GCaMP6 fish was a kind gift from Prof. Arrenberg's lab, University of Tübingen . Both the fish lines were used for calcium imaging experiments.

Setup for stimulation

9 dpf embryos were used for odor stimulation experiments.

Embryos were anesthetized with 0.01% MS-222. After that the embryos were embedded in 1.2 percent agarose gel, and placed on a sylgard plate, which was kindly made for our experiments by Helmut Wratil from Prof. Kloppenberg lab. Sylgard is a silicone elastomer which allows laminar flow of liquids to be maintained on its surface, is stable at room temperature. Once embryos were stable in agarose gel, it was immersed in 100 µl of E3 medium. Small amount of agarose with a thin flattened platinum wire was scratched from the nose and upper lip of the animal, so that the odor could reach the nose of larvae.

The setup was placed at the stage of confocal microscope, and two injection needles were attached to the plate using Blue Tac (a non-odor adhesive). The tips were placed 1.5 cm away in both directions as shown in the (Figure 24) from the nose of the larvae. E3 medium was circulated at the rate of 7.5 ml /minute using a peristaltic pump.

30 µl of stimulus pulses with a pipette were given to the embryo after at an interval of 40-60 sec.

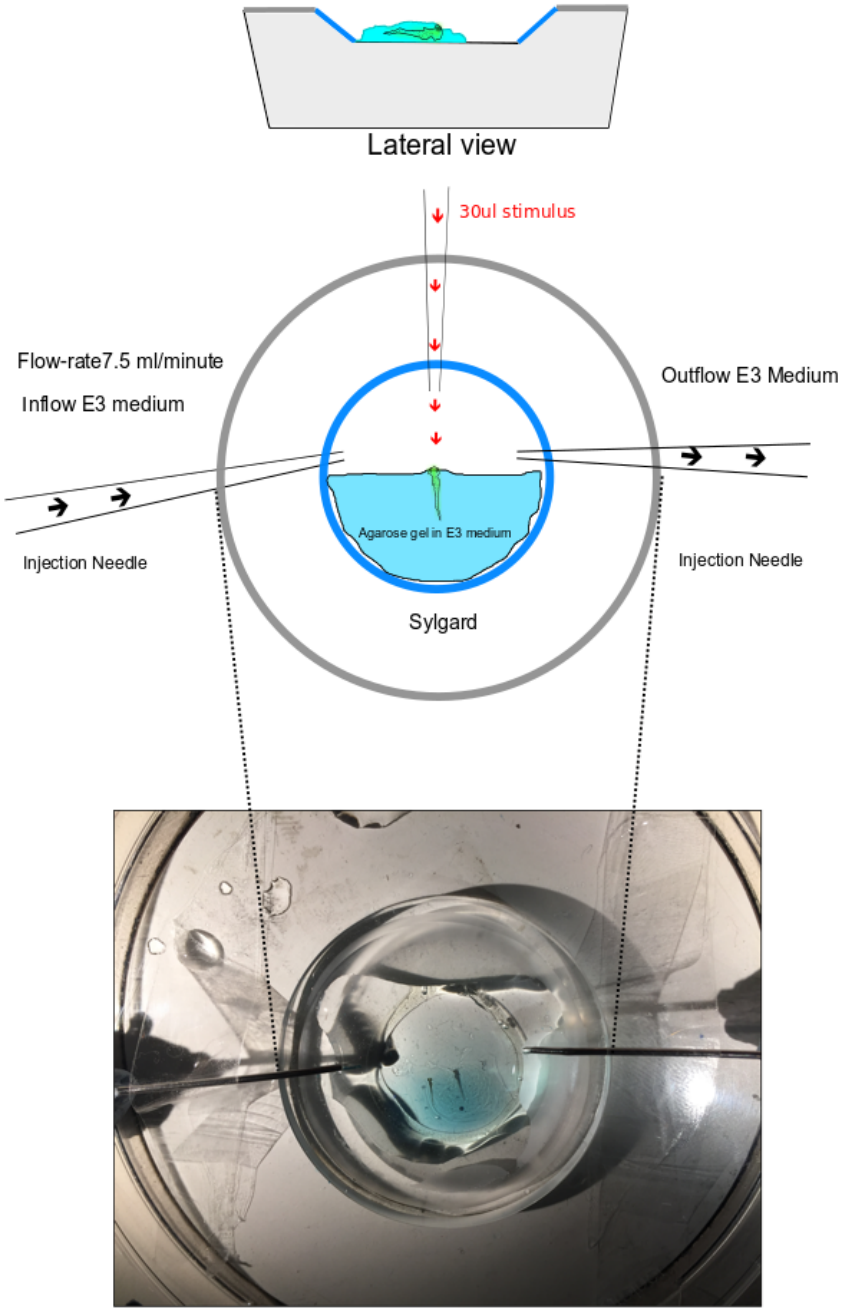

Figure 24: Calcium imaging setup for stimulation of zebrafish larvae. Lateral view of the setup (Top panel). Schematic view of the experimental setup (middle panel). Photograph of the experimental setup bottom panel)

4.14.1 KCL induces a characteristic spike response from neurons in olfactory bulb and telencephalon

Once the larva was embedded in the agarose gel, a 10-minute baseline recording was performed to check the stability of the animal and for motion artefacts. Once the larvae were stable in agarose gel and wriggling of the head could not be observed in a 10-minute recording, the animal was used for experiments, if a lot of wriggling was observed the animal was not used for the experiment or embedded again.

KCL has been used as a positive control in calcium imaging experiments to check for quality of preparation (Chen and Huang, 2017) as it depolarizes the neurons. If the calcium indicator is expressed and functional it will give a characteristic spike response. Once the larva was stable, a pulse of 30 µl of KCL was given to check whether the stimulus was reaching the animal. A characteristic response in the form of fluorescent spike was observed from the larvae olfactory bulb neurons (Figure 25 top panel), on application of KCL. The trace of DF/F0 shows a sudden spike in the fluorescent intensity for nearly all neuron in the olfactory bulb on at 83s in a 2-minute recording (Figure 25, middle panel). The effect of KCL can also be seen at a level of individual neuron, neuron 4 and neuron 76, though they are sitting at different positions in the olfactory bulb and apart from each other, they display a peak rise in the fluorescence on the application of KCL (Figure 25). Further, closely examining the line scan for Neuron 4, close to the application of KCL at 83s, a delay of 1s can be seen after application of stimulus. Neuron 4 undergoes, hyperpolarization, followed by depolarization at 84s and after 2 seconds repolarizes again. Thus, after the addition of the stimulus in the bath application, it takes 1 second for the stimulus to reach the animal.

The depolarization observed on the application of KCL confirms that in the setup was functional, stimulus was reaching with a nose of the larvae and could be used for further experiment.

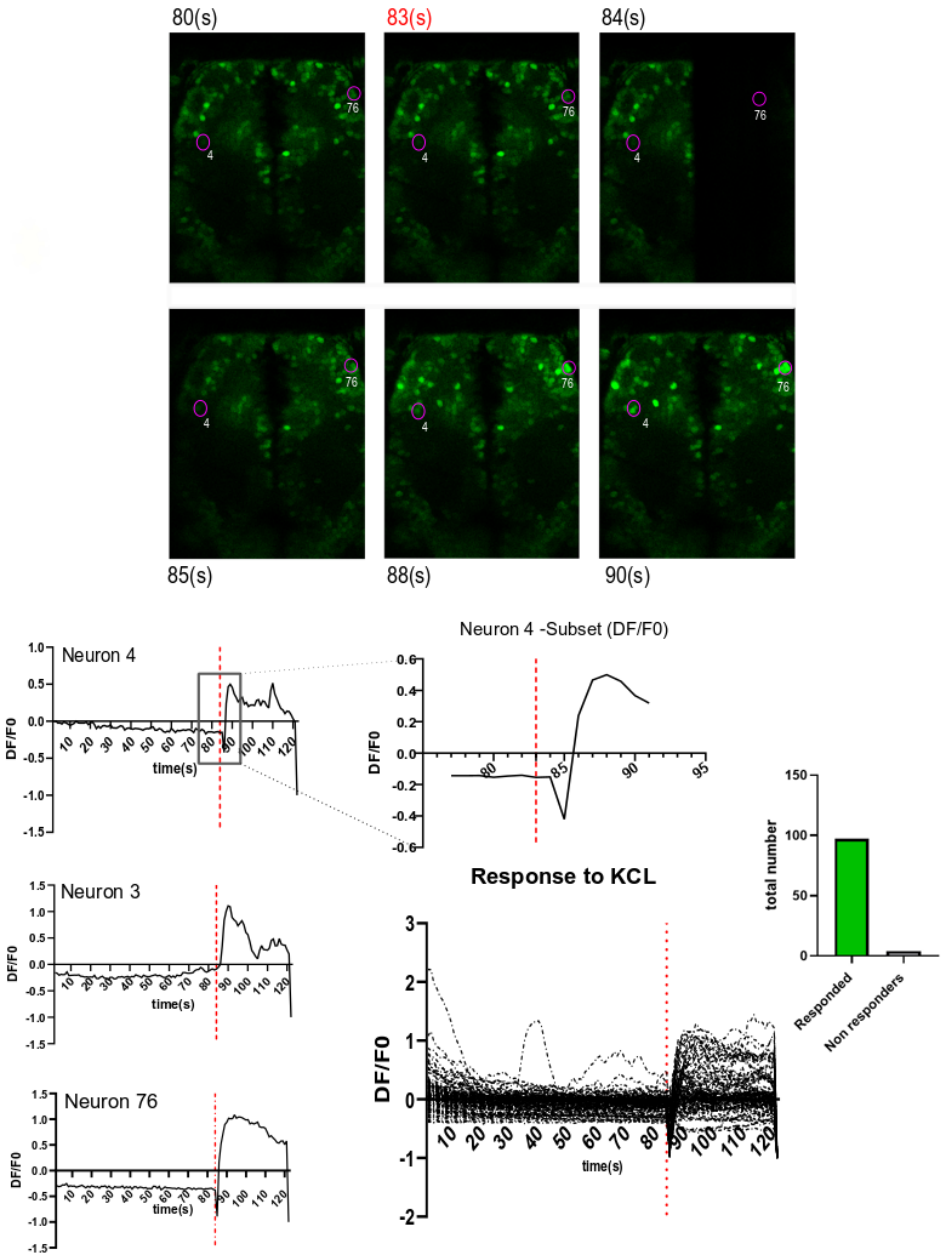

Figure 25: KCL depolarizes neurons in the olfactory bulb. Images of 9dpf larvae during 1M KCL administration at 83s in a 120s recording (Top panel). DF/F0 of neuron 4 on KCL administration (middle panel). DF/FO of all neurons in the olfactory bulb, on applying KCL (Bottom right panel). Total number of responding neurons on KCL application (middle right panel). X-axis is the time in seconds. Recordings were done at a frequency of 1Hz (one frame/second).

4.14.2 Analysis pipeline

Since cells showed a lot of spontaneous activity even without stimulus, we selected two criteria to distinguish a *bona fide* stimulus response from such spontaneous activity. As measuring parameter DF/F0 was chosen. The first criterion was that a peak should exceed 3 standard deviations of the pre stimulus signal, and no such peak was observed during a defined period preceding the stimulus. This period was taken as the first 30 seconds of the recording for Tübingen strain, and in the first 60s in Janelia Campus strain since longer recordings could be obtained in this strain. Additionally, the neuron should not have any peak 3 standard deviations away from the baseline in the 20 seconds before the stimulus presentation, in accordance with published selection criteria (Chia et al., 2019)

The second criterion concerned half width of peak and delay to peak. A half width of maximally 20s and delay to peak for maximally 20 seconds was taken as cut off criterion for selecting neurons, because in the bath application it was observed that 1% methylene blue dye would be completely washed from the stimulating chamber in maximum of 20 seconds. Both criteria together helped in removing spontaneously active neurons from the raw data. An overview of all validated response peaks for cadaverine is shown in Figure 26.

The stimulus consisted of 30 µl pulses. For plotting DF/F0, mean of absolute F values for first 40-60 seconds was taken as F0. ROIs were made encircling the neuron, and line scans of DF/F0 were plotted using a custom written macro for image acquisition software Fiji. This macro was written with the help of Peter Zentis, Imaging facility, CECAD. Vertical lines indicating the time point of stimulus application were added using Graph pad prism software. A custom written MATLAB script was used to check whether the response from the cell's qualifies 3 sigma criteria i.e the peak amplitude of the response should be at least 3 standard deviations away from the mean.

Location of the responding neurons was determined by reference to anatomical markers visible in the fluorescence image as can be seen in the Figure 26.

Analysis pipeline

1.DF/F0 traces were obtained using Fiji (Image J)

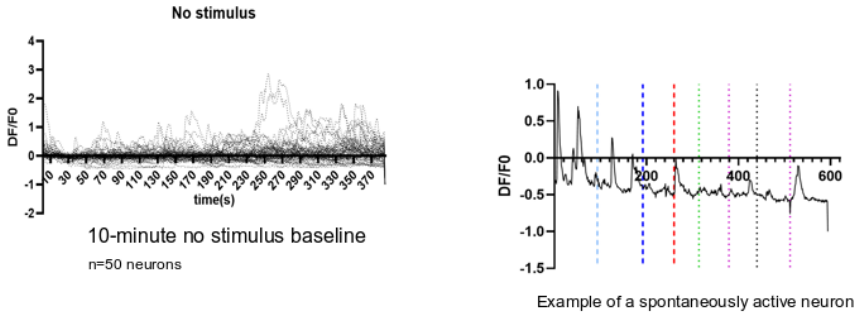

2. All neurons were evaluated on the basis of 3 sigma criteria

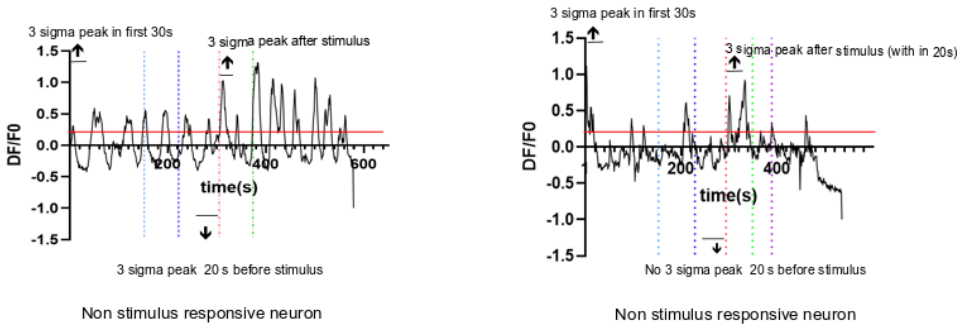

3.Neurons fulfilling the criteria were selected and used for further analysis

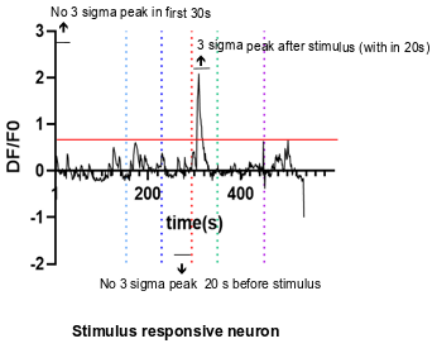

Figure 26 A: The analysis pipeline to screen the stimulus responsive neurons is visualized with representative examples. Dotted lines crossing the x-axis are the time points of individual stimuli (light blue, E3; dark blue neutral, pH; red, alkaline pH; green, cadaverine; violet, 0.1M KCL).Horizontal red line on y axis on graph indicates the threshold value for 3 sigma criteria.

4.14.3 Responses of neurons to cadaverine (Tübingen strain)

Cadaverine triggers innate avoidance behavior in adult zebrafish (Hussain et al., 2013). A single glomerulus was identified in the olfactory bulb as a cadaverine-responsive glomerulus (Dieris et al., 2017). I used 30 µl of 100µM cadaverine solution as positive control to establish the appropriate imaging conditions and analyzed potential cadaverine responses in 342 neurons from the olfactory bulb (Figures 26 B, 27 and 28). In total, six neurons qualified the criteria of a responding neuron (see section Results/ Analysis pipeline). From DF/F0 traces as shown in Figures 26, 27 and 28, some cadaverine-responsive neurons also responded to alkaline pH. One of these six cadaverine responsive neurons also responded to neutral pH.

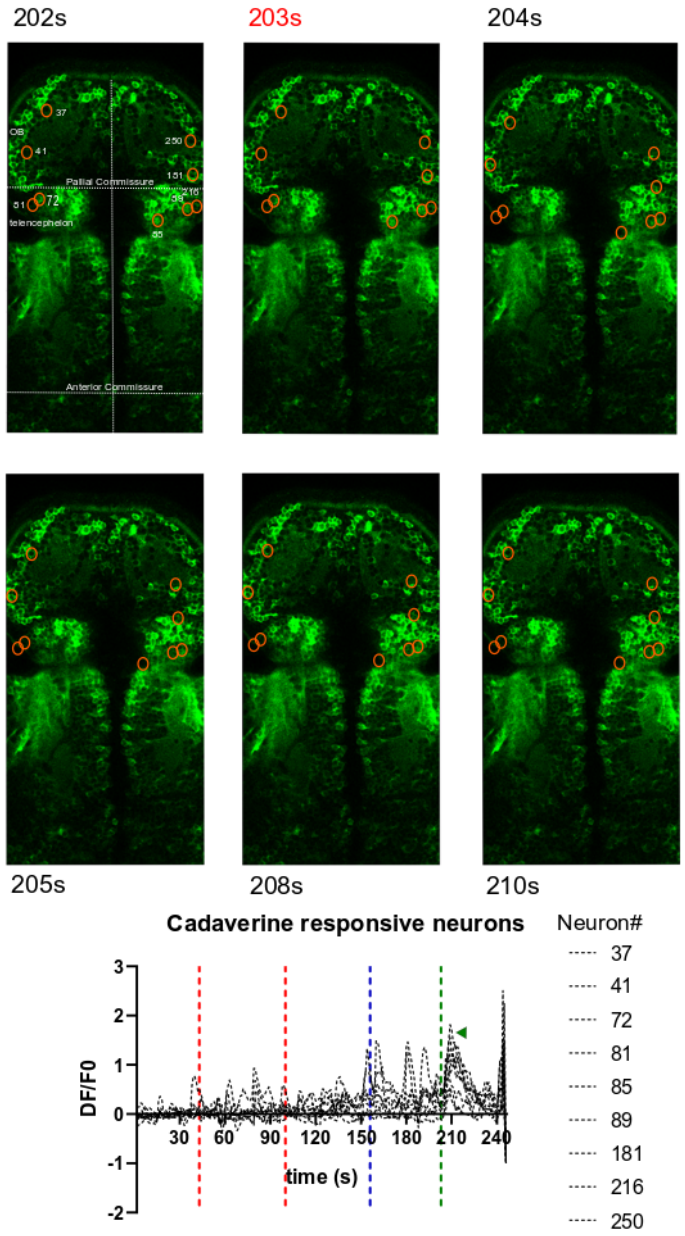

Figure 26 B: Cadaverine responsive neurons in the olfactory bulb. Experiments were conducted on (*elavl3*:: GCaMP6s) Tübingen strain**.** A pulse of cadaverine was given at 203s, indicated by dashed green line (in the graph below). Two pulses of alkaline pH indicated by dashed red line were given before cadaverine at 43s and 98s indicated. Majority of the neurons that responded to cadaverine did not respond to alkaline pH. Few cadaverine responsive neurons responded to neutral pH (indicated by dashed line). White dashed lines represent anatomical markers.

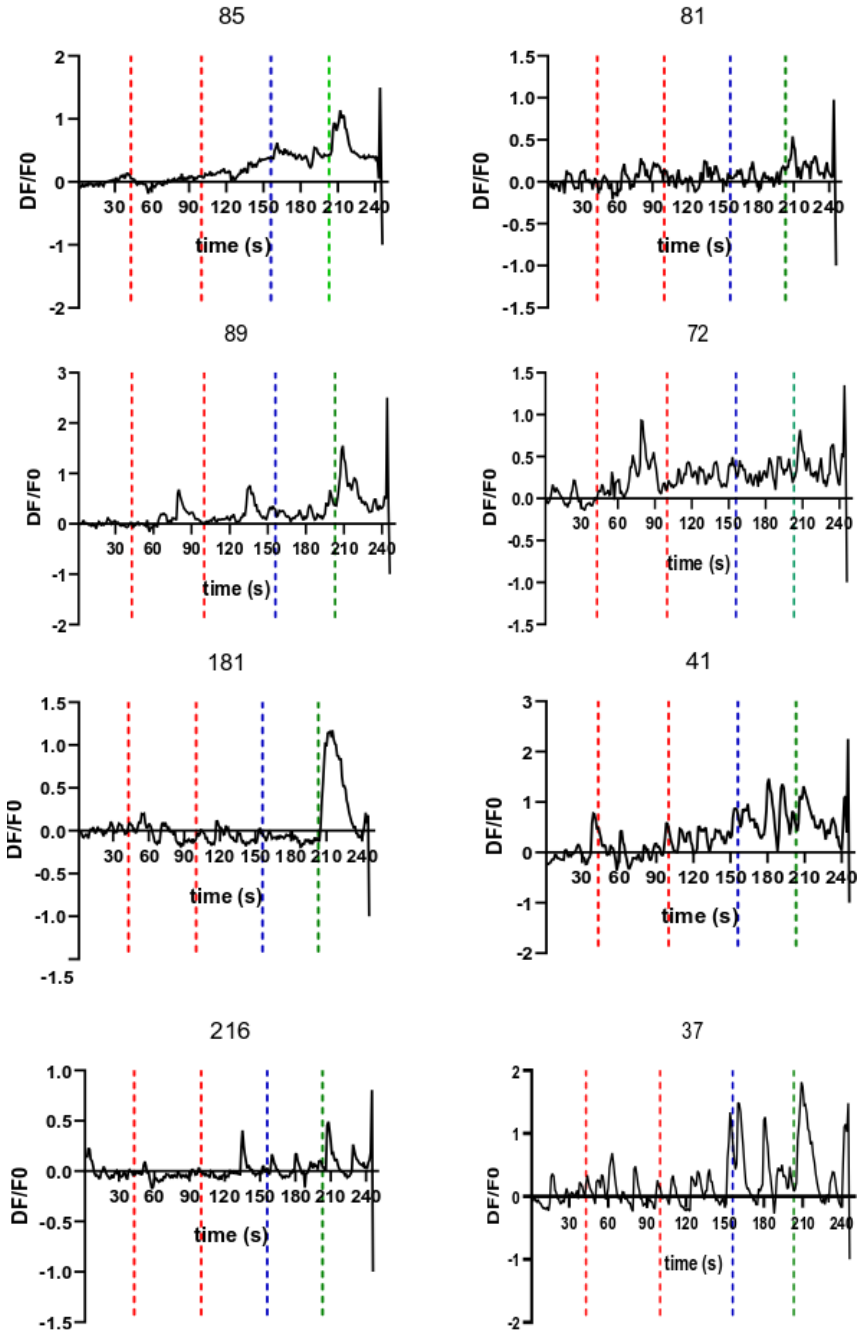

Figure 27: **DF/F0 Traces of individual neurons on cadaverine stimulation at 203s**. One of the neuron that responded to cadaverine also responded to alkaline pH. (indicated as red lines on the graph). Blue dashed line indicates neutral pH, red dashed line indicates alkaline stimulus, green dashed green line on indicates cadaverine stimulus. Sampling frequency 1Hz.

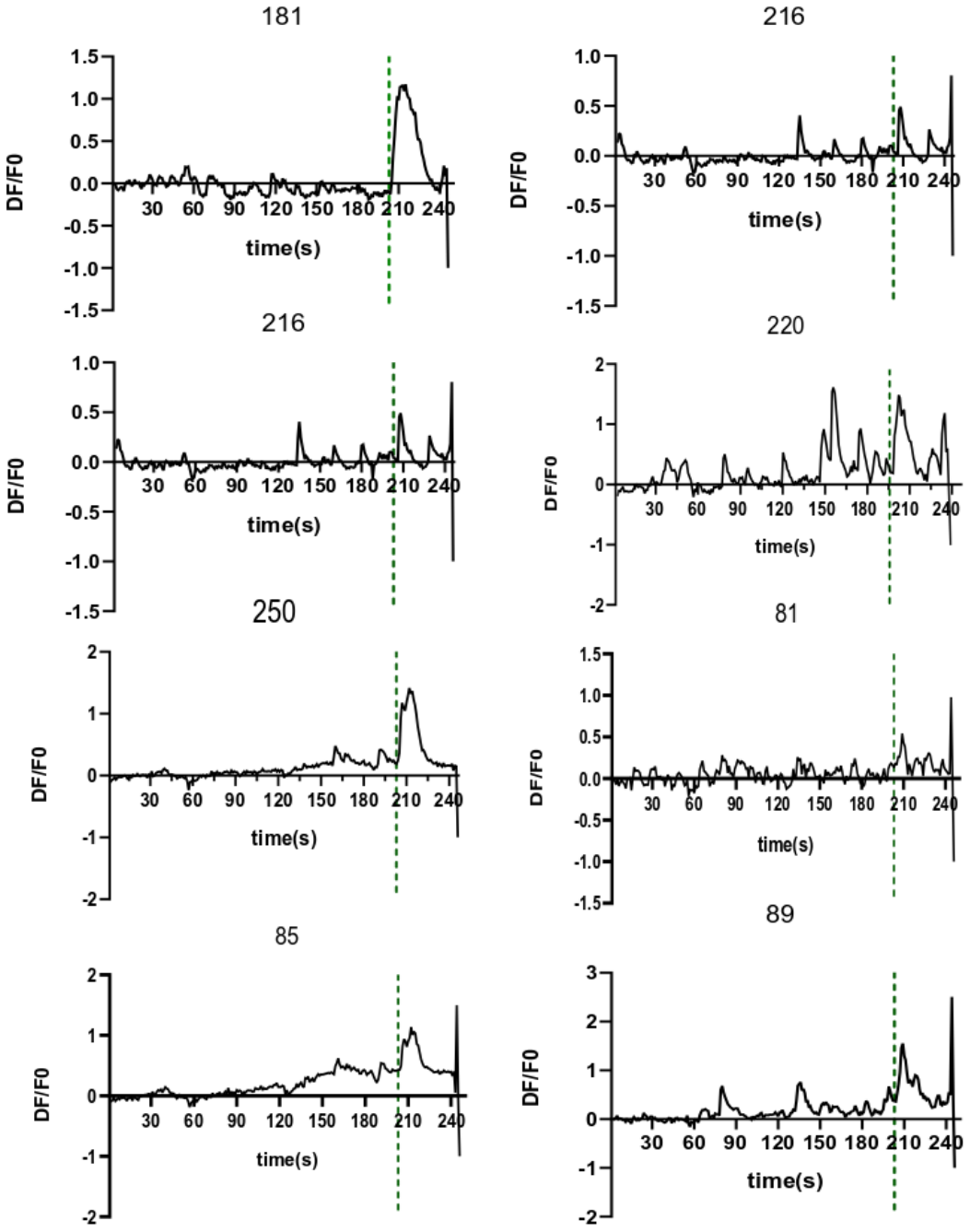

Figure 28: DF/F0 traces of individual neurons with cadaverine as stimulus at 203s (dashed green line).

.

4.14.4 Response of neurons to neutral pH (Tübingen strain)

Some of the neurons in the larva olfactory bulb and telencephalon responded to neutral pH with different amplitudes. These neurons did not exhibit a response peak on application of alkaline pH, at 43 and at 98s. No response peak was observed on the application of cadaverine at 203s (see Figure 29).

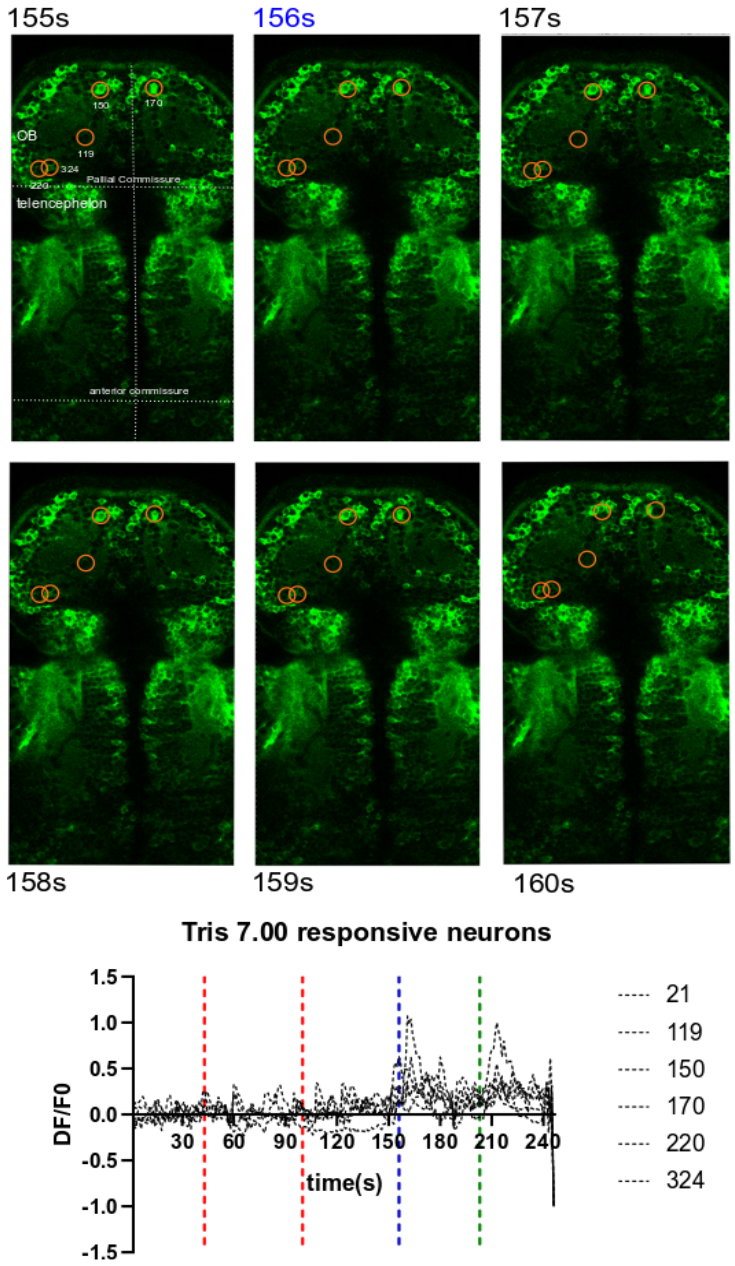

Figure 29: **Response of Neutral pH in the olfactory bulb**. Experiment performed on Tübingen strain fishes. Interestingly the neurons in the olfactory bulb of (*elavl3*:: GCaMP6s) that responded to neutral pH with a response peak (indicated by a blue dashed line, graph in the bottom panel) did not elicit a response peak on stimulation with alkaline pH (dashed red line) at 240s recording. Some (2 out of 5) of the neutral pH responsive neurons also responded to cadaverine (stimulus indicated by dashed green line) on x axis. Sampling frequency 1Hz. White dashed lines represent anatomical markers.

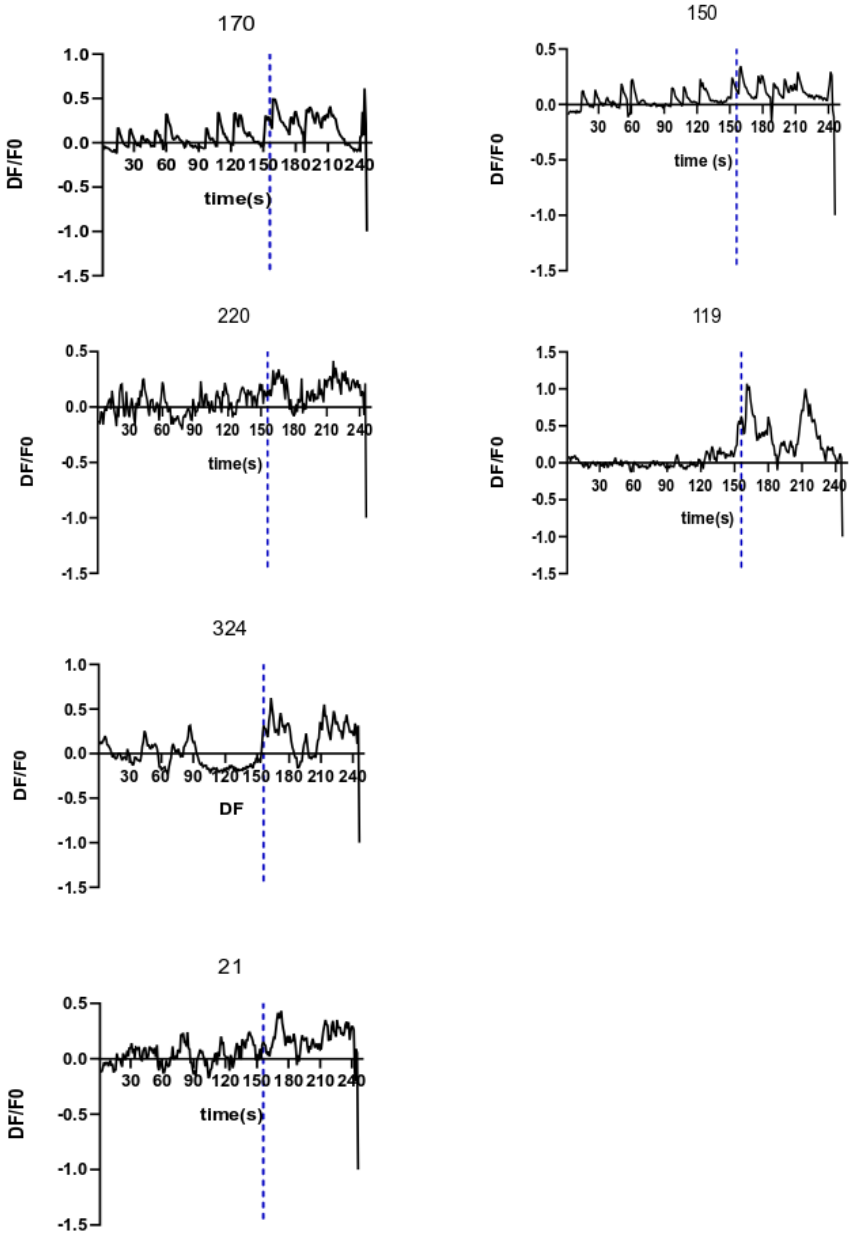

Figure 30: DF/F0 traces of individual neurons (*elavl3*:: GCaMP6s Tübingen strain) Neurons reacted to neutral pH (stimulus application is indicated by a blue dashed line on x-axis). Sampling frequency 1 Hz.

4.14.5 Response of neurons to alkaline pH (Tübingen strain)

Fibers of pallial commissure was used as an anatomical marker to locate the position of medio-dorsal cluster. When alkaline pH was given as an odor stimulus to the larva, a response peak was observed after the stimulation. When the stimulus was repeated at 98s 5 out of 6 alkaline responsive neurons responded again although with varying amplitudes (Figure 31, 32). Interestingly these neurons do not respond with a response peak on the application of neutral pH and cadaverine

4.14.6 Majority of the neurons responding to Cadaverine do not respond to alkaline pH in GCaMP6s larvae at 9 dpf

30 µl of alkaline pH was given as an odor pulse, at 43s as indicated in the line scans of the graphs in Figure (31, 32). Another pulse of 30 µl was given at 98s. Further neutral pH was given as a negative control. Cadaverine was given at 203s. From DF/F0 ratios it can be observed that majority of neurons that gave a response peak to cadaverine, did not show a response peak on the application of alkaline pH. However, one cadaverine responding neuron (neuron 37) also responded to neutral pH.

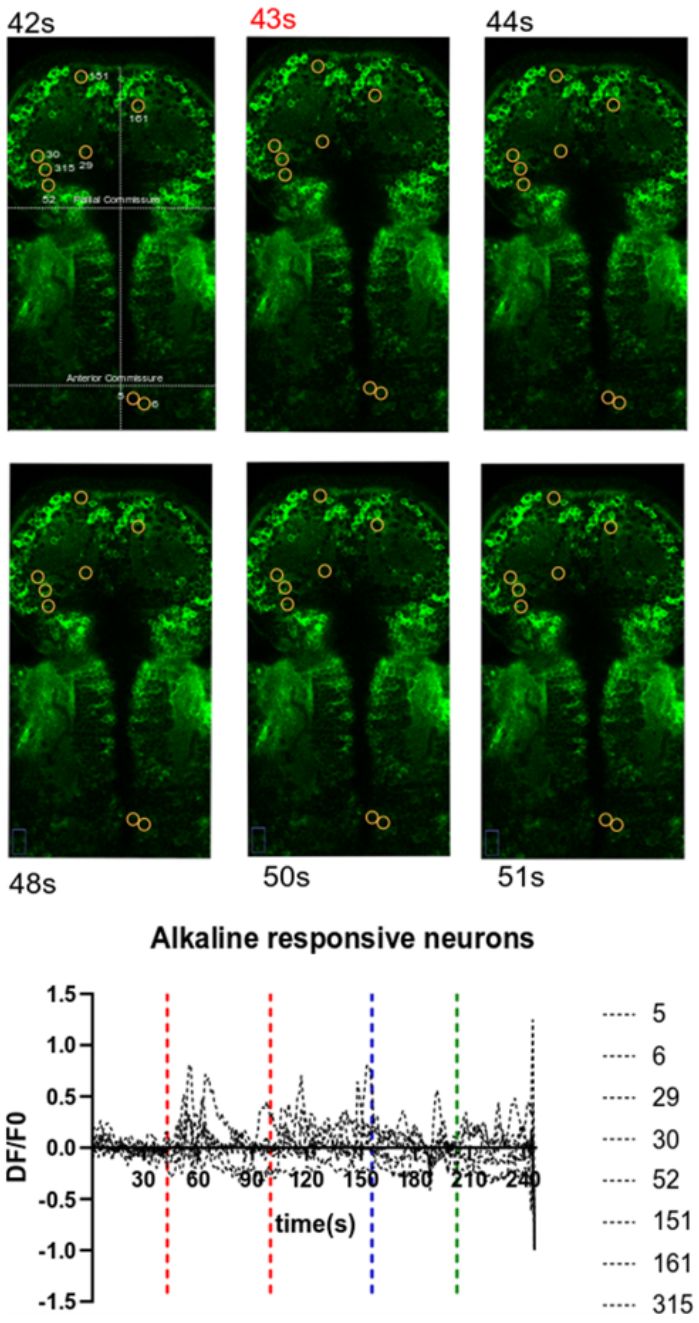

Figure 31: Response of alkaline pH in the olfactory bulb. Experiments performed on Tübingen strain fishes (*elavl3*:: GCaMP6s). Two pulses were given one at 43s as shown in the Figure (top panel), and other at 96s. Neurons that responded to alkaline pH (indicated by red dashed line) did not respond to neutral pH (indicated by dashed blue line on x axis).Cadaverine was given at 203s (indicated by dashed green line). Majority of the neurons that responded to neutral pH did not respond to Cadaverine**.** White dashed lines represent anatomical markers.

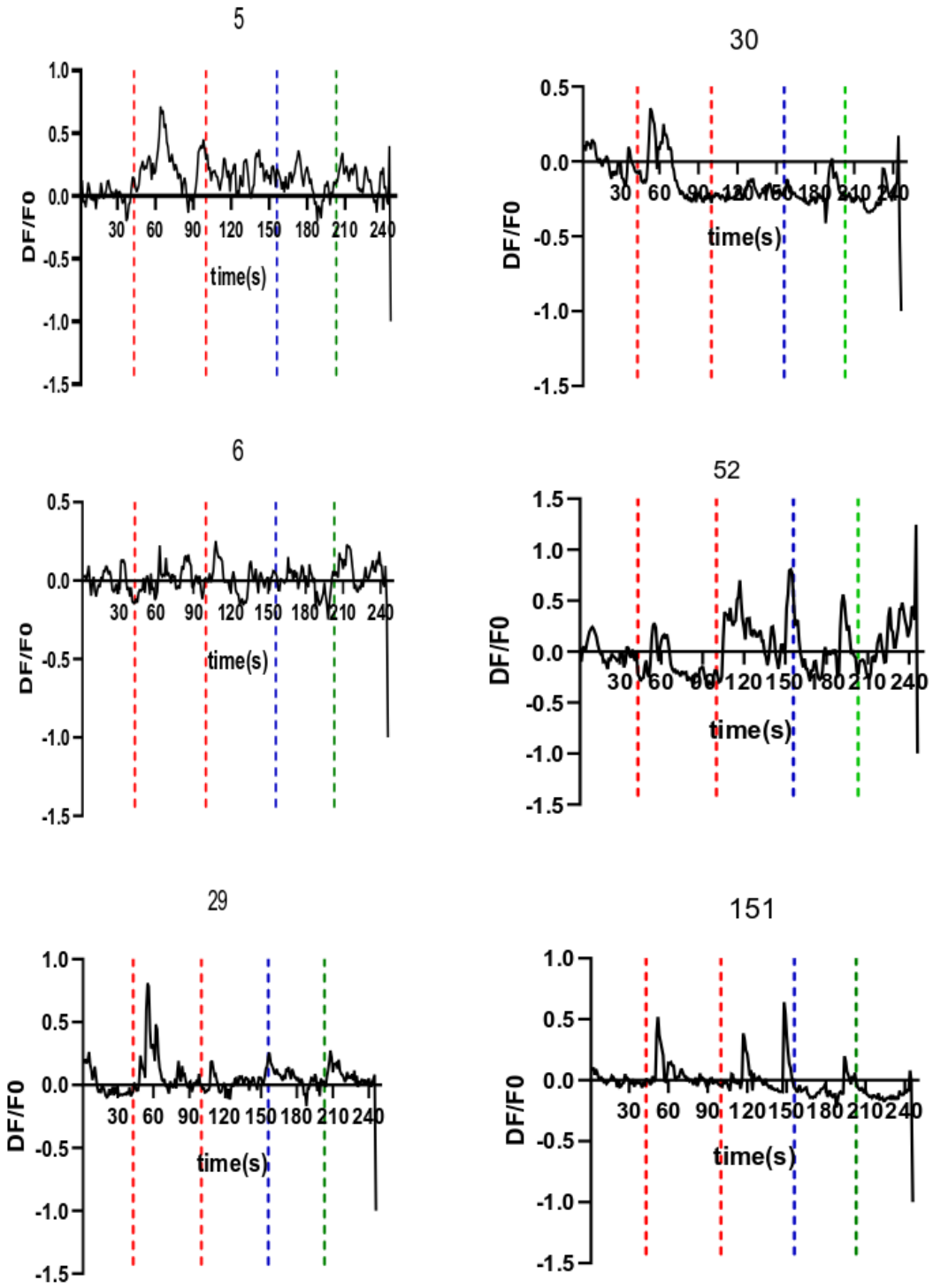

Figure 32: Alkaline response neurons. Experiments performed on Tübingen strain fishes. Pulses of 30µl of alkaline pH (indicated by dashed red line on x axis were given and 6 neurons responded to alkaline pH. Neurons that responded to alkaline pH did not responded cadaverine (see neuron 5, 6, 29, 151). 4 out of 6 neurons responded to the second stimulus of alkaline. None of the alkaline responsive neurons responded to neutral pH (indicated by blue line on x axis) and to cadaverine.

4.14.7 Responses of neurons to Cadaverine (Janelia strain)

We obtained stably expressing GCaMP6s lines with kind co-operation from Misha Ahrens lab at Janelia Campus. The fish lines were raised in our lab, mated after 3 months and 9 dpf embryos were used for experiments.

When a 30 µl pulse of cadaverine was given to the embryos, neurons exhibited a characteristic response spike on stimulation with 30 µl of Cadaverine Figure 33, 34). A total of 356 neurons were analyzed in the olfactory bulb and telencephalon. 8 neurons fulfilled our cutoff criteria as stimulus responsive neuron on the application of cadaverine. Majority of the neurons that responded to stimulus of Cadaverine did not respond to alkaline stimulus (see Figure 33). 1 out 8 Cadaverine responsive neurons also responded to alkaline pH (see Figure 33). E3 medium and Neutral pH was used as negative control. The neurons that responded to cadaverine did not respond to Tris and E3 medium (see Figure 33), indicating the reactivity of theses neurons to cadaverine.

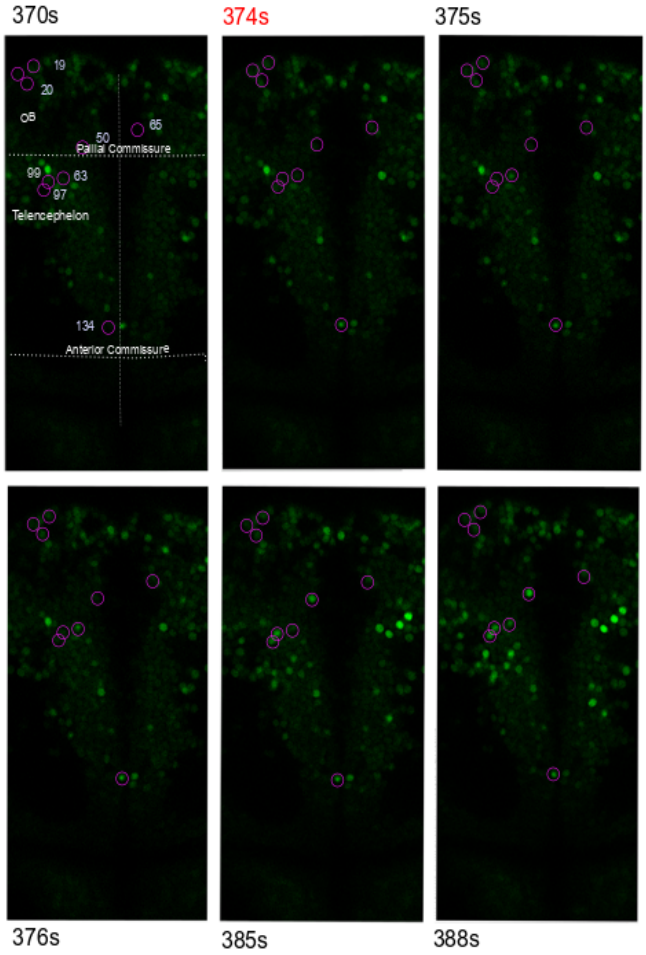

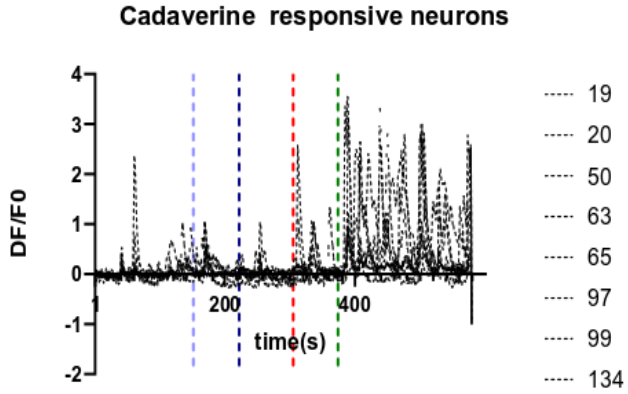

.

Figure legend on next page

Figure 33: Cadaverine responsive neurons in the olfactory bulb Experiments were performed (*elavl3*:: GCaMP6s), Janelia strain fish. A pulse of cadaverine was administered at 374s see top panel, indicated by green dashed line. 30µl of E3 medium was give as negative control at the start of recording at 98s (indicated by a light blue line on x axis), followed by neutral pH (indicated by blue dashed line). A pulse of alkaline pH was given before the administration of cadaverine (indicated by dashed red line) (see graph in the bottom panel). Sampling frequency 1Hz. White dashed lines represent anatomical markers.

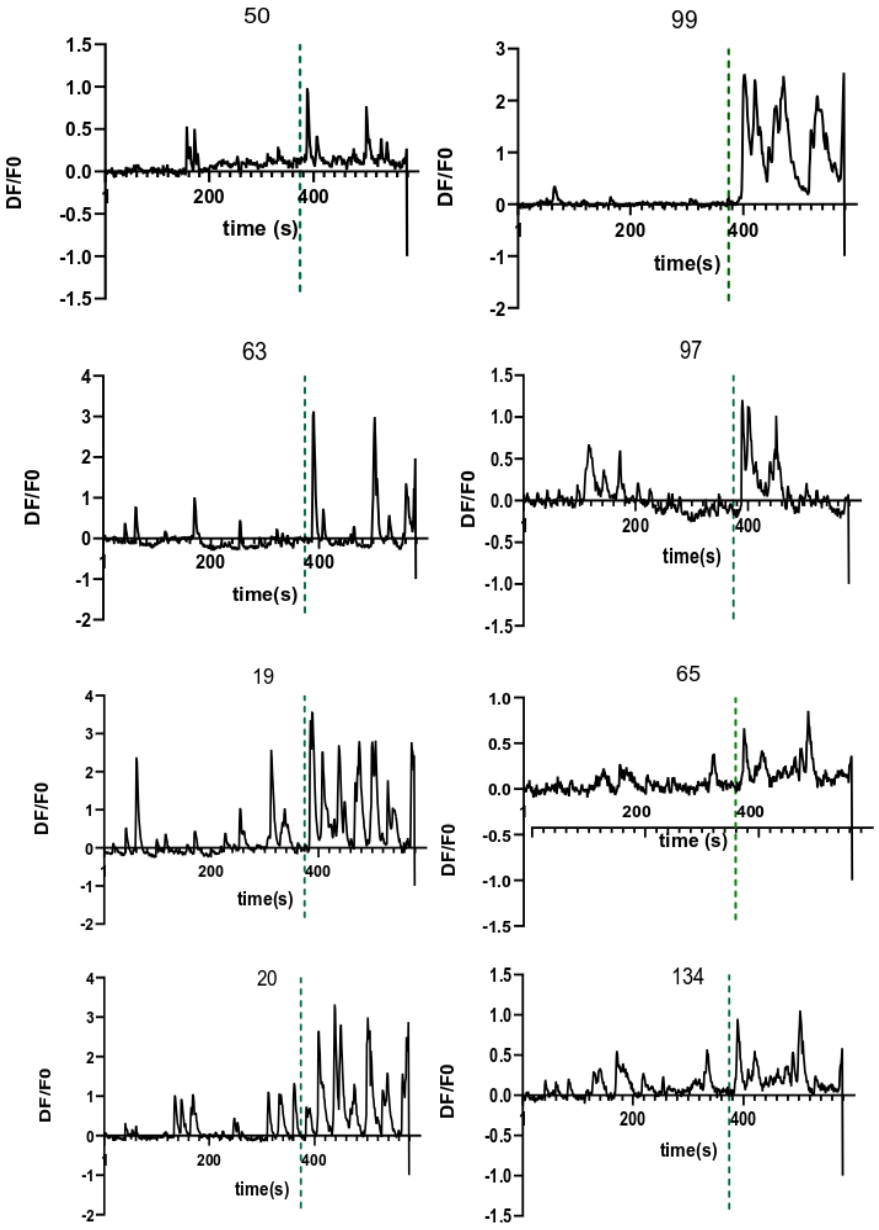

Figure 34: DF/F0 of individual neuron responding to Cadaverine at 374s.

4.14.8 Response of neurons to alkaline pH (Janelia strain)

On introducing a 30 µl odor pulse of alkaline, a spike in the DF/F0 for certain neurons was observed. Around 300 neurons in the olfactory bulb and telencephalon were analyzed. The neurons that qualified the cut off criteria (see section Results /Analysis pipeline) were considered as responsive neurons to alkaline pH. Out of 300 neurons 8 neurons qualified our criteria (see Results/Analysis pipeline). On looking at these neurons on the dorsal surface of larvae, 2 neurons were present at telencephalon, 2 neurons at medio-dorsal cluster, 2 neurons in the dorsal cluster and 1 neuron in the dorsolateral cluster. The position of these neurons was not exclusive to medio-dorsal cluster, as we would have expected (see figure, 25, 42 and 43). 3 out of 6 alkaline responsive neurons also responded to cadaverine (see Figure 37)

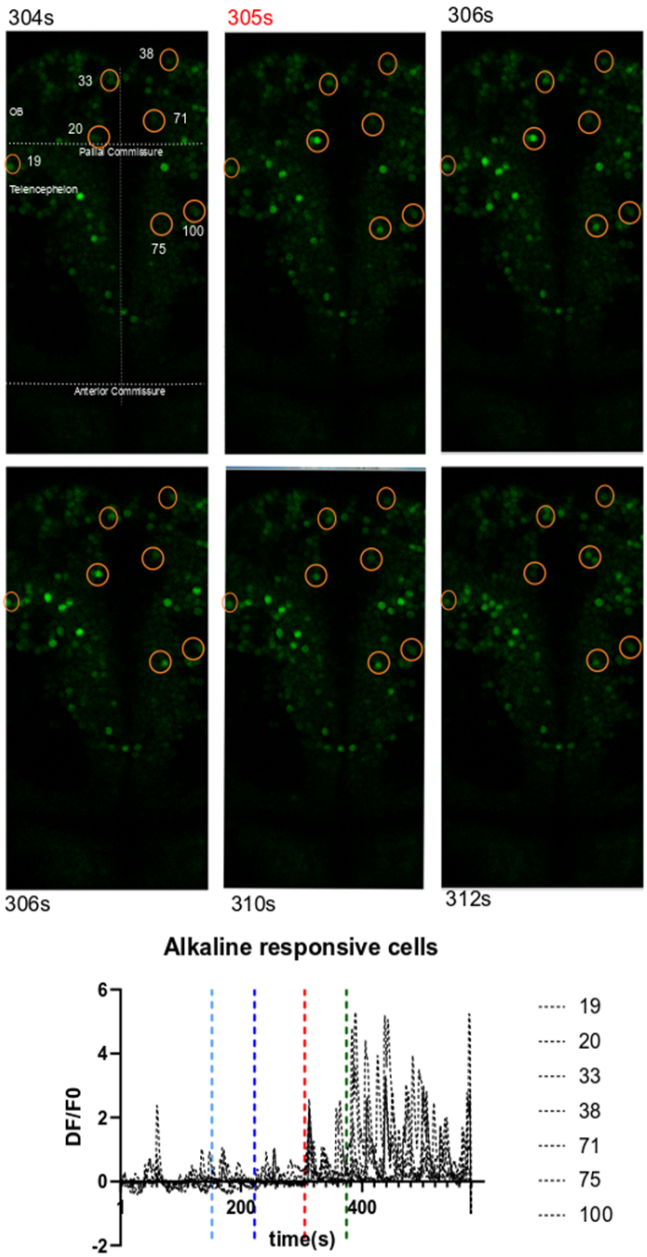

Figure 35: Response of alkaline pH in the olfactory bulb Experiments were performed on (*elavl3*:: GCaMP6s), Janelia strain fish . A pulse was at 305s (top panel) given one at 43s indicated as a dashed line as shown in the Figure (top panel). Neurons that responded to alkaline pH did not respond to Neutral pH (indicated by a blue dashed line on x axis). Cadaverine was given at 374s indicated by a dashed green line. Few neurons that responded to alkaline pH also responded to cadaverine. Majority of the neurons that responded cadaverine did not respond to neutral pH (indicated by dashed dark blue line on the x axis). E3 medium was given as a negative control, neither of alkaline responsive neurons responded to E3. White dashed lines represent anatomical markers.

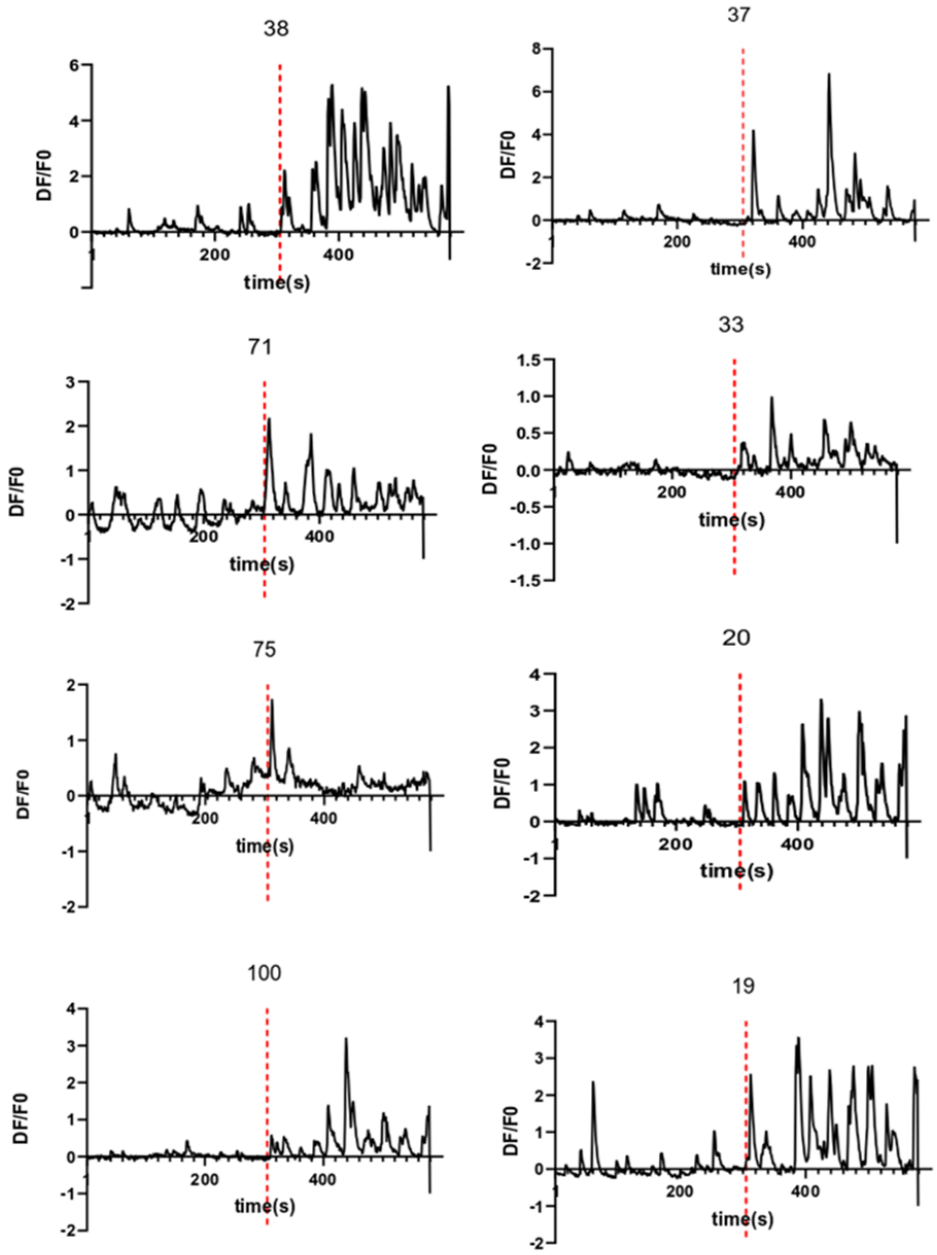

Figure 36: DF/F0 traces of individual neurons that responded to alkaline pH (*elavl3*:: GCaMP6s), Janelia strain (stimulus application indicated by dashed red line on x axis).

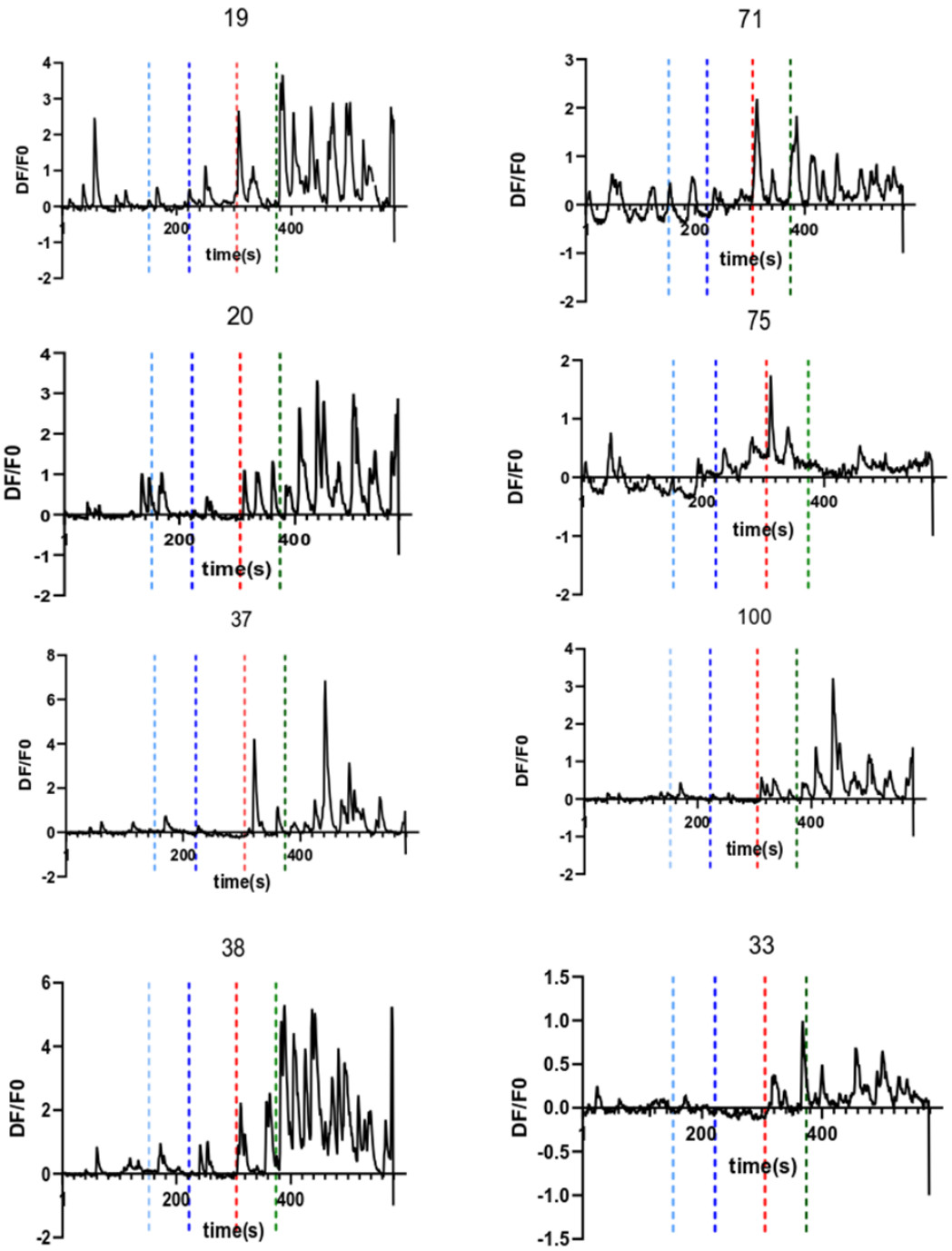

Figure 37: DF/F0 traces of individual neurons (*elavl3*:: GCaMP6s), Janelia strain. A pulse of alkaline pH (indicated by dashed red line on x-axis) was given at 305s. 4 out of 6 neurons that responded to alkaline pH also responded to cadaverine (indicated by dashed green line on x-axis). Neither of the alkaline responsive neurons responded to pH 7.00 or to E3.

4.14.9 Responses of Neutral pH and E3 medium (Janelia strain)

Some neurons in these larvae also responded to neutral pH and E3 medium (Figure 38, 40). However, these responses were not specific to E3 medium or neutral pH. Neurons that respond to neutral pH also responded to E3 medium, alkaline pH and cadaverine (Figure 38, 40). Thus, no specificity in the response could be seen, indicating that these responses can be motion artefacts due to stimulus pulse given to the larva.

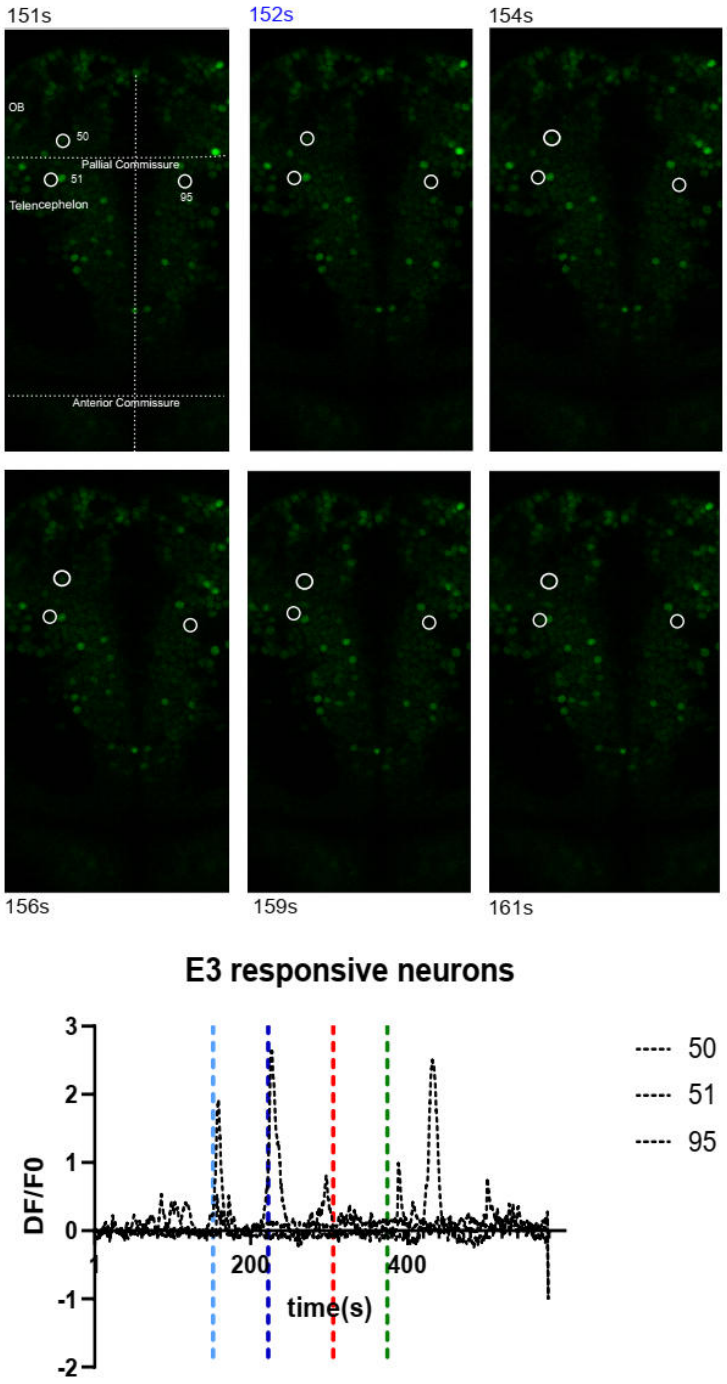

Figure 38: E3 responsive neurons. Few neurons were observed in 9 dpf larve (*elavl3*:: GCaMP6s) larvae that responded to 30µl stimulation of E3 (indicated by light blue line on x-axis, see graph in the bottom panel). E3 responsive neuron also responded to neutral pH (indicated by violet line on the x-axis) and to Cadaverine (indicated by green line on x axis), White dashed lines represents anatomical markers.

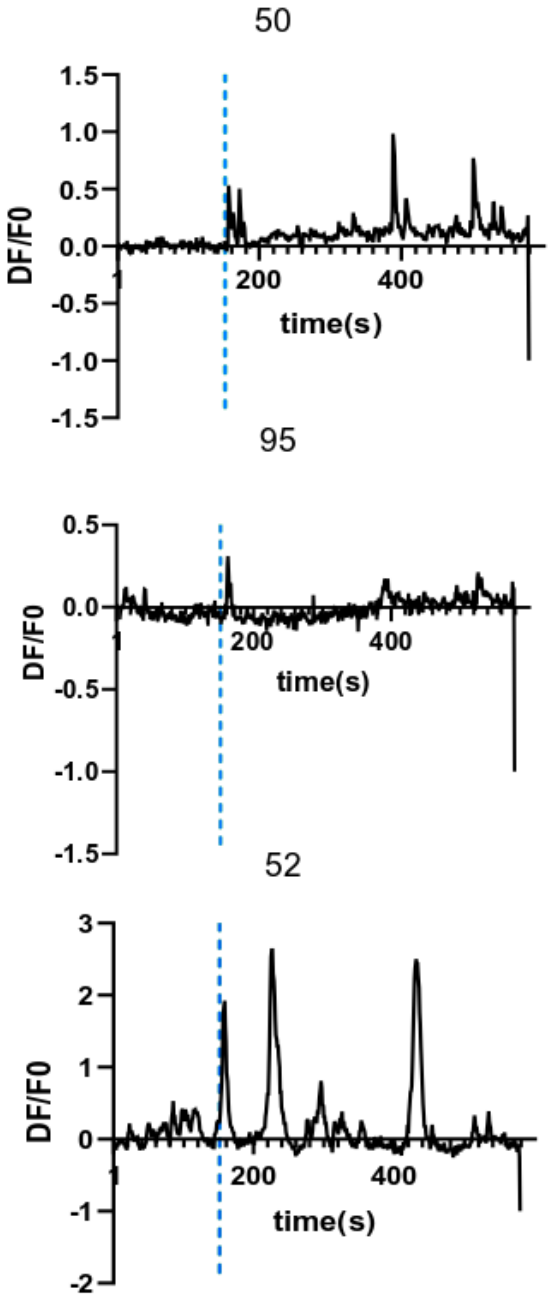

Figure 39: Individual traces of E3 responsive neurons (*elavl3*:: GCaMP6s), Janelia strain The blue dashed line on x-axis indicates the time of stimulus application.

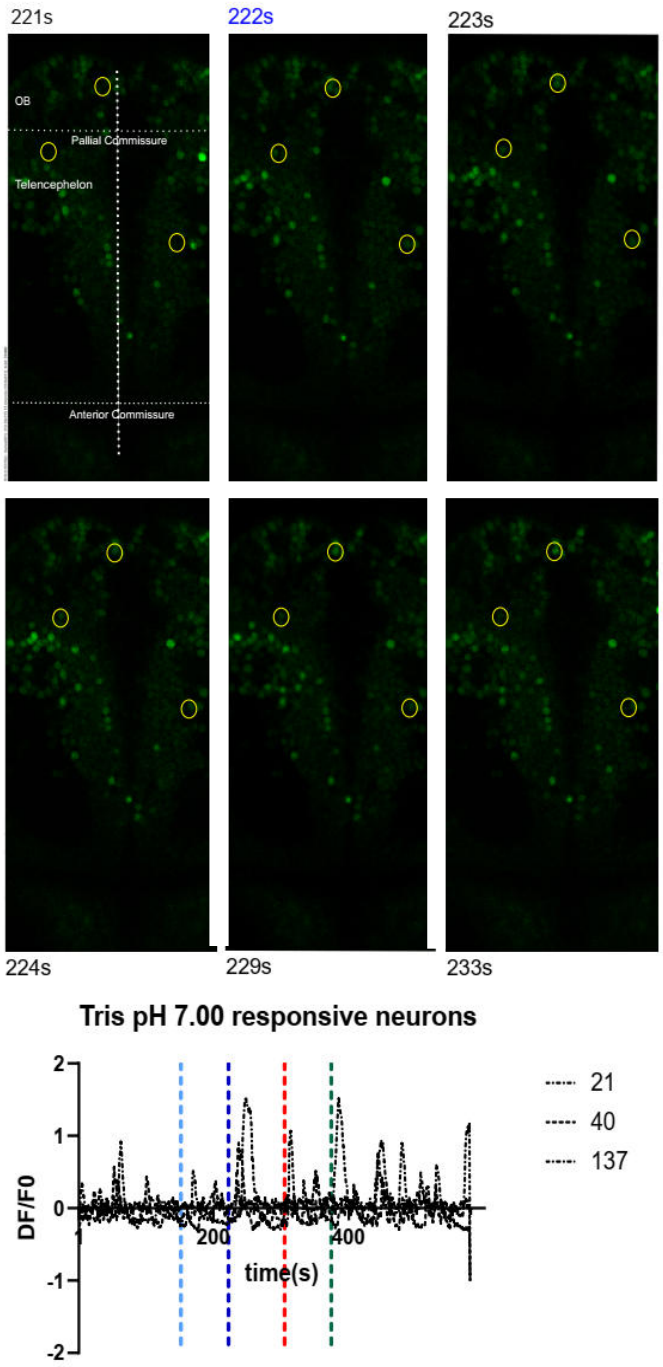

Figure 40: Response of the neuron to neutral pH. Experiments were done on *elavl3*:: GCaMP6s, Janelia strain fishes**.** 30µl of Tris was given at 222s (indicated by dashed green blue line on x-axis).1 out of 3 neutral pH responding neuron also responded to cadaverine(indicated by dashed green line on x-axis) and alkaline pH (indicated by red line on x-axis). Sampling frequency 1 Hz. White dashed lines represent anatomical markers.

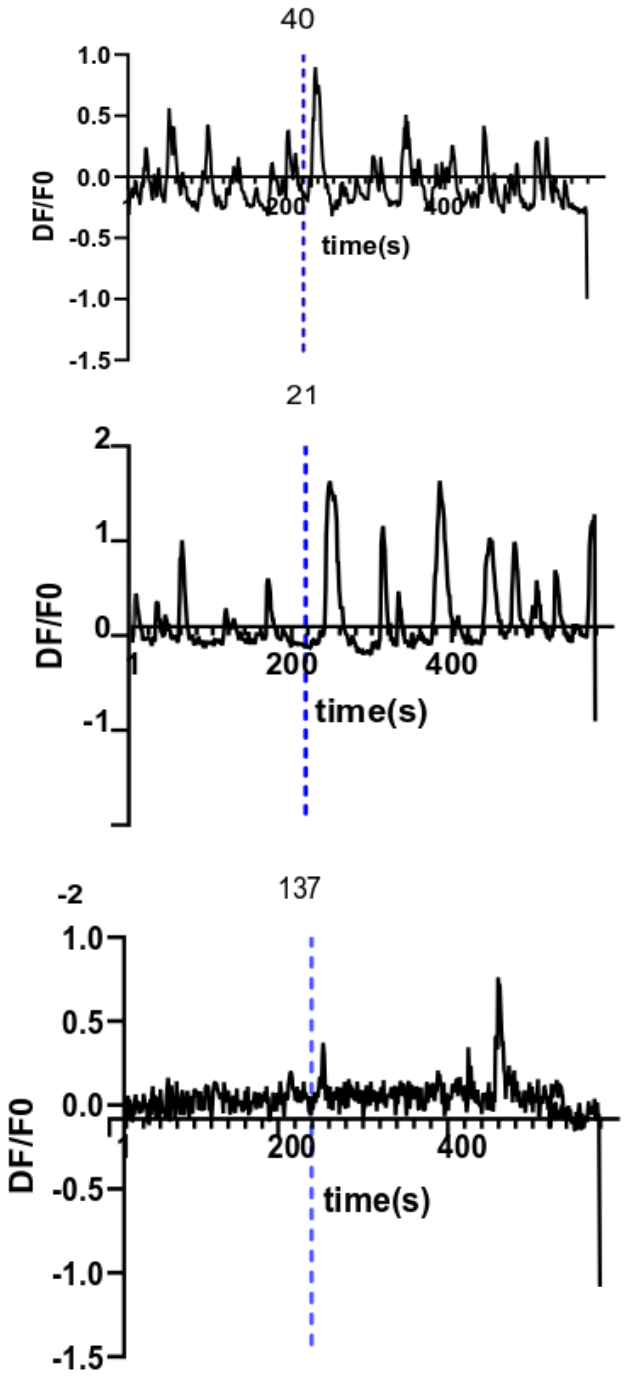

Figure 41: DF/F0 traces pH 7.00 responding neurons (stimulus application is represented by dashed blue line on x-axis).

4.14.10 Medio-dorsal cluster and dorsal cluster predominantly responded to alkaline stimulus in olfactory bulb of elavl3:: GCaMP6s 9 dpf larvae

On observing the videos obtained from calcium imaging experiment for *elavl3*:: GCaMP6s Janelia Campus strain, positions for the Region of Interest (ROI) associated with an odor responsive neuron were traced. Their location was identified using pallial commissure as an anatomical marker situated on the boundary of olfactory bulb and telencephalon. Pooling the data from 4 different larvae analyzed indicated that alkaline responsive neurons were majorly situated in the medio-dorsal (Mdg) and dorsal glomerulus (DG) (Figure 44 top panel). Some of the alkaline responsive neurons were also found in dorsolateral cluster.

Dorsolateral cluster (DLG) in adult zebrafish responded to cadaverine (Dieris et al., 2017). However, in larval zebrafish cadaverine reactivity in olfactory bulb was not limited to dorsolateral cluster. (Figure 42, top panel. Mdg and DG also responded to cadaverine. Neutral pH did not elicit an excitatory response in the olfactory bulb. As majority of the neutral pH responsive neurons were found to be in telencephalon. E3 responsive neurons were found to be distributed throughout olfactory bulb and telencephalon (Figure 42, bottom panel).

In Tübingen strain, *elavl3*::GCaMP6s, alkaline responsive neurons were located in medio-dorsal (Mdg) and dorsal glomerulus (DG) Figure (43, top panel). Dorsolateral cluster responded with very few alkaline responsive neurons (Figure 44, top left graph).

Neutral pH produced no response in the olfactory bulb of zebrafish. Of all the neurons analyzed in 3 larvae, neutral pH responsive neurons were in telencephalon. (Figure 43, bottom left graph). Consistent with the Janelia fish strain, alkaline reactivity in 9 dpf Tubingen strain larvae was also not limited only to medio-dorsal cluster (Figure 43) Similarly , no topology was observed in cadaverine responsive neurons, as they were also present in medio-dorsal (mdg) and dorsal cluster (DG) (Figure 43)

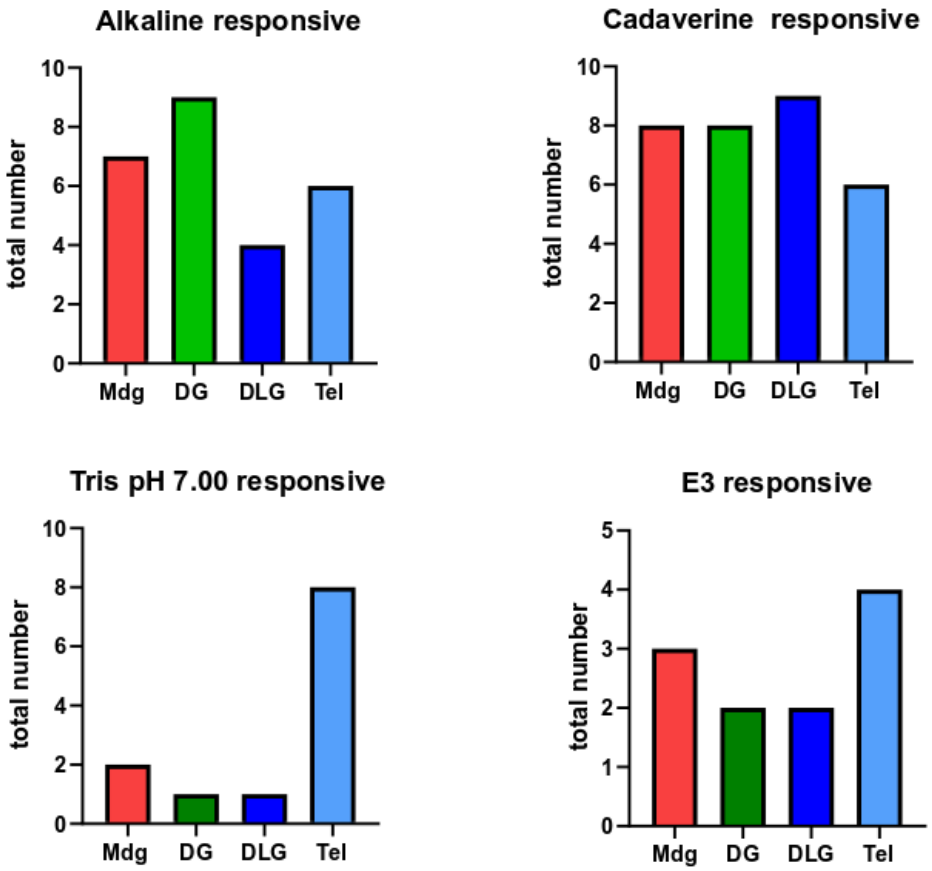

Figure 42: Location of neurons that responded to various stimuli (*elavl3*:: GCaMP6s), Janelia strain The position of neuron was traced to the location of corresponding ROI (Region of interest) on the surface of olfactory bulb. As it can be seen from top panel that alkaline and cadaverine responsive neurons were not clustered to a specific region in the olfactory bulb but were distributed at different locations in the OB. The same can be observed in E3 responsive neurons (bottom panel right graph). Majority of neutral pH (Tris pH 7.00) responsive neurons were in telencephalon (bottom left panel).

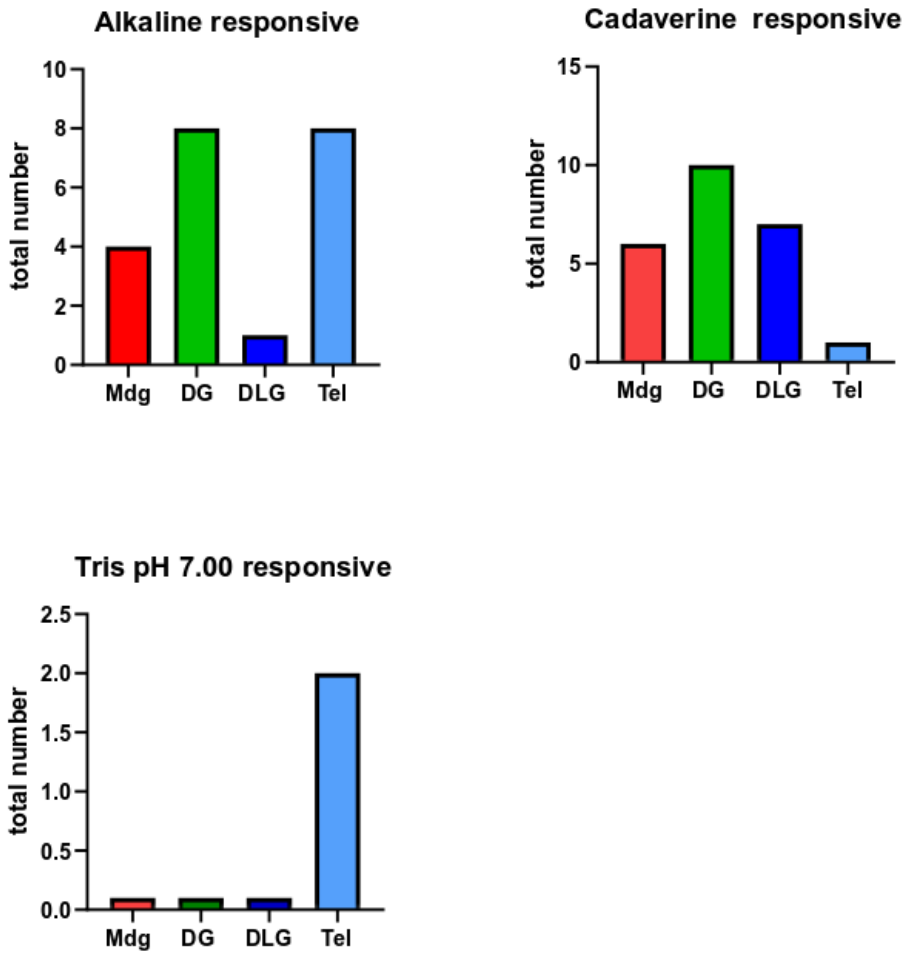

Figure 43: Location of stimulus responsive neurons. (*elavl3*::GCaMP6s), Tübingen strain Alkaline responsive neurons were distributed throughout the OB (top panel right graph). The same could be seen with cadaverine responsive neurons (top right panel). No neutral pH (Tris pH 7.00) responsive neurons were seen in the OB (Bottom left panel). E3 responsive neurons were not able to qualify our criteria both in olfactory bulb as well as in telencephalon, and hence are not represented in the graph.

4.14.11 Neutral pH and E3 medium do not stimulate significant number of neurons in the medio-dorsal and dorsal glomerulus

When the data was pooled from all the recordings and it was observed that neutral pH when tested as an odor in calcium imaging experiments significantly excited a smaller number of neurons/larvae as compared to alkaline pH in medio-dorsal cluster (*p=0.0293, unpaired t-test) (Figure 44, top panel). There was a significant difference in the total number of neurons/larvae that responded to cadaverine in medio-dorsal glomerulus as compared to neutral pH (**p=0.031, unpaired t-test), (Figure44, top panel).

In Dorsal glomerulus alkaline and cadaverine responders/larvae were significantly greater than neutral pH responding neurons (**p=0.0067, unpaired t-test), (*p=0.0406, unpaired t-test) respectively (Figure44, top panel). There was no significant difference in alkaline responders/larvae and cadaverine responders/larvae in dorsal glomerulus.

Neurons in telencephalon responded to all 4-stimului presented to larvae in calcium imaging experiments. There was no significant difference in the number of responding neurons/ larvae in between different stimulus presented (Figure 44, bottom right panel).

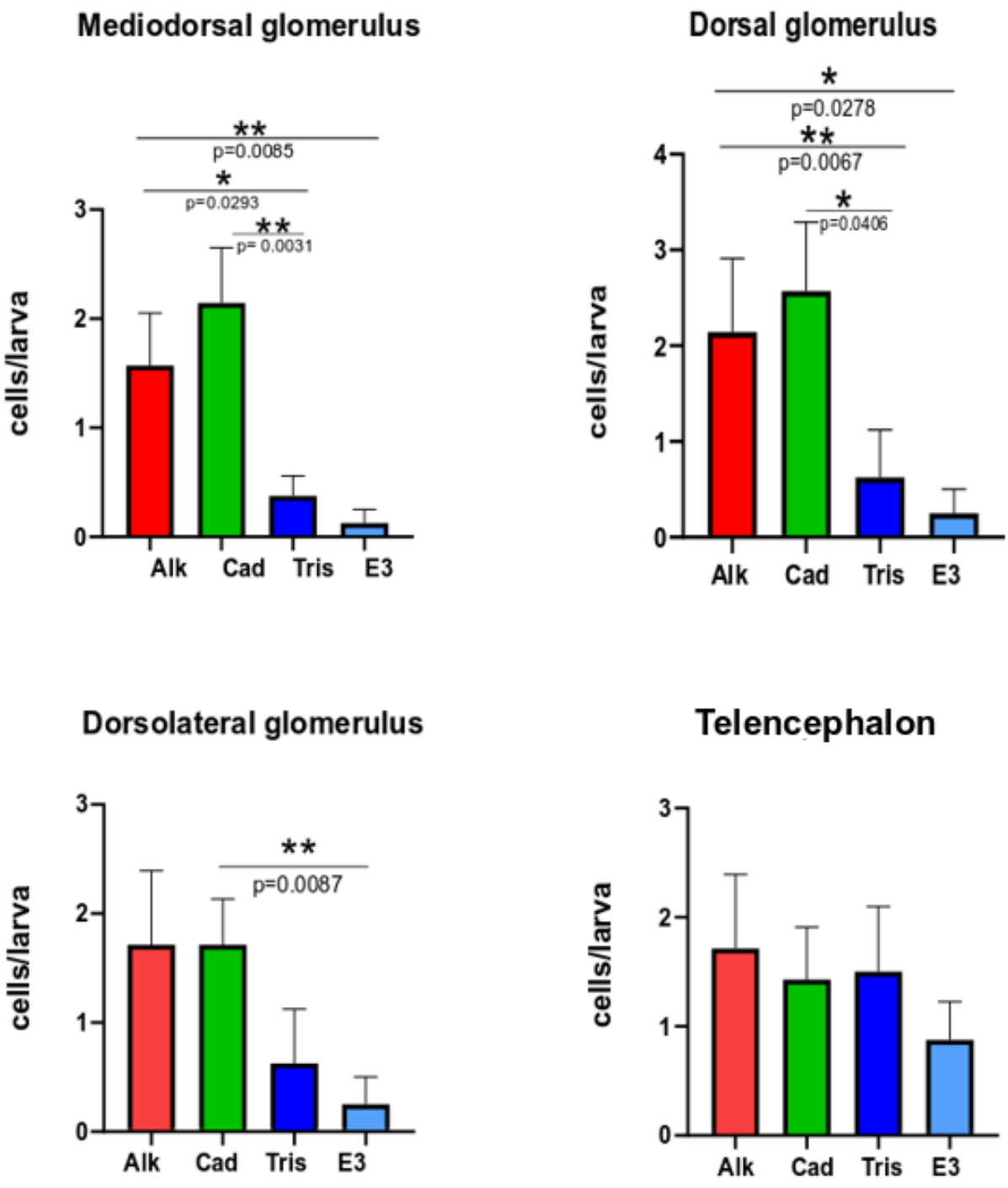

Figure legend on next page

Figure 44 : Neutral pH and E3 medium do not stimulate significant number of neurons in the medio-dorsal and dorsal glomerulus Neutral pH (indicated as Tris) excited significantly a smaller number of neurons/larvae as compared to alkaline pH (Alk) in medio-dorsal cluster (*p=0.0293, unpaired t-test) top panel left. Medio-dorsal cluster (Mdg) also responded to cadaverine. Significant difference in the total number of neurons/larvae was observed that responded cadaverine (cad) as compared to neutral pH (**p=0.031), in medio-dorsal glomerulus. There was no significant difference in the neurons/larvae between neutral pH and E3 responsive neurons. In Dorsal glomerulus alkaline responders/larvae were significantly greater than neutral pH responding neurons (*p=0.0406, unpaired t-test). In dorsolateral cluster there was only significant difference in between cadaverine and E3 responsive neurons (**p=0.0087, unpaired t-test).

4.12 Qualitative analysis of stimulus responsive neurons

4.12.1 Janelia Campus Strain

Based on neuroanatomical locations, neurons were divided either belonging to olfactory bulb or telencephalon. Qualitative properties of the neurons such as half width, amplitude and delay to peak were analysed. In the olfactory bulb, it was found that there was a significant difference in the average half width of alkaline and E3 responsive neurons (**p=0.002, unpaired t test). (Figure 45, top panel). There was also a significant difference in the half width of cadaverine and E3 responsive neurons (**p= 0.002, unpaired t- test). Average half width of neutral pH responsive neurons was also different from E3 responsive neurons (**p= 0.012). However, there was no significant difference in between the amplitudes and delay to peak times among different population of neurons responding to different stimuli (Figure 45), top panel.

In telencephalon, alkaline responsive neurons had the largest half widths and amplitudes when compared to the half widths of cadaverine and neutral pH responsive neurons. However, there was no significant difference in any of the qualitative parameter among the different population of neurons responding to alkaline, neutral pH or to cadaverine (Figure 45, bottom panel).

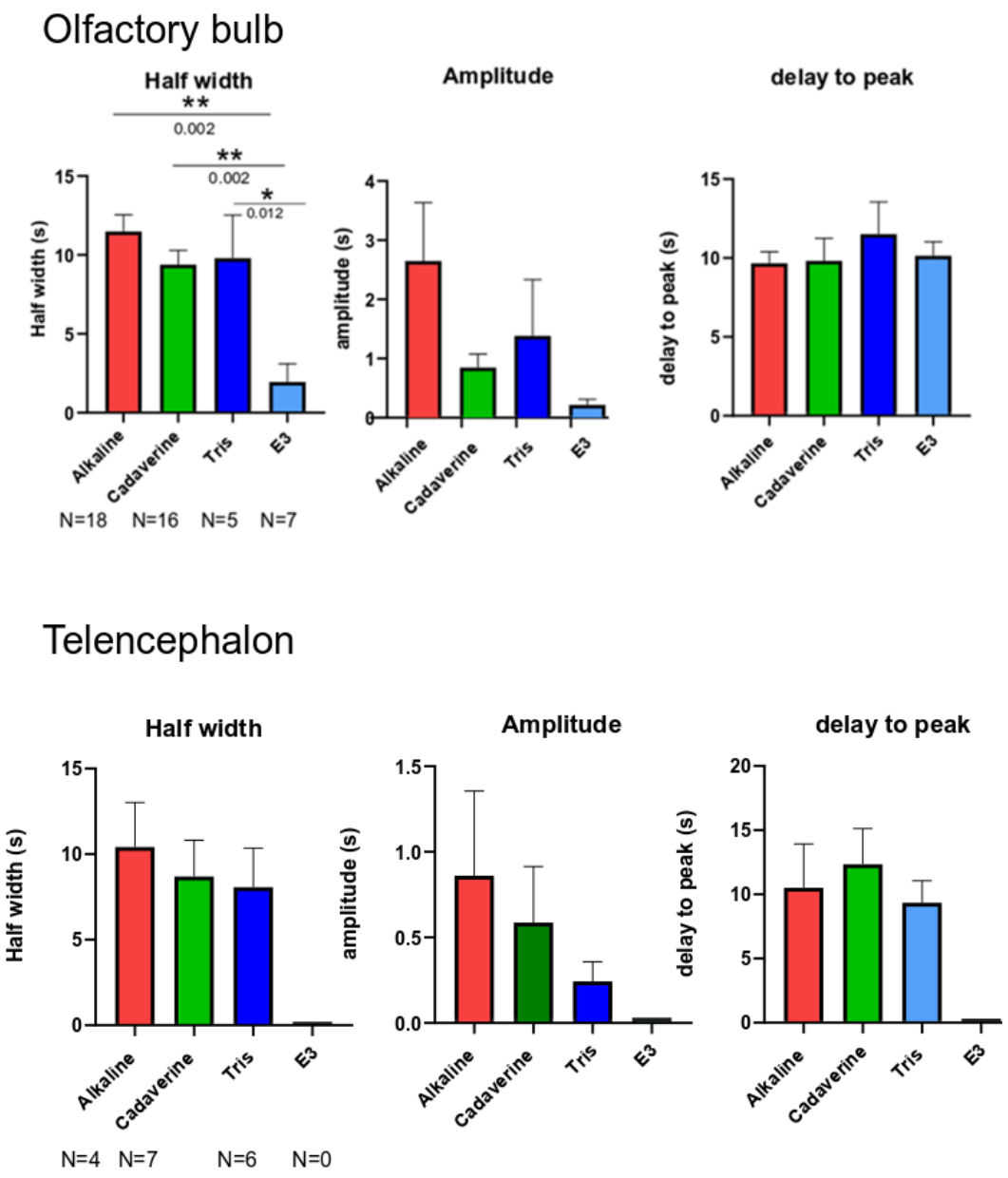

Figure 45: Qualitative analysis of stimulus responsive neurons Janelia strain (*elavl3*::GCaMP6s)

In the olfactory bulb a significant difference in the half widths was observed in between alkaline and cadaverine responsive neurons (*p=0.0465, unpaired t test top panel left graph) In the olfactory bulb, there was also a significant difference in the half width of cadaverine and E3 responsive neurons (**p= 0.002, unpaired t- test). Average half width of neutral pH (indicated as Tris) responsive neurons was also different from E3 responsive neurons (**p= 0.012). However, there was no significant difference in between the amplitudes and delay to peak times among different population of neurons responding to different stimuli, (top panel). In telencephalon, alkaline responsive neurons had the largest half widths and amplitudes when compared to the half widths of cadaverine and neutral pH responsive neurons.

4.12.2 Tübingen Strain

For analysis neurons were segregated based on neuroanatomical locations either belonging to olfactory bulb or telencephalon. On analysing the half width of stimulus responsive neurons in the olfactory bulb, a significant difference was observed in between alkaline and cadaverine responsive neurons (*p=0.0465, unpaired t-test) (Figure46, top panel). There was no significant difference in the half width between alkaline and neutral pH responsive neurons (Figure 46, top panel). No significant difference was found in the amplitudes among neurons responding to different stimuli. Alkaline responsive neurons display the longest delay to peak times and there was a significant difference in delay to peak time between alkaline and neutral pH responsive neurons (*p=0.0147, t-test) (Figure 46, top panel)

In telencephalon, alkaline responsive neurons display the shortest half width and there was a significant difference in the half width among the alkaline and cadaverine responsive neurons (**p=0.0038, unpaired t-test) (Figure 46 bottom panel). Alkaline responsive neurons in telencephalon also displayed the shortest amplitude which was significantly different from cadaverine responsive neurons (*p=0.0164, t-test), and neutral pH responsive neurons (***p=0.006 t-test), while neutral pH responsive neurons (Figure 46, bottom panel). There was no significant difference in the delay to peak response among alkaline, cadaverine and neutral pH responsive neurons.

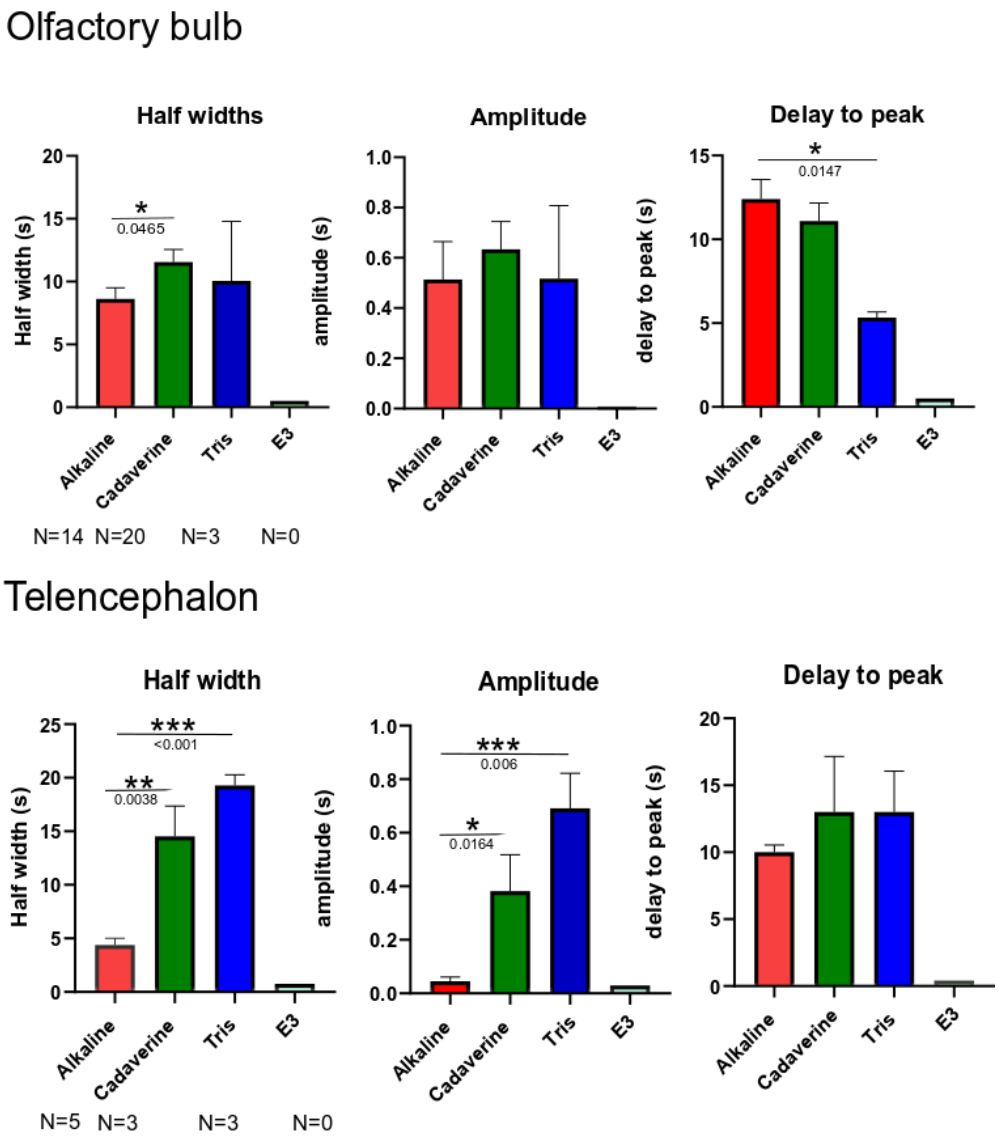

Figure 46: Qualitative analysis of stimulus responsive neurons Tübingen strain (*elavl3::GCaMp6s*)

In the olfactory bulb, a significant difference was observed in the half width between alkaline and cadaverine responsive neurons (*p=0.0465, unpaired t test) top panel. There was no significant difference in the half width between alkaline and Neutral pH responsive neurons, top panel. No significant difference was found in the amplitudes among neurons responding to different stimuli. Alkaline responsive neurons display the longest delay to peak times and there was a significant difference among delay to peak time between alkaline and Neutral pH responsive neurons (*p=0.0147, unpaired t test), top panel)

In telencephalon, alkaline responsive neurons display the shortest half width and there was a significant difference in the half width among the alkaline and Cadaverine responsive neurons (**p=0.0038, unpaired t test) (bottom panel). Alkaline responsive neurons in telencephalon also displayed the shortest amplitude which was significantly different from cadaverine responsive neurons (*p=0.0164, unpaired t test), and Neutral pH responsive neurons (***p=0.006), while Neutral pH responsive neurons, bottom panel. There was no significant difference in the delay to peak response among alkaline, cadaverine and Neutral pH responsive neurons.

5. Discussion

In the last decade zebrafish has emerged as a potent model organism for neuroscience research. They have a well-developed nervous system and have an ability to give behavior output in response to a wide variety of stimuli. The stimulus can be in the form of an odor e.g. cadaverine (Hussain et al., 2013), visual stimulus in the form of moving prey (Bianco et al., 2011), and auditory stimulus (Zeddies and Fay, 2005). Odor information is taken up by the olfactory sensory neurons in the olfactory bulb and processed in the higher olfactory centers such as habenula to give a behavior output (Miyasaka et al., 2009). Attractive and aversive behavior have been studied in adult zebrafish (Hussain et al., 2013), (Namekawa et al., 2018). Amino acids act as an olfactory cue to elicit an attractive response in adult zebrafish via microvillous olfactory sensory neurons (Friedrich and Korsching, 1997; Koide et al., 2009), while cadaverine has found to be eliciting aversive response in adult zebrafish (Hussain et al., 2013), via ciliated olfactory sensory neurons (Dieris et al., 2017)

Crypt neurons project their axons to medio-dorsal cluster of the olfactory bulb, mdg2 (Ahuja et al., 2013). One of the receptors form the ORA gene family “ORA4” was found to be expressed exclusively in crypt neurons, giving them a “one neuron-one receptor type” mode of expression (Oka et al., 2012). Hence it is interesting to find the function of ORA4 receptor and its physiological role in the zebrafish olfaction.

5.1 ORA4 Receptor is not essential for the survival of crypt neurons

A CRISPR/Cas 9 knockout for ORA 4 receptor was generated in our lab (Liu and Korsching unpublished). Using Anti-TrkA antibody staining we found out that crypt neurons do not require the ORA4 receptor to survive. Crypt neurons were also present in ORA4-/- zebrafish. They do not maintain their globular morphology in adult ORA4-/- zebrafish (Figure 13), and were found to be significantly more slender IN ORA4-/- as compared to WT. The olfactory receptors are G-protein coupled receptors, once activated they initiate downstream signaling cascade leading to a variety of physiological processes, (Kang and Koo, 2012). In the absence of ORA4 receptor, the downstream

signaling cascades in the crypt neurons is compromised, which might be affecting the maturation and the development of globular morphology ORA4-/- adult zebrafish. It was also observed that more number of crypt neurons were present in ORA4-/- 6 dpf larval and adult zebrafish as compared to WT. (see figure 13). The rise in the number of crypt neurons in knockout can be a mechanism to compensate for the loss of receptor. The ORA gene family consists of six olfactory genes in teleost fish (7 in zebrafish) which are highly conserved (Saraiva and Korsching, 2007; Zapilko and Korsching, 2016). Neurons may choose another ORA receptor as compensation and thereby survive, similar to what has been observed in another olfactory receptor family (Johnson et al., 2012)

Since crypt neurons survive the ORA4 knockout we can test the role of ORA4 in crypt neuron responses.

First, we checked whether activation by alkaline pH reported in heterologous expression can also be observed in vivo and crypt neurons remain functional in ORA 4-/- background.

To ask this question we needed to know whether alkaline pH (Behrens and Korsching unpublished observation), reported to be a ligand for ORA4 receptor, also reacts to crypt neurons in-vivo in live animal.

5.2 Immediate early genes as a marker for neuronal activity

In the mammalian system, several immediate early genes, such as c-Fos, Arc, p-Erk have been used as indicator of neuronal activity since their expression gets transiently upregulated upon neuronal activation. In this manner, the location of neurons critical for generating different behavior such as attraction, aversion, mating, sleep, pain sensitivity and drug addiction has been identified (Gao and Ji, 2009). The downstream components of mitogen activated proteins (MAP) kinases mediate a wide variety of cellular behaviors in response to an external stimulus (Zarubin and Han, 2005).

Phosphorylated extracellular signal-regulated-kinase (ERK, also known as mitogen-activated MAP kinase) (Ji et al., 1999) has been used in studies to localize active neurons including zebrafish (Dieris et al., 2016). After stimulus or a tissue injury c-Fos starts to be induced after 30-60 minutes, whereas p-Erk can be induced within few minutes of

stimulus (Gao and Ji., 2009). Recent studies with p-Erk showed 7 minutes of stimulus presentation to obtain the best signal to noise ratio in staining of larval zebrafish (Biechl et al., 2016). In my optimization studies 3 minutes of stimulus for adult zebrafish was optimal (Dieris et al., 2017). I found that medio-dorsal cluster was faintly labelled as compared to dorsal and dorsolateral cluster in the olfactory bulb of adult zebrafish on stimulating the fish with alkaline pH (Figure 23). This was unexpected because medio-dorsal cluster (mdg2) is a target glomerulus for crypt neurons (Ahuja et al., 2013). This was the first attempt to the best to our knowledge to check the neural circuits activated in response to alkaline stimulus in adult zebrafish. These results would suggest that olfactory sensory neurons projecting to dorsal and dorsolateral cluster (ciliated neurons) (Friedrich and Korsching, 1998) (Miyasaka et al., 2009) (Dieris et al., 2016), might be reacting to alkaline pH, but do not support such a response for crypt neurons, which do project to one of the mediodorsal glomeruli. However, the high variability of the p-Erk labeling does not allow a firm conclusion. Therefore, we switched to live calcium imaging (see below) to get a clearer understanding of the neural circuits which are activated by alkaline stimulus.

5.3 Zebrafish larval behavior in response to alkaline stimulus

Adult zebrafish displayed attraction to alkaline pH (Ahuja and Korsching, unpublished observation). We wanted to ask whether the same applies to larval zebrafish. Zebrafish larvae display locomotive behavior from 4 dpf onwards (Lindsay and Vogt., 2004). From 5 dpf, the yolk sac supporting the larvae begins to diminish, and they get motivated to look for food source (Lindsay and Vogt., 2004). Two channel choice setup was used to check the response of adult zebrafish presented with 100μM cadaverine (Hussian et al., 2013). For larval zebrafish we made a setup that was much simpler to use. It contained a plexiglass chamber which consisting of 14 lanes 20 cm long, 2cm wide and 10 ml of E3 medium could be added in each lane. 9dpf larvae were used for this setup as it was observed that at 9 dpf majority of larvae displayed locomotive behavior in multilane setup (data not shown). We found that 9 dpf larvae displayed significant attraction to food odor vs E3. There was no significant preference for neutral pH/E3 but there was significant attraction for alkaline pH vs E3 (see Figure 19)

From these experiments it can be concluded that zebrafish larvae preferred alkaline pH over neutral pH or E3 medium. The evaluation for these experiments was cumbersome, as the entire evaluation was performed manually using a video camera and stopping the video after every 30s to mark the position index of the larvae. This process also left room for human error. Therefore, I established an automated tracking system using Rasberry Pi camera with infra-red background.

The increase in the velocity has been used as a parameter for attractive behavior in zebrafish larva (Chen et al., 2019). Along with increase in velocity, there was also a significant decrease in the distance from the center with alkaline pH, i.e larvae preferred to stay close to the source of stimulus. These two parameters indicate a preference for alkalinity by zebrafish larvae, consistent with the initial results with the multilane setup. Animals were not starved before the experiment for the automated tracking system, in contrast to the multilane setup, and hence this preference was not based on the metabolic state of the larvae (results in Figure 19 and 21).

5.4 What could be the physiological meaning of preference for alkaline pH?

Animals effectively secrete ammonia (NH_3) as a product of protein metabolism, to avoid the toxic effects associated with its accumulation in the body fluids (Kumai et al., 2011). Fresh water fish like zebrafish secrete ammonia as a direct waste product because fresh water provides an ambient reservoir for continuous secretion of ammonia (Wright and Wood 1995). There are multiple mechanisms for zebrafish to let go off the ammonia load form the body (Chew et al., 2005). In adults the gills are the major source of ammonia excretion, and the dominant models indicates that branchial ammonia is excreted from freshwater fish mainly through blood to water ammonia gradients (Shih et al., 2008). In zebrafish larvae there are multiple sources of ammonia secretion, including snout, kidneys, and yolk sac, in which yolk sac of larvae plays an important in ammonia secretion (Shih et al., 2008). Ammonia is a strong base, 1M aqueous solution of ammonia has a pH of 11.63, (Ullman Encyclopedia of Industrial Chemistry, 2006). There is a speculation for possibility that attraction for alkalinity might be larval preference for secreted ammonia. Since larvae zebrafish have small size, and limited ability to defend themselves against

predators, they tend to shoal together (Miller and Gerlai, 2007). Thus, sensing secreted ammonia might come as an added advantage indicating a shoal of fish larvae nearby, promoting the survival of zebrafish larvae.

5.5 Ctrax for tracking zebrafish larvae

Ctrax is an open source, freely available machine vision program for estimating simultaneously the orientations of many animals, originally developed to quantify the behavior of multiple walking flies in the arena (Branson et al., 2009). In the recent years, Ctrax has been extensively used to study the behavior of zebrafish larvae (Ingebretson and Masino, 2013). Zebrafish larvae are small compared to adult fish and this presents a challenge in their detection by tracking software. One of the key requirements for detecting the larvae without losing the animal in any frame is a creation of a uniform background. Infra-red light helps in setting a uniform background and increasing the animal body to background contrast, so software can detect the edges of the larvae without losing the larvae in any frame.

Another important issue is the reflection from the edges of the petri-dish. The reflections on the edge are considered as another animal by Ctrax while tracking the larvae, which results in changing the identity of the animal. To solve this issue, I cut out the arena from an agarose-filled large petri dish. The agarose well edges completely removed the reflection of the larvae. We optimized the size and shape of this agarose well, together with agarose concentration and infrared lighting. A 34.5 mm in diameter and 1.5 cm deep agarose well was scooped out in a petri dish filled with 1% agarose gel. Once the experimental conditions are optimized, Ctrax was very effective in tracing the larvae throughout the recording. Occasional jumps were corrected using fix-error MATLAB script (Branson et al., 2009), which helps in maintain the identity of the animal before and after the jupm

5.6 Advantage of Ctrax over id Tracker

Another widely used zebrafish tracking software that can track and maintain the identity of a single fish among a pool of fish is idTracker (Escudero et al., 2014). This makes idTracker suitable for analysing group behaviour in adult zebrafish. I attempted to use idTracker to track the zebrafish larvae. I found that idTracker was able to identify the larvae, and also to track them if there is one larvae/arena (as was the case in my experiments) but it was not able to maintain the identity of that larva over the entire

recording. During recording zebrafish larvae sometimes jumps over few millimetres known as startle reflex (Schier et al., 2019) (Privat and Sumbre, 2020). Larvae usually can get scared or excited by several factors, including the presentation of stimulus in the arena, movement in the surroundings etc. If the jumps in a 3-minute recording are limited to 1 or 2, it does not disturb the overall co-ordinates of the trajectory, but it loses the co-ordinates of the tracking for few frames before and after the jump, and the software does not provide a mechanism to fix the gaps in the trajectory. Thus, after the jump the track is interpreted as belonging to another larva. idTracker also require high speed computers and excellent video quality to get reliable videos, which were not available in the lab.

On the other hand, Ctrax gives a fix-error MATLAB script (Branson et al., 2009), this script helps in fixing the errors such as sudden jumps and identity swapping, which saves a lot of time and reduces the number of trials required due to higher percentage of valid experiments. Ctrax is designed to function with standard laptop and desktop computers and commercially available IR-sensitive cameras, which makes it very user friendly.

5.7 GCaMP as a calcium indicator for analyzing neural networks in zebrafish larvae

Multiple neurons in the nervous system form a functional unit to perform a task. The net outcome of the neuronal activity is in the form of a behavioral output. There are various set of tools and techniques that exist, which have their own set of advantages and disadvantages. Electrophysiological recordings using electrodes have been widely used to study the cellular properties of the neurons (Steriade et al., 2011). These methods havthe advantage of providing detailed temporal resolution but are limited by the number of neurons that can be studied simultaneously.

Optical imaging using bolus loaded of AM esters dyes has allowed for the recording at high spatial resolution from many neurons at the same time (Stosiek et al., 2003; Helmchen and Denk, 2005). The advantage of using calcium indicators over electrophysiological recordings is that it provides a read out of the neural activity from multiple neurons or from a population of neurons. Calcium dyes have been successfully

used in understanding the chemotropic odorant coding in the olfactory bulb of adult zebrafish (Friedrich and Korsching, 1997). Calcium loading dyes results in high background and residual fluorescence as well as nonspecific labelling due to the lack of genetic control (Stosiek et al., 2003). They have also been reported not to be fit for with long imaging sessions due to bleaching (Aramuni and Griesbeck, 2013). Calcium loading dyes and electrode methods are highly invasive to the cell and making the long recording with the tissue much difficult to achieve (Polikov et al., 2005).

Genetically encoded calcium indicators (GECI) with the combination of modern microscopy techniques such as confocal and multi-photon microscopy, have been used for imagining multiple neurons in live zebrafish expressed under the cell specific promoter (Ahrens et al., 2013). GECIs have allowed for the non-invasive measurements for the cellular properties across a neural circuit in a live behaving animal.

GCaMP as a genetically encoded calcium indictor has been useful because it can be introduced into the neurons of interest using a suitable promoter and can measure calcium influx upon voltage changes in the neuron (Nakai et al., 2001). GCaMP-HS as a calcium indicator has been successfully expressed and studied in spinal motor neurons in zebrafish and the fluorescence changes in GCAMP-HS were perfectly matched with actual muscle contraction, indicating the robust calcium dynamics (Muto and Kawakami, 2011).

In the nervous system, to identify the neurons which are responsible for performing a cognitive task, a sensitive calcium indicator is required which can report activity in the individual neuron in vivo. GCaMP3 expressed under the *elavl3* promoter in zebrafish was initially used as calcium indicator to study the attractive/aversive circuits in zebrafish habenula (Krishna et al., 2014). A modified version GCaMP3, with faster kinetics have been developed over the period of time called GCaMP6s. Pan neural expression of GCaMP6s under the *elavl3* promoter have been used to study and analyze the neuronal activity in optokinetic response in the midbrain (Wang et al., 2020) and food seeking behavior in right dorsal habenula (Chen et al., 2019). Selective expression of GCaMP6s in the optic tectum of the midbrain has been used study the prey capture in zebrafish

larvae (Muto and Kawakami., 2016). Thus, making GCaMP6s a non-invasive tissue specific expressing calcium imaging dye.

For our experimental setup we wanted to find the response of alkaline pH in the olfactory bulb of the 9 dpf zebrafish larvae. Imaging experiments were conducted keeping in focus the medio dorsal cluster 2 (mdg2) which is the target area for crypt neurons in the olfactory bulb. Calcium responses were recorded from the mitral and tufted neurons in the OB.

For my experimental findings we did not observed any topology in the alkaline responsive neurons (see Figure 42 and 43). The same was observed for cadaverine responding neurons (see figure 42 and 43). However, in adult zebrafish, a single identified glomerulus was activated in response to 100μM cadaverine (see section figure) which was consistent with the findings of Dieris et al. (2017).

However, I did not observe any topology in the spatial distribution of alkaline-responsive neurons in the adult zebrafish olfactory bulb (see figure 42, 43, 45, 46). This is consistent with a two-photon calcium imaging study by Gerlach et al. (2019), which did not find kin-odor responsive neurons situated exclusively around medio-dorsal cluster. In an earlier study using p-Erk as marker of neuronal activation they had shown crypt neurons to react to zebrafish kin odor (Biechl et al., 2016). Interestingly, in that study, the mediodorsal area did respond specifically to the kin odor. It is possible that despite the higher sensitivity and better time resolution of the calcium-imaging dyes compared to p-Erk labeling, the specificity of calcium imaging dyes is worse due to the high amount of spontaneous calcium fluctuations. This data is preliminary to discuss the qualitative properties of stimulus responsive neurons in the olfactory bulb, a large sample size would be required to analyze in detail qualitative response of neurons to different stimuli.

In my p-Erk experiments I saw a specific response of the dorsolateral cluster (DLG) to cadaverine (see figure 25), consistent with the findings of Dieris et al. (2017). But again, in the calcium-imaging experiments no topology was observed for Cadaverine-responding neurons, which were distributed across all areas of the olfactory bulb (see figure 42).

In contrast to the cadaverine response, the p-Erk response to alkaline pH in adult zebrafish was highly variable (see figure 25), and in particular the mediodorsal cluster seemed mostly less intensely labelled than other glomerular clusters (namely DLG and DG) (see figure 25). While these data are too preliminary to draw any conclusion concerning the localization of alkaline response in the OB they certainly do not support alkaline sensitivity being mediated by OSN projecting to the mediodorsal cluster.

However, in calcium-imaging experiments with larval zebrafish, we observe that alkaline responsive neurons are distributed in mediodorsal (which is the target site for crypt neurons in OB) and dorsal glomeruli (see figure 44). It is conceivable that the maturation of neuronal circuits in the olfactory bulb would increase the calcium oscillations so that the odor-specific component is not robustly detectable in adult fish – the inhibitory interneurons often have later birth periods compared to projection neurons. It can also not be excluded that many OSN would respond to alkaline pH, not necessarily as a receptor-mediated interaction. Another possible interpretation of the results could be that in larval zebrafish crypt neurons might have a role to play in sensing alkalinity and is not consistently maintained into adulthood.

As discussed above, a lot of spontaneous activity in the neurons was observed and up to 90% of the recorded neurons had to be excluded from analysis of imaging data because of that. This is one of the drawbacks of calcium dyes that they pick up calcium oscillations resulting in a background of spontaneous activity, making the post analysis of the imaging data cumbersome. One of the possible solutions for making the analysis easier for the experimenter is a more accurate spatial resolution of the stimulus application and bringing the stimulus exposure to the olfactory epithelium of the larvae within a shorter time range.

Telencephalon is a third relay station in the processing of olfactory information. In adult zebrafish as well as in larvae it receives olfactory information via projection neurons from the olfactory bulb. Dp (dorsal posterior part of telencephalon) which in teleost including zebrafish is homologous to mammalian piriform (olfactory) cortex. Ventral telencephalon also receives projection neurons which is a homolog to the septal area, part of limbic system in mammals (Miyasaka et al., 2014). Hence, it was an interesting question to ask whether the neurons in telencephalon in larval zebrafish respond to olfactory stimulus.

In calcium imaging experiments, along with olfactory bulb, dorso-frontal and dorsal posterior surface of telencephalon was kept in the imaging focus. It was observed that majority of the neurons in telencephalon did not qualify our set criteria as a stimulus responsive neuron (see Results /Analysis pipeline), Figure 44, 45, 56. This implies that neurons in the telencephalon of larval zebrafish experience a lot of calcium fluctuations. In adult zebrafish as well, a high background activity in the telencephalon has been reported independent of stimulus application termed as “representation noise” (Jacobson et al., 2018).

Telencephalon in adult zebrafish has also been reported to exhibit substantial variability and adaptation following stimulus application (Jacobson et al., 2018). Jacobson and colleagues discovered that neurons of (Dp) in telencephalon adapted over trails on stimulus application.

In larval zebrafish, telencephalon as an odor responsive higher brain region has not been studied extensively in calcium imaging studies, one of the possible reasons might be high calcium fluctuations and background noise leading to high variability in the data, as seen in the adult zebrafish. This can be a possible explanation for the variability in the qualitative properties of the stimulus responsive neurons in telencephalon between two strains of fish (see Figure 45 and 46).

It can only be speculated that telencephalon in developing larval zebrafish might be involved in processing multitude of information coming from different sensory modalities, however, role of telencephalon in larval zebrafish as a modulator for sensory information is still under investigation.

In zebrafish larvae, habenula which is part of diencephalon has been studied by various groups as a modulator of olfactory information. Dysfunction or lesion of right dorsal habenula resulted in significant impairment of food seeking behavior (Chen et al., 2019). In zebrafish role of habenula has also been studied in fear and anxiety-related behavior (Hikosaka, 2010), and in modulating inputs from olfactory pathways (Zhang et al., 2017). Thus, it would be interesting to investigate to the response of habenula neurons to olfactory stimuli for further calcium Imaging experiments.

5.8 Controlled odor stimulation by using a microchip

We are currently developing a microchip adapted from (Candelier et al., 2015) in which 5-9 dpf zebrafish larvae can be embedded with agarose gel. The setup will enhance the ability to deliver complex stimuli in precisely controlled with spatio-temporal structures analogous to those encountered in natural conditions. The microfluidic device can deliver multiple chemical stimuli spatial precision (in the range 1-10 ms range), to a larva restrained in agarose gel. The microfluidic device can be combined with confocal microscope with a sampling rate of 1Hz, and the neuronal activity in the olfactory bulb and brain areas can be monitored. However, due to the highly demanding micro-drilling techniques required for making the chip, it did not become ready during the timeframe of my thesis.

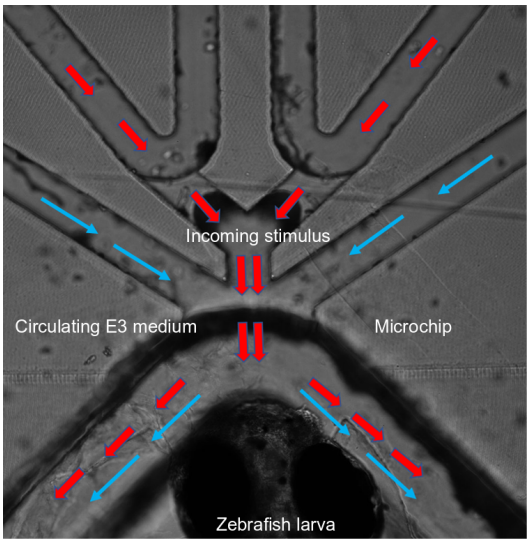

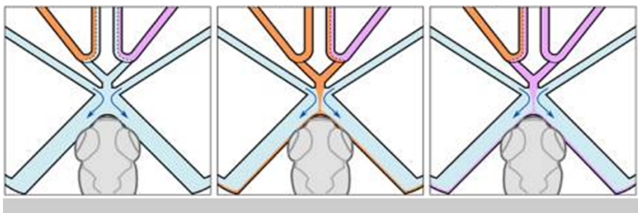

(Candelier et al., 2015)

Figure 47: Maximum projection of the microchip prototype with 9 dpf larvae

6. References

Agetsuma, M., Aizawa, H., Aoki, T., Nakayama, R., Takahoko, M., Goto, M., Sassa, T., Amo, R., Shiraki, T., Kawakami, K., et al. (2010). The habenula is crucial for experience-dependent modification of fear responses in zebrafish. Nat. Neurosci. *13*, 1354–1356.

Ahrens, M.B., Orger, M.B., Robson, D.N., Li, J.M., and Keller, P.J. (2013). Whole-brain functional imaging at cellular resolution using light-sheet microscopy. Nat. Methods *10*, 413–420.

Ahuja, G., Ivandic, I., Saltürk, M., Oka, Y., Nadler, W., and Korsching, S.I. (2013). Zebrafish crypt neurons project to a single, identified mediodorsal glomerulus. Sci Rep *3*, 2063.

Ahuja, G., Bozorg Nia, S., Zapilko, V., Shiriagin, V., Kowatschew, D., Oka, Y., and Korsching, S.I. (2014). Kappe neurons, a novel population of olfactory sensory neurons. Sci Rep *4*, 4037.

Ahuja, G., Reichel, V., Kowatschew, D., Syed, A.S., Kotagiri, A.K., Oka, Y., Weth, F., and Korsching, S.I. (2018). Overlapping but distinct topology for zebrafish V2R-like olfactory receptors reminiscent of odorant receptor spatial expression zones. BMC Genomics *19*, 383.

Akerboom, J., Chen, T.-W., Wardill, T.J., Tian, L., Marvin, J.S., Mutlu, S., Calderón, N.C., Esposti, F., Borghuis, B.G., Sun, X.R., et al. (2012). Optimization of a GCaMP Calcium Indicator for Neural Activity Imaging. J. Neurosci. *32*, 13819–13840.

Alioto, T.S., and Ngai, J. (2005). The odorant receptor repertoire of teleost fish. BMC Genomics *6*, 173.

Amo, R., Fredes, F., Kinoshita, M., Aoki, R., Aizawa, H., Agetsuma, M., Aoki, T., Shiraki, T., Kakinuma, H., Matsuda, M., et al. (2014). The Habenulo-Raphe Serotonergic Circuit Encodes an Aversive Expectation Value Essential for Adaptive Active Avoidance of Danger. Neuron *84*, 1034–1048.

Aramuni, G., and Griesbeck, O. (2013). Chronic calcium imaging in neuronal development and disease. Exp. Neurol. *242*, 50–56.

Ashley, C.C., and Ridgway, E.B. (1968). Simultaneous recording of membrane potential, calcium transient and tension in single muscle fibers. Nature *219*, 1168–1169.

Ashworth, R. (2004). Approaches to measuring calcium in zebrafish: focus on neuronal development. Cell Calcium *35*, 393–402.

Bahl, A., and Engert, F. (2020). Neural circuits for evidence accumulation and decision making in larval zebrafish. Nat. Neurosci. *23*, 94–102.

Baier, H., and Korsching, S. (1994). Olfactory glomeruli in the zebrafish form an invariant pattern and are identifiable across animals. J. Neurosci. *14*, 219–230.

Baier, H., Rotter, S., and Korsching, S. (1994). Connectional topography in the zebrafish olfactory system: random positions but regular spacing of sensory neurons projecting to an individual glomerulus. Proc. Natl. Acad. Sci. U.S.A. *91*, 11646–11650.

Bailey, J., Oliveri, A., and Levin, E.D. (2013). Zebrafish model systems for developmental neurobehavioral toxicology. Birth Defects Res. C Embryo Today *99*, 14–23.

Baird, G.S., Zacharias, D.A., and Tsien, R.Y. (1999). Circular permutation and receptor insertion within green fluorescent proteins. PNAS *96*, 11241–11246.

Barker, A.J., and Baier, H. (2015). Sensorimotor decision making in the zebrafish tectum. Curr. Biol. *25*, 2804–2814.

Basnet, R.M., Zizioli, D., Taweedet, S., Finazzi, D., and Memo, M. (2019). Zebrafish Larvae as a Behavioral Model in Neuropharmacology. Biomedicines *7*.

Behrens, M., Frank, O., Rawel, H., Ahuja, G., Potting, C., Hofmann, T., Meyerhof, W., and Korsching, S. (2014). ORA1, a zebrafish olfactory receptor ancestral to all mammalian V1R genes, recognizes 4-hydroxyphenylacetic acid, a putative reproductive pheromone. J. Biol. Chem. *289*, 19778–19788.

Berg, J., Yang, H., and Jan, L.Y. (2012). Ca2+-activated Cl− channels at a glance. J Cell Sci *125*, 1367–1371.

Bergmann, K., Meza Santoscoy, P., Lygdas, K., Nikolaeva, Y., MacDonald, R.B., Cunliffe, V.T., and Nikolaev, A. (2018). Imaging Neuronal Activity in the Optic Tectum of Late Stage Larval Zebrafish. J Dev Biol *6*.

Berridge, M.J. (1998). Neuronal calcium signaling. Neuron *21*, 13–26.

Berridge, M.J., Lipp, P., and Bootman, M.D. (2000). The versatility and universality of calcium signalling. Nat. Rev. Mol. Cell Biol. *1*, 11–21.

Berridge, M.J., Bootman, M.D., and Roderick, H.L. (2003). Calcium signalling: dynamics, homeostasis and remodelling. Nat. Rev. Mol. Cell Biol. *4*, 517–529.

Bettini, S., Milani, L., Lazzari, M., Maurizii, M.G., and Franceschini, V. (2017). Crypt cell markers in the olfactory organ of Poecilia reticulata: analysis and comparison with the fish model Danio rerio. Brain Struct Funct *222*, 3063–3074.

Bianco, I.H., Kampff, A.R., and Engert, F. (2011). Prey capture behavior evoked by simple visual stimuli in larval zebrafish. Front Syst Neurosci *5*, 101.

Biechl, D., Tietje, K., Gerlach, G., and Wullimann, M.F. (2016). Crypt neurons are involved in kin recognition in larval zebrafish. Sci Rep *6*, 24590.

Biechl, D., Tietje, K., Ryu, S., Grothe, B., Gerlach, G., and Wullimann, M.F. (2017). Identification of accessory olfactory system and medial amygdala in the zebrafish. Sci Rep *7*, 44295.

Bloodgood, B.L., and Sabatini, B.L. (2008). Regulation of synaptic signalling by postsynaptic, non-glutamate receptor ion channels. J. Physiol. (Lond.) *586*, 1475–1480.

van den Bos, R., Althuizen, J., Tschigg, K., Bomert, M., Zethof, J., Filk, G., and Gorissen, M. (2019). Early life exposure to cortisol in zebrafish (Danio rerio): similarities and differences in behaviour and physiology between larvae of the AB and TL strains. Behav Pharmacol *30*, 260–271.

Branson, K., Robie, A.A., Bender, J., Perona, P., and Dickinson, M.H. (2009). High throughput ethomics in large groups of Drosophila. Nat. Methods *6*, 451–457.

Braubach, O.R., Wood, H.-D., Gadbois, S., Fine, A., and Croll, R.P. (2009). Olfactory conditioning in the zebrafish (Danio rerio). Behav. Brain Res. *198*, 190–198.

Braubach, O.R., Fine, A., and Croll, R.P. (2012). Distribution and functional organization of glomeruli in the olfactory bulbs of zebrafish (Danio rerio). J. Comp. Neurol. *520*, 2317–2339, Spc1.

Braubach, O.R., Miyasaka, N., Koide, T., Yoshihara, Y., Croll, R.P., and Fine, A. (2013). Experience-Dependent versus Experience-Independent Postembryonic Development of Distinct Groups of Zebrafish Olfactory Glomeruli. J Neurosci *33*, 6905–6916.

Bromberg-Martin, E.S., Matsumoto, M., and Hikosaka, O. (2010). Dopamine in motivational control: rewarding, aversive, and alerting. Neuron *68*, 815–834.

Brown, J.E., Cohen, L.B., De Weer, P., Pinto, L.H., Ross, W.N., and Salzberg, B.M. (1975). Rapid changes in intracellular free calcium concentration. Detection by metallochromic indicator dyes in squid giant axon. Biophys J *15*, 1155–1160.

Brustein, E., Marandi, N., Kovalchuk, Y., Drapeau, P., and Konnerth, A. (2003). "In vivo" monitoring of neuronal network activity in zebrafish by two-photon Ca (2+) imaging. Pflugers Arch. *446*, 766–773.

Cao, X., and Li, W. (2020). Embryonic substances induce alarm response in adult zebrafish (Danio rerio). J. Fish Biol.

Cao, Y., Oh, B.C., and Stryer, L. (1998). Cloning and localization of two multigene receptor families in goldfish olfactory epithelium. Proc. Natl. Acad. Sci. U.S.A. *95*, 11987–11992.

Chandrasekhar, A., Guo, S., Masai, I., Nicolson, T., and Wu, C.-F. (2017). Zebrafish: from genes and neurons to circuits, behavior and disease. J. Neurogenet. *31*, 59–60.

Chen, Y., and Huang, L.-Y.M. (2017). A simple and fast method to image calcium activity of neurons from intact dorsal root ganglia using fluorescent chemical Ca2+ indicators. Mol Pain *13*, 1744806917748051.

Chen, J.L., Andermann, M.L., Keck, T., Xu, N.-L., and Ziv, Y. (2013a). Imaging Neuronal Populations in Behaving Rodents: Paradigms for Studying Neural Circuits Underlying Behavior in the Mammalian Cortex. J. Neurosci. *33*, 17631–17640.

Chen, T.-W., Wardill, T.J., Sun, Y., Pulver, S.R., Renninger, S.L., Baohan, A., Schreiter, E.R., Kerr, R.A., Orger, M.B., Jayaraman, V., et al. (2013b). Ultrasensitive fluorescent proteins for imaging neuronal activity. Nature *499*, 295–300.

Chen, W.-Y., Peng, X.-L., Deng, Q.-S., Chen, M.-J., Du, J.-L., and Zhang, B.-B. (2019). Role of Olfactorily Responsive Neurons in the Right Dorsal Habenula-Ventral Interpeduncular Nucleus Pathway in Food-Seeking Behaviors of Larval Zebrafish. Neuroscience *404*, 259–267.

Chew, S.F., and Ip, Y.K. (2014). Excretory nitrogen metabolism and defence against ammonia toxicity in air-breathing fishes. J. Fish Biol. *84*, 603–638.

Chia, J.S.M., Wall, E.S., Wee, C.L., Rowland, T.A.J., Cheng, R.-K., Cheow, K., Guillemin, K., and Jesuthasan, S. (2019). Bacteria evoke alarm behaviour in zebrafish. Nat Commun 10, 3831.

Colwill, R.M. (2019). Behavioral studies of stimulus learning in zebrafish larvae. Behav. Processes *164*, 150–156.

Colwill, R.M., and Creton, R. (2011a). Locomotor behaviors in zebrafish (Danio rerio) larvae. Behav. Processes *86*, 222–229.

Colwill, R.M., and Creton, R. (2011b). Imaging escape and avoidance behavior in zebrafish larvae. Rev Neurosci *22*, 63–73.

Cong, L., Wang, Z., Chai, Y., Hang, W., Shang, C., Yang, W., Bai, L., Du, J., Wang, K., and Wen, Q. (2017). Rapid whole brain imaging of neural activity in freely behaving larval zebrafish (Danio rerio). Elife *6*.

Cong, X., Zheng, Q., Ren, W., Chéron, J.-B., Fiorucci, S., Wen, T., Zhang, C., Yu, H., Golebiowski, J., and Yu, Y. (2019). Zebrafish olfactory receptors ORAs differentially detect bile acids and bile salts. J. Biol. Chem. *294*, 6762–6771.

Créton, R., Speksnijder, J.E., and Jaffe, L.F. (1998). Patterns of free calcium in zebrafish embryos. J. Cell. Sci. *111 (Pt 12)*, 1613–1622.

Crivici, A., and Ikura, M. (1995). Molecular and structural basis of target recognition by calmodulin. Annu Rev Biophys Biomol Struct *24*, 85–116.

Dal Maschio, M., Donovan, J.C., Helmbrecht, T.O., and Baier, H. (2017). Linking Neurons to Network Function and Behavior by Two-Photon Holographic Optogenetics and Volumetric Imaging. Neuron *94*, 774-789.e5.

Dana, H., Mohar, B., Sun, Y., Narayan, S., Gordus, A., Hasseman, J.P., Tsegaye, G., Holt, G.T., Hu, A., Walpita, D., et al. (2016). Sensitive red protein calcium indicators for imaging neural activity. Elife *5*.

Dana, H., Sun, Y., Mohar, B., Hulse, B., Hasseman, J.P., Tsegaye, G., Tsang, A., Wong, A., Patel, R., Macklin, J.J., et al. (2018). High-performance GFP-based calcium indicators for imaging activity in neuronal populations and microcompartments. BioRxiv 434589.

Davis, D.J., Bryda, E.C., Gillespie, C.H., and Ericsson, A.C. (2016). Microbial modulation of behavior and stress responses in zebrafish larvae. Behav. Brain Res. *311*, 219–227.

Decker, A.R., McNeill, M.S., Lambert, A.M., Overton, J.D., Chen, Y.-C., Lorca, R.A., Johnson, N.A., Brockerhoff, S.E., Mohapatra, D.P., MacArthur, H., et al. (2014). Abnormal differentiation of dopaminergic neurons in zebrafish trpm7 mutant larvae impairs development of the motor pattern. Dev. Biol. *386*, 428–439.

Dehmelt, F.A., von Daranyi, A., Leyden, C., and Arrenberg, A.B. (2018). Evoking and tracking zebrafish eye movement in multiple larvae with ZebEyeTrack. Nat Protoc *13*, 1539–1568.

Diaz-Verdugo, C., Sun, G.J., Fawcett, C.H., Zhu, P., and Fishman, M.C. (2019). Mating Suppresses Alarm Response in Zebrafish. Curr. Biol. *29*, 2541-2546.e3.

Dieris, M., Ahuja, G., Krishna, V., and Korsching, S.I. (2017). A single identified glomerulus in the zebrafish olfactory bulb carries the high-affinity response to death-associated odor cadaverine. Sci Rep *7*, 40892.

Diggles, B.K., Arlinghaus, R., Browman, H.I., Cooke, S.J., Cowx, I.G., Kasumyan, A.O., Key, B., Rose, J.D., Sawynok, W., Schwab, A., et al. (2017). Responses of larval zebrafish to low pH immersion assay. Comment on Lopez-Luna et al. Journal of Experimental Biology *220*, 3191–3192.

Døving, K.B., Selset, R., and Thomesen, G. (1980). Olfactory sensitivity to bile acids in salmonid fishes. Acta Physiologica Scandinavica *108*, 123–131.

Døving, K.B., Hansson, K.-A., Backström, T., and Hamdani, E.H. (2011). Visualizing a set of olfactory sensory neurons responding to a bile salt. Journal of Experimental Biology *214*, 80–87.

Dreosti, E., Vendrell Llopis, N., Carl, M., Yaksi, E., and Wilson, S.W. (2014). Left-right asymmetry is required for the habenulae to respond to both visual and olfactory stimuli. Curr. Biol. *24*, 440–445.

Duboué, E.R., Hong, E., Eldred, K.C., and Halpern, M.E. (2017). Left Habenular Activity Attenuates Fear Responses in Larval Zebrafish. Curr. Biol. *27*, 2154-2162.e3.

Duchen, M.R. (1999). Contributions of mitochondria to animal physiology: from homeostatic sensor to calcium signalling and cell death. J. Physiol. (Lond.) *516 (Pt 1)*, 1–17.

Dunn, T.W., Gebhardt, C., Naumann, E.A., Riegler, C., Ahrens, M.B., Engert, F., and Del Bene, F. (2016). Neural Circuits Underlying Visually Evoked Escapes in Larval Zebrafish. Neuron *89*, 613–628.

Dwivedi, S., Medishetti, R., Rani, R., Sevilimedu, A., Kulkarni, P., and Yogeeswari, P. (2019). Larval zebrafish model for studying the effects of valproic acid on neurodevelopment: An approach towards modeling autism. J Pharmacol Toxicol Methods *95*, 56–65.

Dynes, J.L., and Ngai, J. (1998). Pathfinding of olfactory neuron axons to stereotyped glomerular targets revealed by dynamic imaging in living zebrafish embryos. Neuron *20*, 1081–1091.

Edwards, J.G., and Michel, W.C. (2002). Odor-stimulated glutamatergic neurotransmission in the zebrafish olfactory bulb. Journal of Comparative Neurology *454*, 294–309.

Eilers, J., and Konnerth, A. (2009). Dye loading with patch pipettes. Cold Spring Harb Protoc *2009*, pdb. prot5201.

Engert, F., and Wilson, S.W. (2012). Zebrafish neurobiology: from development to circuit function and behaviour. Dev Neurobiol *72*, 215–217.

Enjin, A., and Suh, G.S.-B. (2013). Neural mechanisms of alarm pheromone signaling. Mol. Neurons *35*, 177–181.

Esposti, F., Johnston, J., Rosa, J.M., Leung, K.-M., and Lagnado, L. (2013). Olfactory stimulation selectively modulates the OFF pathway in the retina of zebrafish. Neuron *79*, 97–110.

Fernandes, Y., Rampersad, M., Jones, E.M., and Eberhart, J.K. (2019). Social deficits following embryonic ethanol exposure arise in post-larval zebrafish. Addict Biol *24*, 898–907.

Ferraguti, F., and Shigemoto, R. (2006). Metabotropic glutamate receptors. Cell Tissue Res *326*, 483–504.

Ferreira, T., Wilson, S.R., Choi, Y.G., Risso, D., Dudoit, S., Speed, T.P., and Ngai, J. (2014). Silencing of odorant receptor genes by G protein βγ signaling ensures the expression of one odorant receptor per olfactory sensory neuron. Neuron *81*, 847–859.

Fetcho, J.R. (2007). Imaging neuronal activity with calcium indicators in larval zebrafish. CSH Protoc *2007*, pdb. prot4781.

Fetcho, J.R., and O'Malley, D.M. (1997). Imaging neuronal networks in behaving animals. Curr. Opin. Neurobiol. *7*, 832–838.

Franco-Restrepo, J.E., Forero, D.A., and Vargas, R.A. (2019). A Review of Freely Available, Open-Source Software for the Automated Analysis of the Behavior of Adult Zebrafish. Zebrafish *16*, 223–232.

Freifeld, L., Odstrcil, I., Förster, D., Ramirez, A., Gagnon, J.A., Randlett, O., Costa, E.K., Asano, S., Celiker, O.T., Gao, R., et al. (2017). Expansion microscopy of zebrafish for neuroscience and developmental biology studies. Proc. Natl. Acad. Sci. U.S.A. *114*, E10799–E10808.

Friedrich, R.W. (2013). Neuronal computations in the olfactory system of zebrafish. Annu. Rev. Neurosci. *36*, 383–402.

Friedrich, R.W. (2014). Calcium imaging in the intact olfactory system of zebrafish and mouse. Cold Spring Harb Protoc *2014*, 310–316.

Friedrich, R.W., and Korsching, S.I. (1997). Combinatorial and chemotopic odorant coding in the zebrafish olfactory bulb visualized by optical imaging. Neuron *18*, 737–752.

Friedrich, R.W., and Korsching, S.I. (1998). Chemotopic, combinatorial, and noncombinatorial odorant representations in the olfactory bulb revealed using a voltage-sensitive axon tracer. J. Neurosci. *18*, 9977–9988.

Friedrich, R.W., and Wiechert, M.T. (2014). Neuronal circuits and computations: pattern decorrelation in the olfactory bulb. FEBS Lett. *588*, 2504–2513.

Friedrich, R.W., Yaksi, E., Judkewitz, B., and Wiechert, M.T. (2009). Processing of odor representations by neuronal circuits in the olfactory bulb. Ann. N. Y. Acad. Sci. *1170*, 293–297.

Fucile, S. (2004). Ca2+ permeability of nicotinic acetylcholine receptors. Cell Calcium *35*, 1–8.

Fuller, C.L., Yettaw, H.K., and Byrd, C.A. (2006). Mitral neurons in the olfactory bulb of adult zebrafish (Danio rerio): morphology and distribution. J. Comp. Neurol. *499*, 218–230.

Fuss, S.H., and Korsching, S.I. (2001). Odorant feature detection: activity mapping of structure response relationships in the zebrafish olfactory bulb. J. Neurosci. *21*, 8396–8407.

Gahtan, E., Sankrithi, N., Campos, J.B., and O'Malley, D.M. (2002). Evidence for a widespread brain stem escape network in larval zebrafish. J. Neurophysiol. *87*, 608–614.

Gao, Y.-J., and Ji, R.-R. (2009). c-Fos and p-Erk, which is a better marker for neuronal activation and central sensitization after noxious stimulation and tissue injury? Open Pain J *2*, 11–17.

Gayoso, J.Á., Castro, A., Anadón, R., and Manso, M.J. (2011). Differential bulbar and extrabulbar projections of diverse olfactory receptor neuron populations in the adult zebrafish (Danio rerio). J. Comp. Neurol. *519*, 247–276.

Gebhardt, C., Auer, T.O., Henriques, P.M., Rajan, G., Duroure, K., Bianco, I.H., and Del Bene, F. (2019). An interhemispheric neural circuit allowing binocular integration in the optic tectum. Nat Commun *10*, 5471.

Geng, Y., and Peterson, R.T. (2019). The zebrafish subcortical social brain as a model for studying social behavior disorders. Dis Model Mech *12*.

Gerlach, G., Tietje, K., Biechl, D., Namekawa, I., Schalm, G., and Sulmann, A. (2019). Behavioural and neuronal basis of olfactory imprinting and kin recognition in larval fish. Journal of Experimental Biology *222*.

Giovannucci, A., Friedrich, J., Gunn, P., Kalfon, J., Brown, B.L., Koay, S.A., Taxidis, J., Najafi, F., Gauthier, J.L., Zhou, P., et al. (2019). CaImAn an open source tool for scalable calcium imaging data analysis. Elife *8*.

Grienberger, C., and Konnerth, A. (2012). Imaging calcium in neurons. Neuron *73*, 862–885.

Haesemeyer, M., Robson, D.N., Li, J.M., Schier, A.F., and Engert, F. (2018). A Brain-wide Circuit Model of Heat-Evoked Swimming Behavior in Larval Zebrafish. Neuron *98*, 817-831.e6.

Haesemeyer, M., Schier, A.F., and Engert, F. (2019). Convergent Temperature Representations in Artificial and Biological Neural Networks. Neuron *103*, 1123-1134.e6.

Hagey, L.R., Møller, P.R., Hofmann, A.F., and Krasowski, M.D. (2010). Diversity of bile salts in fish and amphibians: evolution of a complex biochemical pathway. Physiol. Biochem. Zool. *83*, 308–321.

Hamdani, E.H., and Døving, K.B. (2002). The alarm reaction in crucian carp is mediated by olfactory neurons with long dendrites. Chem. Senses *27*, 395–398.

Hamdani, E.H., and Døving, K.B. (2006). Specific Projection of the Sensory Crypt Neurons in the Olfactory System in Crucian Carp, Carassius carassius. Chem Senses *31*, 63–67.

Hansen, A., and Zeiske, E. (1993). Development of the olfactory organ in the zebrafish, Brachydanio rerio. J. Comp. Neurol. *333*, 289–300.

Hansen, A., and Zeiske, E. (1998). The peripheral olfactory organ of the zebrafish, Danio rerio: an ultrastructural study. Chem. Senses *23*, 39–48.

Hansen, A., Reutter, K., and Zeiske, E. (2002). Taste bud development in the zebrafish, Danio rerio. Dev. Dyn. *223*, 483–496.

Hansen, A., Rolen, S.H., Anderson, K., Morita, Y., Caprio, J., and Finger, T.E. (2003). Correlation between Olfactory Receptor Cell Type and Function in the Channel Catfish. J. Neurosci. *23*, 9328–9339.

Hansen, A., Anderson, K.T., and Finger, T.E. (2004). Differential distribution of olfactory receptor neurons in goldfish: structural and molecular correlates. J. Comp. Neurol. *477*, 347–359.

Hara, T.J. (1994). Olfaction and gustation in fish: an overview. Acta Physiol. Scand. *152*, 207–217.

Harden, M.V., Newton, L.A., Lloyd, R.C., and Whitlock, K.E. (2006). Olfactory imprinting is correlated with changes in gene expression in the olfactory epithelia of the zebrafish. J. Neurobiol. *66*, 1452–1466.

Hartmann, S., Vogt, R., Kunze, J., Rauschert, A., Kuhnert, K.-D., Wanzenböck, J., Lamatsch, D.K., and Witte, K. (2018). Zebrafish larvae show negative phototaxis to near-infrared light. PLoS ONE *13*, e0207264.

Hashiguchi, Y., and Nishida, M. (2006). Evolution and origin of vomeronasal-type odorant receptor gene repertoire in fishes. BMC Evolutionary Biology *6*, 76.

Hashiguchi, Y., and Nishida, M. (2007). Evolution of trace amine associated receptor (TAAR) gene family in vertebrates: lineage-specific expansions and degradations of a

second class of vertebrate chemosensory receptors expressed in the olfactory epithelium. Mol. Biol. Evol. *24*, 2099–2107.

Heap, L.A., Vanwalleghem, G.C., Thompson, A.W., Favre-Bulle, I., Rubinsztein-Dunlop, H., and Scott, E.K. (2017). Hypothalamic Projections to the Optic Tectum in Larval Zebrafish. Front Neuroanat *11*, 135.

Helmchen, F., and Denk, W. (2005). Deep tissue two-photon microscopy. Nat. Methods *2*, 932–940.

Higashijima, S., Masino, M.A., Mandel, G., and Fetcho, J.R. (2003). Imaging neuronal activity during zebrafish behavior with a genetically encoded calcium indicator. J. Neurophysiol. *90*, 3986–3997.

Hikosaka, O. (2010). The habenula: from stress evasion to value-based decision-making. Nat. Rev. Neurosci. *11*, 503–513.

Hinz, R.C., and de Polavieja, G.G. (2017). Ontogeny of collective behavior reveals a simple attraction rule. Proc. Natl. Acad. Sci. U.S.A. *114*, 2295–2300.

Hinz, C., Gebhardt, K., Hartmann, A.K., Sigman, L., and Gerlach, G. (2012). Influence of kinship and MHC class II genotype on visual traits in zebrafish larvae (Danio rerio). PLoS ONE *7*, e51182.

Hinz, C., Namekawa, I., Namekawa, R., Behrmann-Godel, J., Oppelt, C., Jaeschke, A., Müller, A., Friedrich, R.W., and Gerlach, G. (2013). Olfactory imprinting is triggered by MHC peptide ligands. Sci Rep *3*, 2800.

Howe, H.B., McIntyre, P.B., and Wolman, M.A. (2018). Adult zebrafish primarily use vision to guide piscivorous foraging behavior. Behav. Processes *157*, 230–237.

Hussain, A., Saraiva, L.R., and Korsching, S.I. (2009). Positive Darwinian selection and the birth of an olfactory receptor clade in teleosts. Proc. Natl. Acad. Sci. U.S.A. *106*, 4313–4318.

Hussain, A., Saraiva, L.R., Ferrero, D.M., Ahuja, G., Krishna, V.S., Liberles, S.D., and Korsching, S.I. (2013). High-affinity olfactory receptor for the death-associated odor cadaverine. Proc. Natl. Acad. Sci. U.S.A. *110*, 19579–19584.

Ingebretson, J.J., and Masino, M.A. (2013). Quantification of locomotor activity in larval zebrafish: considerations for the design of high throughput behavioral studies. Front Neural Circuits *7*.

Iwasaki, S., and Ikegaya, Y. (2018). In vivo one-photon confocal calcium imaging of neuronal activity from the mouse neocortex. J. Integr. Neurosci. *17*, 671–678.

Izquierdo, C., Gómez-Tamayo, J.C., Nebel, J.-C., Pardo, L., and Gonzalez, A. (2018). Identifying human diamine sensors for death related putrescine and cadaverine molecules. PLoS Comput. Biol. *14*, e1005945.

Jacobson, G.A., Rupprecht, P., and Friedrich, R.W. (2018). Experience-Dependent Plasticity of Odor Representations in the Telencephalon of Zebrafish. Current Biology *28*, 1-14.e3.

Jesuthasan, S.J., and Mathuru, A.S. (2008). The alarm response in zebrafish: innate fear in a vertebrate genetic model. J. Neurogenet. *22*, 211–228.

Jetti, S.K., Vendrell-Llopis, N., and Yaksi, E. (2014). Spontaneous activity governs olfactory representations in spatially organized habenular microcircuits. Curr. Biol. *24*, 434–439.

Ji, R., Befort, K., Brenner, G.J., and Woolf, C.J. (2002). ERK MAP Kinase Activation in Superficial Spinal Cord Neurons Induces Prodynorphin and NK-1 Upregulation and Contributes to Persistent Inflammatory Pain Hypersensitivity. J Neurosci *22*, 478–485.

Joëls, M., and Baram, T.Z. (2009). The neuro-symphony of stress. Nat. Rev. Neurosci. *10*, 459–466.

Johnson, M.A., Tsai, L., Roy, D.S., Valenzuela, D.H., Mosley, C., Magklara, A., Lomvardas, S., Liberles, S.D., and Barnea, G. (2012). Neurons expressing trace amine-associated receptors project to discrete glomeruli and constitute an olfactory subsystem. Proc. Natl. Acad. Sci. U.S.A. *109*, 13410–13415.

Kalueff, A.V., Stewart, A.M., and Gerlai, R. (2014). Zebrafish as an emerging model for studying complex brain disorders. Trends Pharmacol. Sci. *35*, 63–75.

Kang, N., and Koo, J. (2012). Olfactory receptors in non-chemosensory tissues. BMB Rep *45*, 612–622.

Kaniganti, T., Deogade, A., Maduskar, A., Mukherjee, A., Guru, A., Subhedar, N., and Ghose, A. (2019). Sensitivity of Olfactory Sensory Neurons to food cues is tuned to nutritional states by Neuropeptide Y signalling. BioRxiv 573170.

Kermen, F., Franco, L.M., Wyatt, C., and Yaksi, E. (2013). Neural circuits mediating olfactory-driven behavior in fish. Front Neural Circuits *7*, 62.

Kettunen, P. (2020). Calcium Imaging in the Zebrafish. Adv. Exp. Med. Biol. *1131*, 901–942.

Kibat, C., Krishnan, S., Ramaswamy, M., Baker, B.J., and Jesuthasan, S. (2016). Imaging voltage in zebrafish as a route to characterizing a vertebrate functional connectome: promises and pitfalls of genetically encoded indicators. J. Neurogenet. *30*, 80–88.

Kim, D.H., Kim, J., Marques, J.C., Grama, A., Hildebrand, D.G.C., Gu, W., Li, J.M., and Robson, D.N. (2017). Pan-neuronal calcium imaging with cellular resolution in freely swimming zebrafish. Nat. Methods *14*, 1107–1114.

Koide, T., Miyasaka, N., Morimoto, K., Asakawa, K., Urasaki, A., Kawakami, K., and Yoshihara, Y. (2009). Olfactory neural circuitry for attraction to amino acids revealed by transposon-mediated gene trap approach in zebrafish. Proc. Natl. Acad. Sci. U.S.A. *106*, 9884–9889.

Koide, T., Yabuki, Y., and Yoshihara, Y. (2018). Terminal Nerve GnRH3 Neurons Mediate Slow Avoidance of Carbon Dioxide in Larval Zebrafish. Cell Rep *22*, 1115–1123.

Kokel, D., Bryan, J., Laggner, C., White, R., Cheung, C.Y.J., Mateus, R., Healey, D., Kim, S., Werdich, A.A., Haggarty, S.J., et al. (2010). Rapid behavior—based identification of neuroactive small molecules in the zebrafish. Nat Chem Biol *6*, 231–237.

Korsching, S. (2005). Selective imaging of the receptor neuron population in the olfactory bulb of zebrafish and mice. Chem. Senses *30 Suppl 1*, i101-102.

Korsching, S.I., Argo, S., Campenhausen, H., Friedrich, R.W., Rummrich, A., and Weth, F. (1997). Olfaction in zebrafish: what does a tiny teleost tell us? Semin. Cell Dev. Biol. *8*, 181–187.

Kosaka, T., and Hama, K. (1982). Synaptic organization in the teleost olfactory bulb. J. Physiol. (Paris) *78*, 707–719.

Kotrschal, K., Krautgartner, W.D., and Hansen, A. (1997). Ontogeny of the solitary chemosensory neurons in the zebrafish, Danio rerio. Chem. Senses *22*, 111–118.

Kratz, E., Dugas, J.C., and Ngai, J. (2002). Odorant receptor gene regulation: implications from genomic organization. Trends Genet. *18*, 29–34.

Krishnan, S., Mathuru, A.S., Kibat, C., Rahman, M., Lupton, C.E., Stewart, J., Claridge-Chang, A., Yen, S.-C., and Jesuthasan, S. (2014). The right dorsal habenula limits attraction to an odor in zebrafish. Curr. Biol. *24*, 1167–1175.

Kumai, Y., and Perry, S.F. (2011). Ammonia excretion via Rhcg1 facilitates Na+ uptake in larval zebrafish, Danio rerio, in acidic water. American Journal of Physiology-Regulatory, Integrative and Comparative Physiology *301*, R1517–R1528.

Kumai, Y., Harris, J., Al-Rewashdy, H., Kwong, R.W.M., and Perry, S.F. (2015). Nitrogenous Waste Handling by Larval Zebrafish Danio rerio in Alkaline Water. Physiol. Biochem. Zool. *88*, 137–145.

Kunst, M., Laurell, E., Mokayes, N., Kramer, A., Kubo, F., Fernandes, A.M., Förster, D., Dal Maschio, M., and Baier, H. (2019). A Cellular-Resolution Atlas of the Larval Zebrafish Brain. Neuron *103*, 21-38.e5.

Kwon, H.J., Koo, J.H., Zufall, F., Leinders-Zufall, T., and Margolis, F.L. (2009). Ca2+ Extrusion by NCX Is Compromised in Olfactory Sensory Neurons of OMP−/− Mice. PLoS One *4*.

Larkum, M.E., Watanabe, S., Nakamura, T., Lasser-Ross, N., and Ross, W.N. (2003). Synaptically activated Ca2+ waves in layer 2/3 and layer 5 rat neocortical pyramidal neurons. J. Physiol. (Lond.) *549*, 471–488.

Lee, A., Mathuru, A.S., Teh, C., Kibat, C., Korzh, V., Penney, T.B., and Jesuthasan, S. (2010). The habenula prevents helpless behavior in larval zebrafish. Curr. Biol. *20*, 2211–2216.

Li, Q. (2018). Deorphanization of Olfactory Trace Amine-Associated Receptors. Methods Mol. Biol. *1820*, 21–31.

Li, J., Mack, J.A., Souren, M., Yaksi, E., Higashijima, S., Mione, M., Fetcho, J.R., and Friedrich, R.W. (2005). Early development of functional spatial maps in the zebrafish olfactory bulb. J. Neurosci. *25*, 5784–5795.

Liberles, S.D., and Buck, L.B. (2006). A second class of chemosensory receptors in the olfactory epithelium. Nature *442*, 645–650.

Lindsay, S.M., and Vogt, R.G. (2004). Behavioral responses of newly hatched zebrafish (Danio rerio) to amino acid chemostimulants. Chem. Senses *29*, 93–100.

Lipschitz, D.L., and Michel, W.C. (2002). Amino acid odorants stimulate microvillar sensory neurons. Chem. Senses *27*, 277–286.

Liu, S.J., and Zukin, R.S. (2007). Ca2+-permeable AMPA receptors in synaptic plasticity and neuronal death. Trends Neurosci. *30*, 126–134.

Liu, S.-Q.J., and Cull-Candy, S.G. (2000). Synaptic activity at calcium-permeable AMPA receptors induces a switch in receptor subtype. Nature *405*, 454–458.

Liu, Q., Tang, Z., Surdenikova, L., Kim, S., Patel, K.N., Kim, A., Ru, F., Guan, Y., Weng, H.-J., Geng, Y., et al. (2009). Sensory neuron-specific GPCR Mrgprs are itch receptors mediating chloroquine-induced pruritus. Cell *139*, 1353–1365.

Llano, I., González, J., Caputo, C., Lai, F.A., Blayney, L.M., Tan, Y.P., and Marty, A. (2000). Presynaptic calcium stores underlie large-amplitude miniature IPSCs and spontaneous calcium transients. Nature Neuroscience *3*, 1256–1265.

Lopez-Luna, J., Al-Jubouri, Q., Al-Nuaimy, W., and Sneddon, L.U. (2017). Impact of stress, fear and anxiety on the nociceptive responses of larval zebrafish. PLoS ONE *12*, e0181010.

López-Schier, H. (2019). Neuroplasticity in the acoustic startle reflex in larval zebrafish. Curr. Opin. Neurobiol. *54*, 134–139.

Lukasz, D., and Kindt, K.S. (2018). In Vivo Calcium Imaging of Lateral-line Hair Neurons in Larval Zebrafish. J Vis Exp.

Luo, L., Wen, Q., Ren, J., Hendricks, M., Gershow, M., Qin, Y., Greenwood, J., Soucy, E.R., Klein, M., Smith-Parker, H.K., et al. (2014). Dynamic Encoding of Perception, Memory, and Movement in a C. elegans Chemotaxis Circuit. Neuron *82*, 1115–1128.

Lyons, M.R., and West, A.E. (2011). Mechanisms of specificity in neuronal activity-regulated gene transcription. Prog. Neurobiol. *94*, 259–295.

Lytle, C.R., and Perdue, E.M. (1981). Free, proteinaceous, and humic-bound amino acids in river water containing high concentrations of aquatic humus. Environ. Sci. Technol. *15*, 224–228.

Machluf, Y., Gutnick, A., and Levkowitz, G. (2011). Development of the zebrafish hypothalamus. Ann. N. Y. Acad. Sci. *1220*, 93–105.

Mack-Bucher, J.A., Li, J., and Friedrich, R.W. (2007). Early functional development of interneurons in the zebrafish olfactory bulb. European Journal of Neuroscience *25*, 460–470.

Madeira, N., and Oliveira, R.F. (2017). Long-Term Social Recognition Memory in Zebrafish. Zebrafish *14*, 305–310.

Mahabir, S., and Gerlai, R. (2017). The Importance of Holding Water: Salinity and Chemosensory Cues Affect Zebrafish Behavior. Zebrafish *14*, 444–458.

Marques, J.C., Li, M., Schaak, D., Robson, D.N., and Li, J.M. (2020). Internal state dynamics shape brainwide activity and foraging behaviour. Nature *577*, 239–243.

Mathuru, A.S., and Jesuthasan, S. (2013). The medial habenula as a regulator of anxiety in adult zebrafish. Front Neural Circuits *7*, 99.

Michel, W.C., and Lubomudrov, L.M. (1995). Specificity and sensitivity of the olfactory organ of the zebrafish, Danio rerio. J. Comp. Physiol. A *177*, 191–199.

Miklavc, P., and Valentinčič, T. (2012). Chemotopy of amino acids on the olfactory bulb predicts olfactory discrimination capabilities of zebrafish Danio rerio. Chem. Senses *37*, 65–75.

Miller, N., and Gerlai, R. (2007). Quantification of shoaling behaviour in zebrafish (Danio rerio). Behavioural Brain Research *184*, 157–166.

Miller, N.Y., and Gerlai, R. (2011). Shoaling in zebrafish: what we don't know. Rev Neurosci *22*, 17–25.

Miyasaka, N., Sato, Y., Yeo, S.-Y., Hutson, L.D., Chien, C.-B., Okamoto, H., and Yoshihara, Y. (2005). Robo2 is required for establishment of a precise glomerular map in the zebrafish olfactory system. Development *132*, 1283–1293.

Miyasaka, N., Morimoto, K., Tsubokawa, T., Higashijima, S., Okamoto, H., and Yoshihara, Y. (2009). From the olfactory bulb to higher brain centers: genetic visualization of secondary olfactory pathways in zebrafish. J. Neurosci. *29*, 4756–4767.

Miyasaka, N., Arganda-Carreras, I., Wakisaka, N., Masuda, M., Sümbül, U., Seung, H.S., and Yoshihara, Y. (2014). Olfactory projectome in the zebrafish forebrain revealed by genetic single-neuron labelling. Nat Commun *5*, 3639.

Miyawaki, A., Llopis, J., Heim, R., McCaffery, J.M., Adams, J.A., Ikura, M., and Tsien, R.Y. (1997). Fluorescent indicators for Ca2+ based on green fluorescent proteins and calmodulin. Nature *388*, 882–887.

Morita, Y., and Finger, T.E. (1998). Differential projections of ciliated and microvillous olfactory receptor neurons in the catfish, Ictalurus punctatus. Journal of Comparative Neurology *398*, 539–550.

Muto, A., and Kawakami, K. (2011). Imaging functional neural circuits in zebrafish with a new GCaMP and the Gal4FF-UAS system. Commun Integr Biol *4*, 566–568.

Muto, A., and Kawakami, K. (2013). Prey capture in zebrafish larvae serves as a model to study cognitive functions. Front Neural Circuits *7*, 110.

Muto, A., and Kawakami, K. (2016). Calcium Imaging of Neuronal Activity in Free-Swimming Larval Zebrafish. Methods Mol. Biol. *1451*, 333–341.

Muto, A., and Kawakami, K. (2018). Ablation of a Neuronal Population Using a Two-photon Laser and Its Assessment Using Calcium Imaging and Behavioral Recording in Zebrafish Larvae. J Vis Exp.

Muto, A., Ohkura, M., Kotani, T., Higashijima, S., Nakai, J., and Kawakami, K. (2011). Genetic visualization with an improved GCaMP calcium indicator reveals spatiotemporal activation of the spinal motor neurons in zebrafish. Proc. Natl. Acad. Sci. U.S.A. *108*, 5425–5430.

Muto, A., Lal, P., Ailani, D., Abe, G., Itoh, M., and Kawakami, K. (2017). Activation of the hypothalamic feeding centre upon visual prey detection. Nat Commun *8*, 15029.

Nakai, J., Ohkura, M., and Imoto, K. (2001). A high signal-to-noise Ca(2+) probe composed of a single green fluorescent protein. Nat. Biotechnol. *19*, 137–141.

Nakamura, T., and Gold, G.H. (1987). A cyclic nucleotide-gated conductance in olfactory receptor cilia. Nature *325*, 442–444.

Namekawa, I., Moenig, N.R., and Friedrich, R.W. (2018). Rapid olfactory discrimination learning in adult zebrafish. Exp Brain Res *236*, 2959–2969.

Nasiadka, A., and Clark, M.D. (2012). Zebrafish breeding in the laboratory environment. ILAR J *53*, 161–168.

Neher, E., and Sakaba, T. (2008). Multiple roles of calcium ions in the regulation of neurotransmitter release. Neuron *59*, 861–872.

Niell, C.M., and Stryker, M.P. (2008). Highly Selective Receptive Fields in Mouse Visual Cortex. J. Neurosci. *28*, 7520–7536.

Nikonov, A.A., Finger, T.E., and Caprio, J. (2005). Beyond the olfactory bulb: an odotopic map in the forebrain. Proc. Natl. Acad. Sci. U.S.A. *102*, 18688–18693.

Niswender, C.M., and Conn, P.J. (2010). Metabotropic Glutamate Receptors: Physiology, Pharmacology, and Disease. Annu Rev Pharmacol Toxicol *50*, 295–322.

Norton, W., and Bally-Cuif, L. (2010). Adult zebrafish as a model organism for behavioural genetics. BMC Neurosci *11*, 90.

Norton, W.H.J., Manceau, L., and Reichmann, F. (2019). The Visually Mediated Social Preference Test: A Novel Technique to Measure Social Behavior and Behavioral Disturbances in Zebrafish. Methods Mol. Biol. *2011*, 121–132.

Oka, Y., and Korsching, S.I. (2011). Shared and unique G alpha proteins in the zebrafish versus mammalian senses of taste and smell. Chem. Senses *36*, 357–365.

Oka, Y., Saraiva, L.R., and Korsching, S.I. (2012). Crypt neurons express a single V1R-related ora gene. Chem. Senses *37*, 219–227.

Orger, M.B., and Baier, H. (2005). Channeling of red and green cone inputs to the zebrafish optomotor response. Vis. Neurosci. *22*, 275–281.

Orrenius, S., Zhivotovsky, B., and Nicotera, P. (2003). Regulation of cell death: the calcium-apoptosis link. Nat. Rev. Mol. Cell Biol. *4*, 552–565.

Paredes, R.M., Etzler, J.C., Watts, L.T., Zheng, W., and Lechleiter, J.D. (2008). Chemical calcium indicators. Methods *46*, 143–151.

Parisi, V., Guerrera, M.C., Abbate, F., Garcia-Suarez, O., Viña, E., Vega, J.A., and Germanà, A. (2014). Immunohistochemical characterization of the crypt neurons in the olfactory epithelium of adult zebrafish. Ann. Anat. *196*, 178–182.

Parolini, M., Ghilardi, A., De Felice, B., and Del Giacco, L. (2019). Environmental concentration of fluoxetine disturbs larvae behavior and increases the defense response at molecular level in zebrafish (Danio rerio). Environ Sci Pollut Res Int *26*, 34943–34952.

Pelkowski, S.D., Kapoor, M., Richendrfer, H.A., Wang, X., Colwill, R.M., and Creton, R. (2011). A novel high-throughput imaging system for automated analyses of avoidance behavior in zebrafish larvae. Behav. Brain Res. *223*, 135–144.

Pérez-Escudero, A., Vicente-Page, J., Hinz, R.C., Arganda, S., and de Polavieja, G.G. (2014a). idTracker: tracking individuals in a group by automatic identification of unmarked animals. Nat. Methods *11*, 743–748.

Pérez-Escudero, A., Vicente-Page, J., Hinz, R.C., Arganda, S., and de Polavieja, G.G. (2014b). idTracker: tracking individuals in a group by automatic identification of unmarked animals. Nat. Methods *11*, 743–748.

Polikov, V.S., Tresco, P.A., and Reichert, W.M. (2005). Response of brain tissue to chronically implanted neural electrodes. J. Neurosci. Methods *148*, 1–18.

Portugues, R., and Engert, F. (2009). The neural basis of visual behaviors in the larval zebrafish. Curr. Opin. Neurobiol. *19*, 644–647.

Portugues, R., Severi, K.E., Wyart, C., and Ahrens, M.B. (2013). Optogenetics in a transparent animal: circuit function in the larval zebrafish. Curr. Opin. Neurobiol. *23*, 119–126.

Pozzan, T., Arslan, P., Tsien, R.Y., and Rink, T.J. (1982). Anti-immunoglobulin, cytoplasmic free calcium, and capping in B lymphocytes. J. Cell Biol. *94*, 335–340.

Privat, M., and Sumbre, G. (2020). Naturalistic Behavior: The Zebrafish Larva Strikes Back. Curr. Biol. *30*, R27–R29.

Quirin, S., Vladimirov, N., Yang, C.-T., Peterka, D.S., Yuste, R., and Ahrens, M.B. (2016). Calcium imaging of neural circuits with extended depth-of-field light-sheet microscopy. Opt Lett *41*, 855–858.

Randlett, O., Wee, C.L., Naumann, E.A., Nnaemeka, O., Schoppik, D., Fitzgerald, J.E., Portugues, R., Lacoste, A.M.B., Riegler, C., Engert, F., et al. (2015). Whole-brain activity mapping onto a zebrafish brain atlas. Nat Methods *12*, 1039–1046.

Reilly, C.E. (2001). Mitral cell activity patterns optimise to reflect odour representation. J. Neurol. *248*, 641–643.

Reinig, S., Driever, W., and Arrenberg, A.B. (2017). The Descending Diencephalic Dopamine System Is Tuned to Sensory Stimuli. Curr. Biol. *27*, 318–333.

Renninger, S.L., and Orger, M.B. (2013). Two-photon imaging of neural population activity in zebrafish. Methods *62*, 255–267.

Rink, E., and Wullimann, M.F. (2004). Connections of the ventral telencephalon (subpallium) in the zebrafish (Danio rerio). Brain Research *1011*, 206–220.

Rizzuto, R., and Pozzan, T. (2006). Microdomains of intracellular Ca2+: molecular determinants and functional consequences. Physiol. Rev. *86*, 369–408.

Robles, E. (2017). The power of projectomes: genetic mosaic labeling in the larval zebrafish brain reveals organizing principles of sensory circuits. J. Neurogenet. *31*, 61–69.

Rochefort, N.L., Garaschuk, O., Milos, R.-I., Narushima, M., Marandi, N., Pichler, B., Kovalchuk, Y., and Konnerth, A. (2009). Sparsification of neuronal activity in the visual cortex at eye-opening. Proc. Natl. Acad. Sci. U.S.A. *106*, 15049–15054.

Rogers, M., and Dani, J.A. (1995). Comparison of quantitative calcium flux through NMDA, ATP, and ACh receptor channels. Biophys. J. *68*, 501–506.

Saint-Amant, L., and Drapeau, P. (1998). Time course of the development of motor behaviors in the zebrafish embryo. J. Neurobiol. *37*, 622–632.

Saint-Amant, L., and Drapeau, P. (2003). Whole-cell patch-clamp recordings from identified spinal neurons in the zebrafish embryo. Methods Cell Sci *25*, 59–64.

Saraiva, L.R., and Korsching, S.I. (2007). A novel olfactory receptor gene family in teleost fish. Genome Res. *17*, 1448–1457.

Saraiva, L.R., Ahuja, G., Ivandic, I., Syed, A.S., Marioni, J.C., Korsching, S.I., and Logan, D.W. (2015). Molecular and neuronal homology between the olfactory systems of zebrafish and mouse. Sci Rep *5*, 11487.

Sato, T., Hamaoka, T., Aizawa, H., Hosoya, T., and Okamoto, H. (2007a). Genetic single-cell mosaic analysis implicates ephrinB2 reverse signaling in projections from the posterior tectum to the hindbrain in zebrafish. J. Neurosci. *27*, 5271–5279.

Sato, Y., Miyasaka, N., and Yoshihara, Y. (2005). Mutually Exclusive Glomerular Innervation by Two Distinct Types of Olfactory Sensory Neurons Revealed in Transgenic Zebrafish. J. Neurosci. *25*, 4889–4897.

Sato, Y., Miyasaka, N., and Yoshihara, Y. (2007b). Hierarchical Regulation of Odorant Receptor Gene Choice and Subsequent Axonal Projection of Olfactory Sensory Neurons in Zebrafish. J. Neurosci. *27*, 1606–1615.

Schärer, Y.-P.Z., Shum, J., Moressis, A., and Friedrich, R.W. (2012). Dopaminergic modulation of synaptic transmission and neuronal activity patterns in the zebrafish homolog of olfactory cortex. Front Neural Circuits *6*, 76.

Schwaller, B. (2010). Cytosolic Ca2+ Buffers. Cold Spring Harb Perspect Biol *2*, a004051.

Severi, K.E., Böhm, U.L., and Wyart, C. (2018). Investigation of hindbrain activity during active locomotion reveals inhibitory neurons involved in sensorimotor processing. Sci Rep *8*, 13615.

Shams, S., Seguin, D., Facciol, A., Chatterjee, D., and Gerlai, R. (2017). Effect of social isolation on anxiety-related behaviors, cortisol, and monoamines in adult zebrafish. Behav. Neurosci. *131*, 492–504.

Shaner, N.C., Campbell, R.E., Steinbach, P.A., Giepmans, B.N.G., Palmer, A.E., and Tsien, R.Y. (2004). Improved monomeric red, orange and yellow fluorescent proteins derived from Discosoma sp. red fluorescent protein. Nat. Biotechnol. *22*, 1567–1572.

Shao, X., Lakhina, V., Dang, P., Cheng, R.P., Marcaccio, C.L., and Raper, J.A. (2017). Olfactory sensory axons target specific protoglomeruli in the olfactory bulb of zebrafish. Neural Dev *12*, 18.

Sharma, K., Ahuja, G., Hussain, A., Balfanz, S., Baumann, A., and Korsching, S.I. (2016). Elimination of a ligand gating site generates a supersensitive olfactory receptor. Sci Rep *6*, 28359.

Shih, T.-H., Horng, J.-L., Hwang, P.-P., and Lin, L.-Y. (2008). Ammonia excretion by the skin of zebrafish (Danio rerio) larvae. Am. J. Physiol., Cell Physiol. *295*, C1625-1632.

Shimazaki, T., Tanimoto, M., Oda, Y., and Higashijima, S.-I. (2019). Behavioral Role of the Reciprocal Inhibition between a Pair of Mauthner Neurons during Fast Escapes in Zebrafish. J. Neurosci. *39*, 1182–1194.

Simpson, J.H., and Looger, L.L. (2018). Functional Imaging and Optogenetics in Drosophila. Genetics *208*, 1291–1309.

Smith, S.J., and Zucker, R.S. (1980). Aequorin response facilitation and intracellular calcium accumulation in molluscan neurones. J Physiol *300*, 167–196.

Sneddon, L.U., Lopez-Luna, J., Wolfenden, D.C.C., Leach, M.C., Valentim, A.M., Steenbergen, P.J., Bardine, N., Currie, A.D., Broom, D.M., and Brown, C. (2017). Response to: Responses of larval zebrafish to low pH immersion assay. Comment on Lopez-Luna et al. J. Exp. Biol. *220*, 3192–3194.

Speca, D.J., Lin, D.M., Sorensen, P.W., Isacoff, E.Y., Ngai, J., and Dittman, A.H. (1999). Functional identification of a goldfish odorant receptor. Neuron *23*, 487–498.

Spence, R., Gerlach, G., Lawrence, C., and Smith, C. (2008). The behaviour and ecology of the zebrafish, Danio rerio. Biol Rev Camb Philos Soc *83*, 13–34.

Spilioti, M., Vargesson, N., and Neri, P. (2016). Quantitative assessment of intrinsic noise for visually guided behaviour in zebrafish. Vision Res. *127*, 104–114.

Steele, C.W., Owens, D.W., and Scarfe, A.D. (1990). Attraction of zebrafish, Brachydanio rerio, to alanine and its suppression by copper. Journal of Fish Biology *36*, 341–352.

Steele, W.B., Mole, R.A., and Brooks, B.W. (2018). Experimental Protocol for Examining Behavioral Response Profiles in Larval Fish: Application to the Neuro-stimulant Caffeine. J Vis Exp.

Stosiek, C., Garaschuk, O., Holthoff, K., and Konnerth, A. (2003). In vivo two-photon calcium imaging of neuronal networks. PNAS *100*, 7319–7324.

Svoboda, K., and Yasuda, R. (2006). Principles of two-photon excitation microscopy and its applications to neuroscience. Neuron *50*, 823–839.

Tabor, R., Yaksi, E., Weislogel, J.-M., and Friedrich, R.W. (2004). Processing of odor mixtures in the zebrafish olfactory bulb. J. Neurosci. *24*, 6611–6620.

Takahashi, M., Narushima, M., and Oda, Y. (2002). In vivo imaging of functional inhibitory networks on the mauthner cell of larval zebrafish. J. Neurosci. *22*, 3929–3938.

Takahashi, M., Inoue, M., Tanimoto, M., Kohashi, T., and Oda, Y. (2017). Short-term desensitization of fast escape behavior associated with suppression of Mauthner cell activity in larval zebrafish. Neurosci. Res. *121*, 29–36.

Thommesen, G. (1983). Morphology, distribution, and specificity of olfactory receptor neurons in salmonid fishes. Acta Physiol. Scand. *117*, 241–249.

Thouvenin, O., and Wyart, C. (2017). Tracking microscopy enables whole-brain imaging in freely moving zebrafish. Nat. Methods *14*, 1041–1042.

Tian, L., Hires, S.A., Mao, T., Huber, D., Chiappe, M.E., Chalasani, S.H., Petreanu, L., Akerboom, J., McKinney, S.A., Schreiter, E.R., et al. (2009). Imaging neural activity in worms, flies and mice with improved GCaMP calcium indicators. Nat. Methods *6*, 875–881.

Tsang, B., Ansari, R., and Gerlai, R. (2019). Dose dependent behavioral effects of acute alcohol administration in zebrafish fry. Pharmacol. Biochem. Behav. *179*, 124–133.

Tsien, R.Y. (1980). New calcium indicators and buffers with high selectivity against magnesium and protons: design, synthesis, and properties of prototype structures. Biochemistry *19*, 2396–2404.

Valente, A., Huang, K.-H., Portugues, R., and Engert, F. (2012). Ontogeny of classical and operant learning behaviors in zebrafish. Learn. Mem. *19*, 170–177.

Vogt, R.G., Lindsay, S.M., Byrd, C.A., and Sun, M. (1997). Spatial patterns of olfactory neurons expressing specific odor receptor genes in 48-hour-old embryos of zebrafish Danio rerio. J. Exp. Biol. *200*, 433–443.

Wakisaka, N., Miyasaka, N., Koide, T., Masuda, M., Hiraki-Kajiyama, T., and Yoshihara, Y. (2017). An Adenosine Receptor for Olfaction in Fish. Current Biology *27*, 1437-1447.e4.

Wang, K., Hinz, J., Zhang, Y., Thiele, T.R., and Arrenberg, A.B. (2020). Parallel Channels for Motion Feature Extraction in the Pretectum and Tectum of Larval Zebrafish. Cell Rep *30*, 442-453.e6.

Wee, C.L., Song, E.Y., Johnson, R.E., Ailani, D., Randlett, O., Kim, J.-Y., Nikitchenko, M., Bahl, A., Yang, C.-T., Ahrens, M.B., et al. (2019). A bidirectional network for appetite control in larval zebrafish. Elife *8*.

Wetzker, R., and Böhmer, F.-D. (2003). Transactivation joins multiple tracks to the ERK/MAPK cascade. Nat. Rev. Mol. Cell Biol. *4*, 651–657.

White, E.J., Kounelis, S.K., and Byrd-Jacobs, C.A. (2015). Plasticity of glomeruli and olfactory-mediated behavior in zebrafish following detergent lesioning of the olfactory epithelium. Neuroscience *284*, 622–631.

Widmann, C., Gibson, S., Jarpe, M.B., and Johnson, G.L. (1999). Mitogen-activated protein kinase: conservation of a three-kinase module from yeast to human. Physiol. Rev. *79*, 143–180.

Wong, S.T., Trinh, K., Hacker, B., Chan, G.C., Lowe, G., Gaggar, A., Xia, Z., Gold, G.H., and Storm, D.R. (2000b). Disruption of the type III adenylyl cyclase gene leads to peripheral and behavioral anosmia in transgenic mice. Neuron *27*, 487–497.

Wright, P.A., and Wood, C.M. (2009). A new paradigm for ammonia excretion in aquatic animals: role of Rhesus (Rh) glycoproteins. J. Exp. Biol. *212*, 2303–2312.

Yabuki, Y., Koide, T., Miyasaka, N., Wakisaka, N., Masuda, M., Ohkura, M., Nakai, J., Tsuge, K., Tsuchiya, S., Sugimoto, Y., et al. (2016). Olfactory receptor for prostaglandin F2α mediates male fish courtship behavior. Nat. Neurosci. *19*, 897–904.

Yaksi, E., von Saint Paul, F., Niessing, J., Bundschuh, S.T., and Friedrich, R.W. (2009). Transformation of odor representations in target areas of the olfactory bulb. Nat. Neurosci. *12*, 474–482.

Yang, L., Jiang, H., Wang, Y., Lei, Y., Chen, J., Sun, N., Lv, W., Wang, C., Near, T.J., and He, S. (2019). Expansion of vomeronasal receptor genes (OlfC) in the evolution of fright reaction in Ostariophysan fishes. Commun Biol *2*, 235.

Yokogawa, T., Hannan, M.C., and Burgess, H.A. (2012). The dorsal raphe modulates sensory responsiveness during arousal in zebrafish. J. Neurosci. *32*, 15205–15215.

Yoshihara, Y. (2014). Zebrafish Olfactory System. In The Olfactory System: From Odor Molecules to Motivational Behaviors, K. Mori, ed. (Tokyo: Springer Japan), pp. 71–96.

Zapilko, V., and Korsching, S.I. (2016). Tetrapod V1R-like ora genes in an early-diverging ray-finned fish species: the canonical six ora gene repertoire of teleost fish resulted from gene loss in a larger ancestral repertoire. BMC Genomics *17*, 83.

Zariwala, H.A., Borghuis, B.G., Hoogland, T.M., Madisen, L., Tian, L., De Zeeuw, C.I., Zeng, H., Looger, L.L., Svoboda, K., and Chen, T.-W. (2012). A Cre-Dependent GCaMP3 Reporter Mouse for Neuronal Imaging In Vivo. J Neurosci *32*, 3131–3141.

Zarubin, T., and Han, J. (2005). Activation and signaling of the p38 MAP kinase pathway. Cell Research *15*, 11–18.

Zeddies, D.G., and Fay, R.R. (2005). Development of the acoustically evoked behavioral response in zebrafish to pure tones. J. Exp. Biol. *208*, 1363–1372.

Zhang, B.-B., Yao, Y.-Y., Zhang, H.-F., Kawakami, K., and Du, J.-L. (2017). Left Habenula Mediates Light-Preference Behavior in Zebrafish via an Asymmetrical Visual Pathway. Neuron *93*, 914-928.e4.

Zhou, S., Chen, Q., Di Paolo, C., Shao, Y., Hollert, H., and Seiler, T.-B. (2019). Behavioral profile alterations in zebrafish larvae exposed to environmentally relevant concentrations of eight priority pharmaceuticals. Sci. Total Environ. *664*, 89–98.

Zohar, Y., Muñoz-Cueto, J.A., Elizur, A., and Kah, O. (2010). Neuroendocrinology of reproduction in teleost fish. Gen. Comp. Endocrinol. *165*, 438–455.

7. Appendix

7.1 Abbreviations

ATP Adenosine triphosphate
BSA Bovine serum albumin
CAM calmodulin
cAMP cyclic adenosine monophosphate
CNG cyclic nucleotide gated ion channels
CRISPR Clustered Regularly Interspaced Short Palindromic Repeats
DAPI 4',6- Diamidino-2-Phenylindole
dlG dorso-lateral cluster of glomeruli
DMSO Dimethylsulfoxide
dpf days post fertilization
GECI Genetically encoded calcium Indicators
GPCR G Protein coupled receptors
GTP guanine triphosphate
IEG immediate early genes
IHC immuno-histochemistry
OB olfactory bulb
OE olfactory epithelium
OR olfactory receptor
OSN olfactory sensory neurons
PBS phosphate buffered saline
PCR polymerase chain reaction
p-Erk phosphorylated extracellular -signal regulated kinase
rpm rounds per minute
TAAR trace amine-associated receptor
V1R/V2R vomeronasal receptor type 1 and 2
RT room temperature
PFA Paraformaldehyde

7.2 Macro for obtaining raw data from Fiji

```
FoStart=0;
FoEnd=30;

path=File.openDialog("Please open file");
dir=File.getParent(path);
file=File.getName(path);
resultDir=dir+File.separator+substring(file, 0, lengthOf(file)-4);
if(!File.exists(resultDir)){
	File.makeDirectory(resultDir);
}
open(path);
currentImg=getImageID();
run("To ROI Manager");

Stack.getDimensions(width, height, channels, slices, frames);
roiInt=newArray(frames);
for (roi = 0; roi < roiManager("count"); roi++) {
	//selectImage(currentImg);
	Array.fill(roiInt, 0);
	roiManager("Select", roi);
	for (frame = 1; frame < frames; frame++) {
		Stack.setFrame(frame);
		roiManager("Select", roi);
		getStatistics(area, mean, min, max, std, histogram);
		roiInt[frame-1]=mean;
	}

	//Array.show(roiInt);
	FoArray=Array.slice(roiInt,FoStart,FoEnd);
```

```
	Array.getStatistics(FoArray, min, max, mean, stdDev);
	FoValue=mean;
	//print(FoValue);
	roiFFo=newArray(roiInt.length);
	for (i = 0; i < roiInt.length; i++) {
		roiFFo[i]=roiInt[i]/FoValue;
	}
	roiDeltaF=newArray(roiInt.length);
	roiDeltaFFo=newArray(roiInt.length);
	for (i = 0; i < roiInt.length; i++) {
		roiDeltaF[i]=roiInt[i]-FoValue;
		roiDeltaFFo[i]=roiDeltaF[i]/FoValue;
	}
	//Array.show(roiFFo);
	Plot.create("deltaF/Fo plot Roi"+roi, "frame", "deltaF/Fo", roiDeltaFFo);
	Plot.update();
	plotImg=getImageID();
	rename("deltaF over Fo plot");
	plotTitle=getTitle();
	saveResults();
	waitForUser("check");
	close();


}
function saveResults(){
	run("Clear Results");
	for (i = 0; i < roiInt.length; i++) {
		setResult("Frame", nResults, i+1);
		setResult("Flu [a.u.]", nResults-1,roiInt[i]);
```

```
		setResult("F/Fo", nResults-1,roiFFo[i]);
		setResult("deltaF", nResults-1,roiDeltaF[i]);
		setResult("deltaF/Fo", nResults-1,roiDeltaFFo[i]);
		if(i==0){
			setResult("Fo [a.u.]", nResults-1,FoValue);
			setResult("Fo 1st frame", nResults-1,FoStart);
			setResult("Fo last frame", nResults-1,FoEnd);
		}

	}
	resultPath=resultDir+File.separator+roi+1+"_"+"resultTable.csv";
	saveAs("results", resultPath);
	selectImage(plotImg);
	selectWindow(plotTitle);
	resultPath=resultDir+File.separator+roi+1+"_"+"deltaFFo-plot.png";
	saveAs("png", resultPath);


}
```

7.3 Erklärung

Ich versichere, dass ich die von mir vorgelegte Dissertation selbständig angefertigt, dass ich alle Angaben zu den verwendeten Quellen und Hilfsmitteln gemacht habe und dass ich die Orte angegeben habe, an denen die Arbeit - einschließlich Tabellen, Karten und Abbildungen -, die im Wortlaut oder in der Bedeutung anderen Werken entnommen sind, in jedem Einzelfall entlehnt worden ist; dass diese Dissertation noch keiner anderen Fakultät oder Universität zur Prüfung vorgelegt worden ist, dass sie noch nicht veröffentlicht worden ist; und dass ich eine solche Veröffentlichung nicht vor Abschluss des Promotionsverfahrens vornehmen werde. Die Bestimmungen der Promotionsordnung sind mir bekannt. Die von mir vorgelegte Dissertation ist von Prof. Dr. Sigrun Korsching betreut worden

Köln, 15.06.2020

7.4 Acknowledgement

First, I would like to thank Prof. Dr. Sigrun Korsching for being my immediate supervisor and accepting me a graduate student to pursue my doctoral studies in her research group. During my doctoral training, her mentoring and valuable feedbacks has helped me not only to develop as a graduate student but also as an individual. Thanking you!

I would also like to thank Prof. Dr. Peter Kloppenburg, as my co-supervisor and member of my thesis advisory committee. Inputs from him and his research group has immensely helped in shaping the project. I would like to thank Dr. Leo Kurian, as my tutor and member of thesis advisory committee.

Thanks to Prof. Dr. Tobias Bollenbach for agreeing to serve as a chairperson of the examination committee.

Many thanks to Prof. Arrenberg, University of Tübingen and his research group for agreeing to train me on calcium imaging techniques. With their help I was able to solve many technical issues in imaging experiments. Thanks again!

Thanks to Peter Zentis, CECAD, for helping to analyse imaging data. Thanks to the team at University workshop in helping to solve technical issues in our experimental setup.

I would like to also thank graduate school organisers, Dr. Isabell Witt, Katerina Vlantis, and Kathy Jörgens, for taking care of scientific and non-scientific issues for graduate students. Thanks to Katerina again for being a big help to us while organising RTG-NCA Neuroday in Koln!

Thanks to all my graduate school colleagues especially Phillip, Madhuri, Babis, Nasim, Tarun, Merle and Katharina for their scientific input and wonderful time at the graduate school retreats!!

And for my lab colleagues, I would like to thank Dr. Gaurav Ahuja a former postdoc in our lab for teaching me several techniques during the initial months of my graduate training. Dr. Milan Dieris, former member of the lab for teaching me microscopy! I would also like to thank Dr. Kanika Sharma, Dr. Adnan Syed for being nice friend and colleagues. Thanks

to Kanika for being a patient listener in all my talks! Many thanks to Shahzeb for nice time during Goettingen meeting, and for being a patient neighbour in sharing his stationary! Thanks to Gunes, Asma, Marc, Daniel, Alex, Liane for being wonderful lab colleagues and bringing fun to the lab. Thanks to Mehmet, for taking care of the fish facility.

I would like to take the opportunity to thanks my family and friends for their constant support. Many thanks to Jim Hutton for all pep talks to keep me motivated!

Lastly, thanks to RTG-NCA and DFG for supporting me during my graduate studies at the University of Cologne

Manish Tomar